Functional characterisation of *in vitro* synthesised G-protein coupled receptors in polymersomes

Dissertation
Zur Erlangung des Grades
"Doktor der Naturwissenschaften"

Am Fachbereich Biologie
der Johannes Gutenberg-Universität, Mainz

Sylvia May
Geboren am 15.02.1982 in Ludwigshafen am Rhein

Mainz, 2012

Dekan:

1. Berichterstatter:
2. Berichterstatter:

Tag der mündlichen Prüfung:02.07.2012

Zusammenfassung

Membranproteine spielen eine wichtige Rolle in physiologischen Prozessen. Daher ist es nicht verwunderlich, dass Fehlfunktionen von Membranproteinen häufig Krankheitsbildern zugrunde liegen. Dies erklärt auch das große wissenschaftliche Interesse an Membranproteinen und speziell an G-Protein gekoppelten Rezeptoren (GPCR), der größten Subfamilie der Membranproteine. GPCRs stellen daher ein herausragendes Target für die pharmazeutische Wirkstoffentwicklung dar. Aufgrund ihrer hohe Selektivität und Sensitivität sind Membranproteine auch für die Detektion geringster Stoffmengen mittels Biosensoren sehr interessant. Trotz diesem großen Interesse an GPCRs und ihrer wachsenden Bedeutung als Angriffspunkte neuer Medikamente, ist es noch nicht gelungen Struktur, Funktion und endogene Liganden aller bekannten Rezeptoren vollständig aufzuklären. Dies liegt an der hydrophoben Natur der Membranproteine und den damit verbundenen Schwierigkeiten bei Überexpression, Aufreinigung, Rekonstitution und Handhabung. Auch die geringe Stabilität Lipid basierter Membransysteme als Plattform für Screeningsysteme und Biosensoren bereitet Schwierigkeiten für industrielle Anwendungen.

In den letzten Jahren wurde die *in vitro* Synthese von Proteinen zu einer interessanten Alternative, um Membranproteine mit höheren Ausbeuten in biomimetischen Membransystemen herzustellen. Hierfür werden Membranproteine in Gegenwart von Lipidvesikeln oder planaren Membransystemen mit Hilfe von Zellextrakten synthetisiert. Diese zellfreie Methode reduziert zelluläre Einflüsse auf die Proteinausbeute und erleichtert die Anpassung der Expressionsbedingungen. Die direkte Proteinsynthese in Gegenwart biomimetischer Membranen erspart außerdem langwierige Aufreinigungs- und Rekonstituierungsprozesse. Auch für die empfindlichen lipidischen Systeme wurde eine vielversprechende Alternative gefunden. Amphiphile Block-Copolymere zeigen in wässrigen Lösungen ähnliches membranbildendes Verhalten wie Lipide. Allerdings weisen diese besseren Eigenschaften bezüglich Stabilität und Widerstandskraft auf.

Ziel dieser Arbeit war es, durch die innovative Kombination von *in vitro* Synthese und Block-Copolymer basierten Membransystemen ein GPCR-funktionalisiertes Membransystem zu entwickeln, welches zur Charakterisierung von GPCRs genutzt werden kann. Die *in vitro* Expression der GPCRs, Dopamin Rezeptor 1 (DRD1) und 2 (DRD2), im polymeren Membransystem wurde mittels Immunodetektion nachgewiesen. Als polymeres Membransystem wurden Diblock- sowie Tribock-Polymersome verwendet, wobei Anitkörper-Bindungsstudien auf eine bevorzugte Orientierung der Rezeptoren in Triblock-Polymersomen hinwiesen. Die Funktionalität des DRD2 wurde durch einen Liganden-Austausch-Assay auf immobilisierten DRD2-funktionalisierten Triblock-Polymersomen nachgewiesen, wobei eine Verschiebung der Bindungskurve im Vergleich zu zellulären Systemen auf einen Einfluss der modifizierten Proteinumgebung hinweist.

Abstract

Membrane proteins play an indispensable role in physiological processes. It is, therefore, not surprising that many diseases are based on the malfunction of membrane proteins. Hence membrane proteins and especially G-protein coupled receptors(GPCRs)- the largest subfamily- have become an important drug target. Due to their high selectivity and sensitivity membrane proteins are also feasible for the detection of small quantities of substances with biosensors. Despite this widespread interest in GPCRs due to their importance as drug targets and biosensors there is still a lack of knowledge of structure, function and endogenous ligands for quiet a few of the previously identified receptors.

Bottlenecks in over-expression, purification, reconstitution and handling of membrane proteins arise due to their hydrophobic nature. Therefore the production of reasonable amounts of functional membrane proteins for structural and functional studies is still challenging. Also the limited stability of lipid based membrane systems hampers their application as platforms for screening applications and biosensors.

In recent years the *in vitro* protein synthesis became a promising alternative to gain better yields for expression of membrane proteins in bio-mimetic membrane systems. These expression systems are based on cell extracts. Therefore cellular effects on protein expression are reduced. The open nature of the cell-free expression systems easily allows for the adjustment of reaction conditions for the protein of interest. The cell-free expression in the presence of bio-mimetic membrane systems allows the direct incorporation of the membrane proteins and therefore skips the time-consuming purification and reconstitution processes. Amphiphilic block-copolymers emerged as promising alternative for the less stable lipid-based membrane systems. They, like lipids, form membraneous structures in aqueous solutions but exhibit increased mechanical and chemical stability.

The aim of this work was the generation of a GPCR-functionalised membrane system by combining both promising alternatives: *in vitro* synthesis and polymeric membrane systems. This novel platform should be feasible for the characterisation of the incorporated GPCR. Immunodetection of Dopamine receptor 1 and 2 expressed in diblock- and triblock-polymersomes demonstrated the successful *in vitro* expression of GPCRs in polymeric membranes. Antibody binding studies suggested a favoured orientation of dopamine receptors in triblock-polymersomes. A dopamine-replacement assay on DRD2-functionalised immobilised triblock-polymersomes confirmed functionality of the receptor in the polymersomes. The altered binding curve suggests an effect of the altered hydrophobic environment presented by the polymer membrane on protein activity.

Contents

1 Motivation

Membrane proteins play an indispensable role in cell communication, adhesion, energy conversion, signal recognition, transduction, amplification and sensing. Among the membrane proteins the G-protein-coupled receptors (GPCRs) form the largest family and they can be activated by a wide variety of stimuli, such as light, hormones, neurotransmitters and odorants. Many diseases are based on the malfunction of seven-transmembrane proteins, hence nowadays about 40-60% of the descriptive drugs on the market or in development target these GPCRs [23]. But yet there is still a remarkable amount of orphan receptors, with unknown endogenous ligands. A more detailed knowledge about their structure and function increases their importance as drug targets in the future [63]. Therefore, a lot of effort is put into the development of screening assays to identify both endogenous ligands as well as new potential drugs and high throughput methods for the analysis of membrane protein structures. Hence, it is crucial to find feasible methods to immobilise GPCRs in a functional conformation onto appropriate hydrophobic surfaces. These functionalised surfaces should be stable against air and strain as well as capable for parallel and high throughput screening.

2 Introduction

2.1 GPCRs and their importance as targets for the pharmaceutical industry

Since the first description of selectivity of agents by distribution and action by Paul Ehrlicher in 1913 the knowledge about the reasons for selectivity increased immense. In the beginning receptors were only identified according to the response different agents caused in various target tissues or cells [12]. Soon it became clear, that the response could not only rely on the distribution in different target tissues cause different agents elicited different responses in the same tissue [13]. Earl Sutherland spurred the understanding of receptor signaling with the discovery of cyclic adenosine monophosphate (cAMP) as the first second messenger [15]. With further studies, it was shown, that many receptors require a coupled G-Protein [14] for cAMP activation and signal transduction into the cells. The possibility to determine the DNA sequence and clone genes of interest into vectors for overexpression in cell lines further improved the investigation of G-protein coupled receptors (GPCRs) function and signaling. The first crystal structure of one of those GPCRs, bovine rhodopsin, was reported in 2000 by Palczewski [16]. Nowadays it is well known, that these GPCRs are membrane spanning proteins with seven transmembrane regions. On the intracellular region they are coupled to various G-proteins which are activated

by conformational changes of the receptors caused by ligand binding. These ligands can be as diverse as light, odorants, neurotransmitters, biogenic amines, hormones, proteins, amino acids, ions, protons, nucleotides, chemokines and proteins. The activated G-protein transduces the receptor signal into the cells using various signaling pathways [17], [18]. The signal is terminated by receptor desensitisation. This internalisation of active receptors is mediated by phosphorylation and subsequent arrestin binding which induces the formation of clathrin coated pits and finally endocytosis of the formed vesicles [19]. But there are also a lot of other mechanisms which regulate GPCR induced signaling within cells [20].

Today the GPCRs constitute the largest gene family in mammalians. The elucidation of the human genome in 2001 revealed that 2% of the human genome encode for GPCRs [22]. They are divided into 5 main families (glutamate, rhodopsin, adhesion, frizzled/taste2 and secretion) based on phylogenetic analyses [21]. Although the understanding of GPCRs has much improved since their first discovery, and advanced gene expression analysis including side directed mutagenesis and bioinformatic methods became available [22] for enforced characterization of receptors and their ligands there are still a lot of orphan receptors with unknown endogenous ligands. Therefore a lot of effort is put on the deorphanisation and different strategies like fluorescent imaging plate reader screening have been devised [22]. The identification of endogenous ligands often reveals the physiological role of the receptor and therefore also its involvement in diseases and its potential as drug target. The importance of the GPCRs as drug targets is illustrated by the fact that approximately 40% of all approved drugs target GPCRs [23] with upward trend for drugs in development. Studies, comparing disease related proteins with drug target proteins, showed that only a small portion of disease related proteins are targeted by current drugs [23]. These studies also demonstrated that more and more drugs in development target proteins that were not prior drug targets. In the past, many drugs were developed as follow-up drugs for already known target proteins. They were found through traditional chemical screening methods and therefore often only acted on the symptoms of a disease but not on the protein causing the disease [23]. This shows, that a detailed knowledge of the molecular structure and function of proteins and thus the genetic basis of diseases will help to develop more tailored drugs which target proteins directly related to diseases. Biochemical methods like side directed mutagenesis and computational predictions based on known crystal structures of model GPCRs deeply improved the characterisation of ligand binding sites. But still they are mostly based on a few know crystal structures of some model GPCRs cause crystallisation of functional membrane proteins is still challenging. Especially membrane proteins, and therefore GPCRs as the largest family, will becoming more important for future drug development cause they are more easily addressable than cytosolic proteins due to the still challenging transport of drugs across biological membranes.

2.2 Dopamine receptor as a model protein for GPCRs

Dopamine receptors mediate some important neuronal functions and thus they play an essential role in physiological mechanisms of the central nervous system like memory, regulation of motor activity, attention, cognition, motivation, emotion, drug addiction, reward and neuroendocrine processes. Therefore they are common targets for antipsychotic drugs in psychological disorders like schizophrenia and Parkinson's disease [26]. In 1979 Kebabian and Calne proposed to divide the dopaminergic receptors into two classes - D_1 receptors which stimulate adenylate cyclase and the D_2 receptors which transduce their signal cAMP independent [24]. This classification was confirmed by pharmacological, biological and physiological studies. Gene cloning procedures revealed that there are altogether 5 dopamine receptor subtypes which show a high homology of their membrane domains and also the pharmacological characteristics are similar within the two classes: D_1-like receptors(D_1 and D_5) and D_2-like receptors (D_2, D_3 and D_4) [25]. Today it is also known that the various dopamine receptors can build heterodimers with synergistic effects and even specific transduction pathways [27]. For the D_2receptors it was recently shown that they also form heterodimers with Neurotensin1 receptor [35] and receptors for Somatostatin [36]. Those findings might be of importance for further studies on the physiological role of the dopamine receptors and their future as efficient drug targets.

2.2.1 Structure and signaling pathways of dopamine receptors

As members of the large GPCR-family all dopamine receptor subtypes have seven membrane-spanning α helices with considerable conserved amino-acid sequences in the transmembrane regions within the same class of dopamine receptors [25]. All dopamine receptors subtypes have the orientation in the cell membrane in common: extracellular N-terminus and intracellular C-terminus. The C-terminus contains phosphorylation and palmitoylation sites in both subfamilies and is longer for the D_1-like receptors than for the D_2-like [25], [28]. The length of the N-terminus is similar for all subtypes but it carries variable amounts of glycosylation sites Fig.1; [25]. Several amino acids of the transmembrane regions form the binding pocket for ligands Fig.1. This might be the reason, why ligands easily discriminate between the two subfamilies, but not between members of the same subfamily [28], due to the high homology of the transmembrane regions.

The receptors couple to their G-proteins via the 3rd intracellular loop. The D_1-like receptors couple to stimulating G-proteins (G_s/G_{olf}) and activate adenylate cyclase and the D_2-like receptors couple to inhibitory G-proteins (G_i/G_o) which inhibit adenylate cyclase. These different signaling pathways cause an D_2/D_1 antagonism: neurons carrying both receptors are

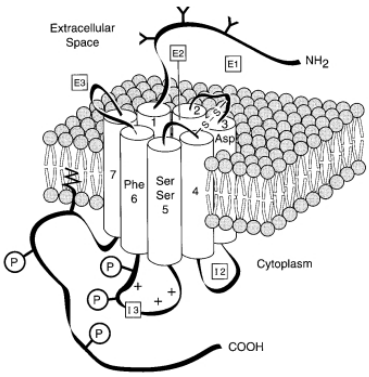

Figure 1: Structure of dopamine receptors: All receptors have 7 transmembrane domains (1-7) and three extracellular loops (E1-E3) and three intracellular loops (I2, I3; I1 not shown between 1 and 2). The 3rd intracellular loop is longer for the DRD2 receptor than for the DRD1. The residues involved in dopamine binding are highlighted in the transmembrane domains. Potential glycosylation sites are marked on the extracellular N-terminus. Potential phosphorylation sites are marked on the 3rd intracellular loop and C-terminus. The disulfide bridge between E1 and E2 is supposed to stabilise the structure [25].

activated by D_1 receptors but the signal is extenuated by the concurrent activation of D_2 receptors [29]. The D_2 receptors also impact several additional signaling pathways like phospholipase activity, ion channels, MAP(mitogen-activated protein) kinases and the Na^+/H^+ exchanger. Those additional pathways are mostly addressed by the $G_{\beta\gamma}$ subunits of the $G_{i/o}$-proteins which are released by receptor activation of the $G_{i/o}$-proteins [30]. Recently it could be demonstrated that DRD2 can also regulate the AkT-GSK3 (Akt/Glycogen Synthase Kinase 3) pathway by a G-protein independent signaling that involves a signaling complex of β-arrestin 2, Akt(a non-specific serine/threonine-protein kinase) and the multimeric protein phosphatase PP2A [33], [34].

The DRD2-gene is located on chromosome 11 and is composed of eight exons, seven of which are coding. The alternative splicing of the sixth exon causes the two isoforms -D_{2L} and D_{2S}- [28] which differ in the length of the 3rd intracellular loop [31]. There is still some disagreement if these isoforms may be responsible for the coupling to different G-proteins. But there is also some evidence, that the binding to a particular G-protein is restricted by the cell-type and availability of the G-protein [30]. Usiello [32] found that the two isoforms have distinct functions in vivo. The D_{2L} isoform acts mostly on the postsynaptic sites of dopaminergic neurons and the D_{2S} isoform shows mainly presynaptic autoreceptor function.

The dopamine receptors are mostly expressed in the brain Fig.2, but can also be found in the pituitary and the periphery [25]; Fig.3.

Brain region	Receptor subtype									
	D_1		D_2		D_3		D_4		D_5	
	mRNA	Receptor	mRNA	Receptor	mRNA	Receptor	mRNA	Receptor	mRNA	Receptor
Caudate nucleus	+++	+++	+++	+++	+/−	+/−	−	+/−	+	++
Putamen	+++	+++	+++	+++	+/−	+/−	−	+/−	+	++
Nucleus accumbens	+++	+++	+++	+++	++	++	−	+/−	+	++
Islands of Calleja	++	++	++	++	+++	+++	−	+/−	−	++
Olfactory tubercle	++	++	++	++	++	++	−	+/−	−	+
Globus pallidus										
External segment	+	+	−	++	−	+	−	+	−	+
Internal segment	−	++	−	+/−	−	+	−	+	−	−
Thalamus	+/−	+	+	+/−	+	+	−	+	−	+
Subthalamic nucleus	−	+	−	−	−	−	−	−	−	−
Hypothalamus	−	+	−	+/−	+	+	−	+	−	+
Substantia nigra										
Pars compacta	+/−	+	++	++	+	+	−	−	−	+
Pars reticulata	+	++	−	+	+	+	−	+	−	−
Ventral tegmental area	−	−	−	−	+	+	−	−	−	+
Red nucleus	−	+	−	+	−	−	−	−	−	−
Hippocampus	+/−	+	+/−	++	+	+	+	+	+	
Cortex										
Frontal	++	++	+/−	+	+	+	+	+	−	++
Motor	++	++	+/−	+/−	−	−	+	+	+	++
Insular and cingular	++	++	+/−	+/−	−	−	+	+	−	−
Somatosensory	++	++	+	+/−	−	−	−	−	−	++
Temporal	++	++	+	+	+	+	+	+	+	+
Occipital	++	++	+	+/−	−	−	+	+	−	++
Amygdala	−	+		+	+	+	−	−	−	−
Cerebellum	+	+	+	+	+	+	−	−	−	+

Figure 2: Distribution of dopamine receptors in the brain. The table demonstrates the relative abundance between brain regions for each receptor subtype [37].

Tissue	Receptor Type	Function
Blood vessels		
Adventitia	D_2-like	Inhibition of NE release
Media	D_1-like	Vasodilatation
Intima	D_2-like	Unknown
Adrenal gland		
Glomerulosa	D_1-like	Unknown
	D_2-like	Inhibition of aldosterone secretion
Medulla	D_1-like	Stimulation of E/NE release
	D_2-like	Inhibition of E/NE release
Kidney		
Glomerulus	D_1-like	Increase of filtration rate
Juxtaglomerular apparatus	D_1-like	Stimulation of renin secretion
Proximal tubule	D_1-like	Inhibition of Na^+ reabsorption
Ascending limb of loop of Henle	D_1-like	Inhibition of Na^+ reabsorption
Cortical collecting duct	D_1-like	Inhibition of Na^+ reabsorption
	D_2-like	Inhibition of vasopressin action
Sympathetic ganglia/ endings	D_2-like	Inhibition of NE release
Heart	D_4	Unknown

NE, norepinephrine; E, epinephrine.

Figure 3: Distribution and function of peripheral dopamine receptors [25].

2.2.2 Pathophysiological role of DRD2

Four major neuronal systems of the brain use dopamine as the principal neurotransmitter to modulate via the several dopamine receptor subtypes locomotor behavior (nigrostriatal system), motivated behavior (mesolimbic system), learning and memory (mesocortical system), and the release of prolactin (tuberoinfundibular system) [40], [38]. Studies in DRD2 knock-out mice revealed the physiological role of DRD2. It plays an important role in adaptive functions that improve fitness, reproductivity, success and survival as well as in motor coordination, locomotor activity, executive planning, motivation or aversion and social dominance [38]. The DRD2 is also involved in the reward system and the regulation of food intake [38] and influences the preference for alcohol [40]. Also the involvement in insulin secretion and β-cell proliferation could be shown recently [39], [38]. Beside other regulatory systems the DRD2 influences also the learning from negative prediction errors [41] and bad outcomes [42] as well as the immunoregulation of T-cells [43].

Although the increased knowledge about the physiological function of each dopamine receptor subtype, relating dopamine receptor function to psychological disorders and distinct diseases is still challenging. Complicated by the fact that activation of these receptors produces a wide range of functional responses which are also dependent upon the activity state and localisation of the dopamine receptors. Additionally the lack of absolutely selective agonists and antagonists for each receptor subtype hampers further investigations about distinct contributions of each receptor subtype to different disorders.

Despite all these bottlenecks there is reliable evidence for the involvement of DRD2 in several psychological disorders [49] and diseases [27]. The first association people normally have is the relation between dopamine and Parkinson's disease. In fact, the death of dopaminergic neurons in the striatum and therefore the loss of presynaptic DRD2 receptors plays a crucial role in the progression of this disease [27], [37], [49]. On the other hand hyperactive dopaminergic signal transduction presumably through DRD2 and its dimers as well as mutated DRD2 in the central nervous system is associated with the pathophysiology of schizophrenia (the dopamine hypothesis) [44]- [48]. Alterations of DRD2 density and DRD2 dysfunction in general seem to have a bearing on the pathogenesis of ADHD (Attention-Deficit Hyperactivity Disorder) [27], [50], [52] and substance abuse [27], [51] and may contribute to some symptoms of Huntigton's disease [56]. Due to the involvement of the DRD2 in the rewarding system and the learning from good and bad outcomes, mutations, the ratio of splice variants and dysfunctions of DRD2 confer to vulnerability to substance abuse and alcoholism [40], [41], [53]. Also psychological disorders like bipolar disorder [49], [44] and impulsive disorder [41] are related to mutations in the DRD2 gene. The TaqI A polymorphism which alters DRD2 expression levels in the striatum could be associated with the risk for obesity and substance abuse [52], [54], [55].

Altered immunoresponse was reported in Parkinson's and Schizophrenia patients [43]. There are also some hints, that DRD2 dysfunction may lead to glucose intolerance, as patients showed glucose intolerance after prolonged treatment with neuroleptic drugs (DRD2 agonist) [39]. As the DRD2-DRD1 dimer plays a crucial role in the maturation, differentiation and growth of striatal neurons alterations in the expression of both receptors may also influence the dimerisation. Therefore altered dimerisation may affect cognition, learning and memory as well as being at the origin of diseases like schizophrenia, Parkinson's Disease, depression and drug abuse [57], [58].

The contribution of DRD2 in so many different diseases accounts for its importance as drug target. In 2007 the DRD2 alone was targeted by 40 distinct approved drugs [23]. But still there are no absolutely selective drugs for the dopamine receptor subtypes but only pharmaceuticals with different affinities [46], [59]. Therefore medication with dopamine agonists or antagonists still causes a lot of undesirable side effects like extrapyramidal or endocrine symptoms [49] or glucose intolerance [39] or even influences decision making [41]. So there is still a lot of potential for new drugs targeting the DRD2. Some basic approaches are already in discussion in the literature, like the use and development of bivalent ligands [48] to address the dopamine receptor dimers or to target the β-arrestin signaling pathway [60].

2.3 Bottlenecks in membrane protein synthesis and ligand screening

As shown above membrane proteins and especially GPCRs are of a tremendous interest for medicine and the pharmaceutical industry. To study the physiology and pathophysiology as well as the potential as new drug targets it is necessary to produce these proteins in a large scale in their physiological conformation in a cheap, stable and easy to handle format. The most common way is still the cloning of the gene of interest and subsequent overexpression of the protein of interest in cell cultures. However this method has some widely known limitations: It is difficult or even impossible to express proteins which are modified e.g. with radioactive labelled amino acids or - even worse - which are toxic for the host cell. Problems may also arise due to aggregation and degradation of the produced proteins in the host cells [61]. Especially the expression of membrane proteins is difficult because the insertion of many membrane proteins into the cell membrane of the host cells is critical. One problem is the lack of transport mechanisms for the insertion of the large amount of over expressed membrane proteins into the cell membrane. As the membrane proteins need the hydrophobic environment of the cell membrane for folding into their active conformation this insertion is crucial to obtain functional membrane proteins. If the membrane proteins are incorporated into the cell membrane they often have channel-forming or transport activities and influence the metabolism of the cell. These

properties of membrane proteins often lead to stress or even toxicity for the host cells. In consequence of these effects a strong selection against high-expressing clones occurs which results in low expression yields. On the other hand the specific cell physiology of the host cells effects the expression of the protein of interest. Differences in posttranslational modification processes, codon usage or the prevalent reducing environment are important factors for successful protein expression [62]. These differences often lead to insufficient amounts of expressed target protein or even to incorrect folded or truncated proteins. Furthermore the high complexity of most biological membranes and the host cells makes it difficult to investigate the protein of interest without any side effects or cross talk in signal transduction. These limitations in accurate signal detection and the often low concentration of the protein of interest in the cell membrane necessitate complicate isolation procedures. After the overexpression in cell lines, the proteins need to be extracted with the help of detergents from the native cell membrane, purified and subsequently reconstituted into the bio-mimetic membrane surfaces for further studies of function and structure or the use in biosensing and screening applications. This process is time consuming and often the membrane proteins loose their functional integrity during this process [71]. As the study of membrane proteins is still challenging [72] and there is often a lack of reproducibility the cell-free biosynthesis of proteins has become an attractive alternative for protein biosynthesis [69].

2.4 Cell-free synthesis of membrane proteins

Cell-free expression systems are already a routine technique for the production and analysis of soluble proteins. During the last decade they also have become more and more an effective tool for the production of membrane proteins for structural and functional analysis.

2.4.1 Cell-free expression systems

Cell-free protein biosynthesis systems are based on cell lysates derived from different cell types. The most commonly used systems are produced from *Escherichia coli*, wheat germ embryos, rabbit reticulocytes or insect cell lines [73]. These lysates include all macromolecular components (ribosomes, tRNAs, aminoacyl tRNA synthethases, initiation, elongation, and termination factors) for the translation reaction [64]. The translation machinery of a cell is normally able to produce proteins from all kinds of mRNA templates as long as their ribosome binding side is compatible with the ribosomes. This qualifies the *in vitro* synthesis of proteins to be annotated as a generic platform, on which virtually any protein can be synthesised, even the structure-function-sensitive membrane proteins. Therefore all genes which shall be expressed

in a cell-free expression system require a ribosome binding side which is compatible to the ribosomes in the lysate [61]. Additionally to the lysate the cell-free expression systems contain ions (buffer), energy sources like ATP or GTP, an energy regeneration system, amino acids, the four ribonucleoside triphosphates, and cofactors to perform protein synthesis.

In coupled (transcription and translation) cell-free expression systems a prokaryotic phage RNA polymerase is combined with the cell lysates which transcribes the DNA template (plasmids or PCR products) into mRNA Fig.4a. Therefore the DNA templates require an appropriate promoter (T7, SP6 or others) for the RNA polymerase [64]. For an efficient protein synthesis DNA templates must also contain a translation initiation signal such as a Kozak (eukaryotic systems) or a Shine-Dalgarno (prokaryotic systems) sequence and a translation and transcription termination region [65].

An alternative to the cell lysate based cell-free expression systems is the PURE (protein synthesis using recombinant elements) system [85]. In this system nearly the complete translation machinery is reconstituted from recombinant proteins produced from conventional expression in *E.coli* and subsequent purification. The ribosomes are also purified from *E.coli*. However the protein yields are lower than for the lysate based systems, this system is used for analytical scale production of proteins. The well defined conditions of this system are advantageous especially for the study of folding pathways and translation kinetics [73].

2.4.2 Advantages of cell-free protein synthesis

Cell-free protein synthesis has emerged as a feasible method to overcome the obstacles linked with the over-expression of proteins in cell lines. One indispensable advantage of these expression systems is the possibility to synthesise proteins which are toxic for living cells like membrane proteins. The open nature of the system allows the easy modification of the reaction conditions. Therefore the modification of proteins with unnaturally modified or isotope/fluorescent-labelled amino acids [74] can be performed at high rate and specificity of incorporation [63]. Combined with the higher purity of the cell-free synthesised proteins (only the added DNA template is expressed) this labelling strategy results in a lower background in analytical applications.

The open nature also offers multitudinous possibilities to adapt the expression conditions to the protein of interest. Thus it was possible to increase the overall protein yield of these systems. Additionally the limited yields of one compartment batch reactions due to the rapid depletion of precursors and accumulation of inhibitory by-products were overcome by the development of continuous exchange strategies Fig.4b. In this mode the reaction mixture is connected by a

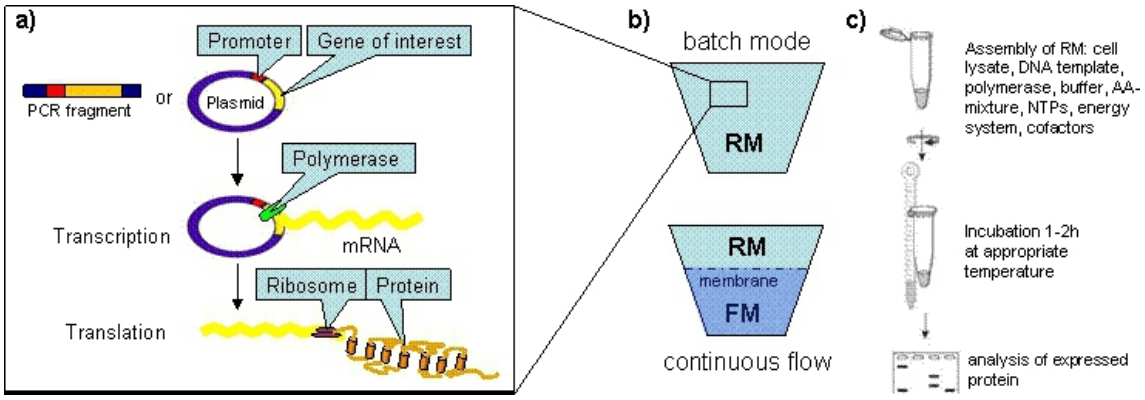

Figure 4: Cell-free expression systems: a) Cell free expression reaction in a coupled system. First the DNA template is transcribed into mRNA by a phage RNA polymerase. This mRNA is subsequently translated into the protein of interest. b) The cell-free protein expression can be run in two different modes. In the batch mode all components are added at the beginning in one vial. In the continuous flow mode the RM is coupled to a FM via a permeable membrane. This allows the continuous supply of the RM with precursors and the removal of inhibitory by-products from the RM leading to longer reaction times and therefore higher yields. c) General protocol for cell-free expression kits; RM = reaction mixture; FM = feeding mixture; AA = amino acids; NTPs = nucleoside triphosphates

semipermeable membrane to a feeding mixture providing a reservoir of precursors like nucleoside triphosphates, energy sources and amino acids [73]. These optimizations made the cell-free expression feasible for high-yield expression of proteins.

Due to the fact, that the cell-free expression system still contains all essential components for protein synthesis, the expressed proteins fold immediately into their appropriate tertiary structure and even post-translational modifications such as glycosylation or phosphorylation can take place in the eukaryotic cell-free reactions [70], [81].

It was demonstrated for several membrane proteins including GPCRs that the addition of mild detergents [83] and co-expression of apolipoproteins in combination with lipids could facilitate the folding of the expressed proteins [72], [73], [75], [84]. Even membrane proteins which are synthesised as precipitates showed a better solubility with mild detergents and functionality in contrast to membrane proteins from cell based systems, where they often build insoluble aggregates and inclusion bodies [65].Those cell-free expressed and solubilised membrane proteins can subsequently be reconstituted into liposomes [71], [76]. Synthesised membrane proteins can also directly be inserted into an hydrophobic environment provided by added membraneous lipid structures as microsomes or liposomes during expression [65]- [67]. This should lead to a prevalent inside out orientation within the lipid vesicles which significantly facilitates functional assays [73]. Recently new strategies for solubilising membrane proteins using amphipols emerged [77]. These amphiphilic polymers may become interesting alternatives for detergents. Their common structure provides a hydrophilic backbone making them water-soluble with hydrophobic chains for engaging membrane proteins. These strategies Fig.5 permit solubility and alleviates the correct folding of membrane proteins. Also the direct incorporation of a GPCR into a tethered lipid bilayer by *in vitro* synthesis has been reported [94].

2.4.3 Applications of cell-free produced membrane proteins

The successful production of membrane proteins in cell-free systems with good yields and serviceable purity, homogeneity and integrity [73] opened up new possibilities in proteomic research [82].

Especially the easy labelling of membrane proteins during cell-free synthesis and the resulting low background promotes their use in structural characterisation by NMR [73], [75], [78], [80] even directly from the reaction mixture without further purification [82].One remaining bottleneck in NMR analysis of membrane proteins is their structural complexity and flexibility and the required hydrophobic environment which often avert clear peaks in the spectra [73]. Also a first 3D crystal structure of a cell-free produced membrane protein has been reported [79]. But crystallisation of membrane proteins remains challenging [72]. Further methods used in

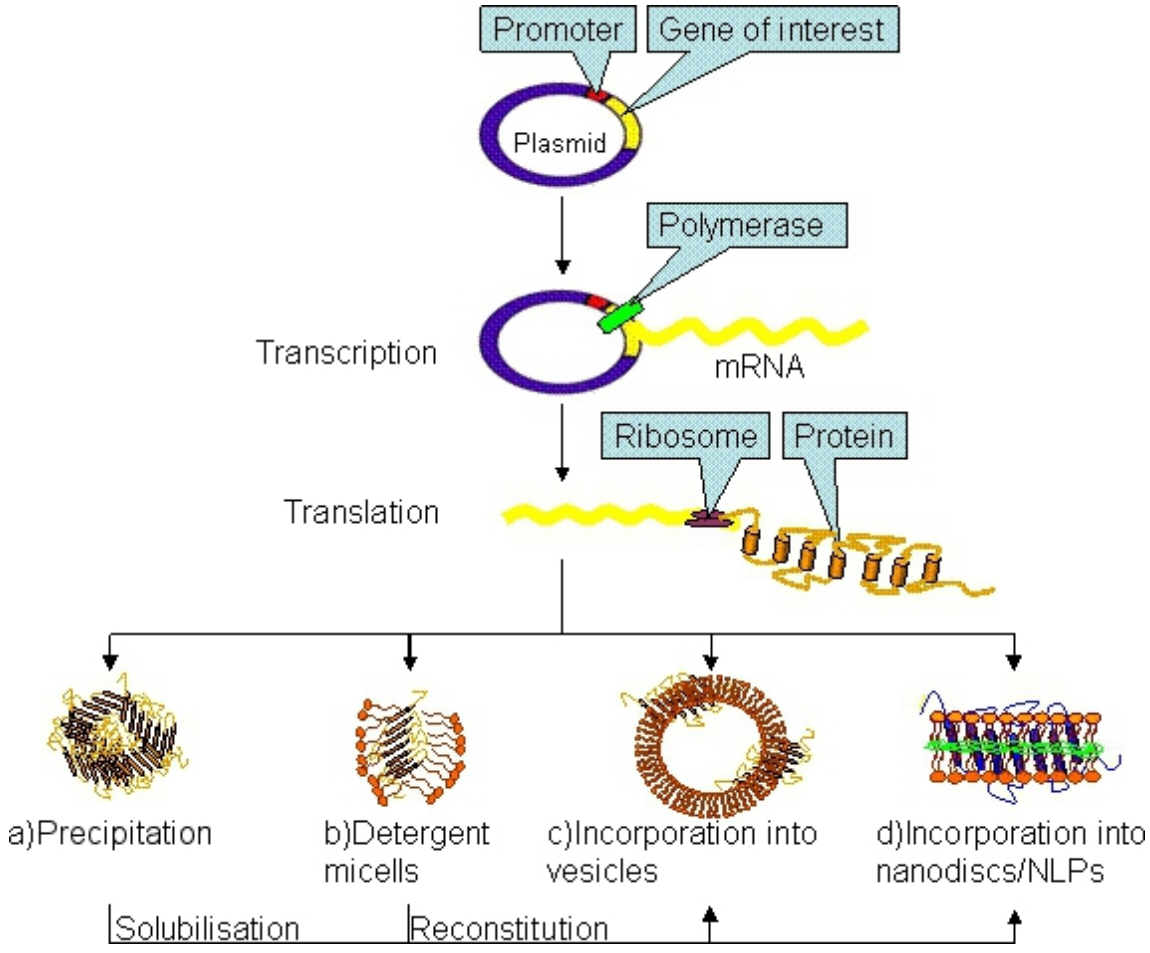

Figure 5: The cell-free protein expression systems allow the production of membrane proteins in soluble forms. Therefore different methods are available: a) production as precipitate with subsequent solubilisation with mild detergents and reconstitution into lipid bilayers b) production in detergent micelles with subsequent reconstitution into lipid bilayers c) direct incorporation into vesicles d) direct incorporation into nanodiscs/nanolipoprotein particles (NLPs)

structural analysis of cell-free produced membrane proteins are circular dichroism and electron microscopy [73]. The simultaneous cell-free production of different membrane proteins offers a new approach for oligomerisation studies [75]. But also other protein interactions can be studied by the use of cell-free protein synthesis combined with dual labelling and fluorescence cross-correlation spectroscopy [86].

The short reaction time and the multiple templates (mRNA, DNA, PCR products) compatible with cell-free synthesis make this technology appealing for the construction and screening of mutagenesis and gene libraries [81]. The produced proteins can directly be arrayed by specific trapping techniques [73]. C-terminal labelling of proteins with tetracysteine motifs which form a fluorescent complex after binding to biarsenicl ligands [87] were used for real-time monitoring of protein synthesis in cell-free extracts. This method can be used for high-throughput screening of pharmaceutical translation-inhibitors [81].

Also the functional characterisation of cell-free produced membrane proteins is within the focus of current research. Although the development of functional assays for membrane proteins is still challenging there are several successful approaches with well defined model systems. Substrate specificity and kinetic parameters of some transporters and channels have been published which correlate with the data obtained from cell based systems [73]. Also ligand binding experiments and competitive assays [62], [73] with reconstituted cell-free expressed GPCRs as well as competitive assays with directly *in vitro* synthesised GPCRs into nanolipoprotein particles (NLPs) [84] have been reported. The cell-free methods exhibit high potentials for miniaturization and high-throughput protein arrays [81]. For soluble proteins there are already several approaches published [81], [65], [88]. For protein arrays with membrane proteins the requirements for correct folding often hamper the development of an appropriate approach. For bacteriorhodopsin a functional array device has been published recently [89].

The incorporation of cell-free expressed membrane proteins into liposomes blazes a trail towards the development of artificial cells. Although it is still a long way to go the first attempts are already published [90]. But also the use of proteoliposomes for medical applications is up for discussion [76].

2.5 Advantages of bio-mimetic surfaces as platform for biosensors and screening applications

In every organism the cell membrane plays an indispensable role in the interaction of extracellular and intracellular compartments. Perceptive abilities like sense of smell, taste, vision, touch or hearing but also nerve conductivity are triggered by the biochemical signals interacting

with their specific receptors in the cell membrane. The conformational changes in the receptor molecules following binding events lead to different signal transduction pathways within the cells. The high complexity of biological cell membranes generated by a wide variety of highly specific receptor molecules allow the parallel transduction of different signals. Modern nanobiotechnology aims to mimic this principle of parallel registration by specifically biofunctionalisation of small arrays on solid surfaces like electrodes or semiconductors. These biochips or biosensors will allow the determination of bioactive molecules with high specificity at lowest concentrations. This approach will enable the easy screening of potential pharmacological active substances as well as the screening for endogenous ligands for new receptors. With improvements in reproducibility, cost reduction and stability the use of these biomimetic platforms as routine applications in genomics and proteomics is realistic.

2.5.1 The biological membrane

Biological membranes form a lipid bilayer barrier (6-10nm) in order to prevent uncontrolled exchange of intracellular and extracellular components, such as proteins, ions and metabolites. But they also allow the formation of intracellular compartments with distinct functions such as organelles or vesicles. Proteins embedded in and associated with the lipid bilayer render the strict barrier towards a selectively permeable communication platform. The individuality of each cell is obtained by the varying lipid composition of the membrane and the specific set of proteins which serve as channels, pumps, energy transducers, enzymes or receptors. The mass ratio of lipids and proteins also vary from 1:4 to 4:1 in different cell types. Carbohydrates which are linked to the lipids or proteins round off the individual 'fingerprint' of each cell Fig.6. But even for one cell the outer and inner leaflet of the bilayer membrane do not consist of exactly the same components. Due to the fluid structure of the leaflets, lipids can diffuse rapidly laterally but they do very slowly cross over into the other plane (flip-flop), whereas proteins vary markedly in their lateral mobility and do not rotate across the bilayer. Therefore biological membranes are often regarded as two-dimensional solutions of oriented proteins and lipids (fluid mosaic model [91]). The fluidity of the bilayer is controlled by the chemical properties of the membrane lipids and the lipid composition [92].

Because of the complexity of biological membranes, there is a clear need for bio-mimetic membrane platforms development, in which one or few membrane components can be isolated and studied [93].

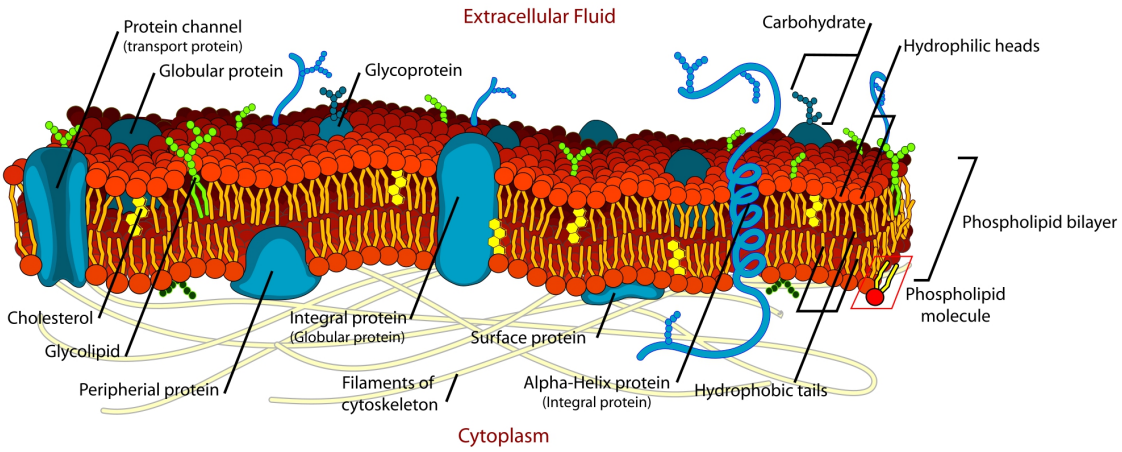

Figure 6: Schematic of a biological cell membrane (original from LadyofHats Mariana Ruiz): The core structure -the lipid bilayer- is formed by membrane lipids like phosphoglycerides, sphingomyelin and glycolipids. Those amphiphilic molecules with a hydrophilic head group and two hydrophobic acyl chains spontaneously form a bilayer structure in water. This self-assembly process is mainly driven by hydrophobic interactions. The fluidity of the membranes is determined by the length of the acyl chains, the degree of saturation of the acyl chains and the amount of cholesterol inserted into the bilayer [92]. The folding, structure and function of the integral proteins is influenced by the physical properties of the bilayer. The complex organization of the membrane accomplishes their diverse functions and biological activity.

2.5.2 Lipid based bio-mimetic membrane platforms

During the past decades a lot of effort was put on the development of different lipid based model systems (Fig.7) to mimic the biological membrane. Four major model systems have emerged to be most applicable for membrane characterisation and proteomic applications: liposomes, black lipid membranes (BLM), solid supported bilayer lipid membranes (sBLM) and tethered bilayer lipid membranes (tBLM). These well defined systems should facilitate the structural and functional study of membrane proteins which recommend an hydrophobic environment to fold into their active conformation. This approach also affords the use of surface sensitive techniques for characterisation of the membrane proteins which are not applicable to living cells e.g. optical or electrochemical methods.

Liposomes

Due to their amphiphilic and bulky structure most phospholipids and glycolipids favour to form bilayer structures in aqueous solutions. This self assembly process is driven by hydrophobic interactions between the acyl chains of the lipids. The resulting bilayer structure is stabilised by van-der Waals attractive forces between the hydrocarbon tails as well as by electrostatic interactions and hydrogen-bond formation between the polar head groups of the lipids and the surrounding water molecules, respectively. These non-covalent interactions lead to some biologically important properties of lipid bilayers:

- they tend to be extensive
- they strive to close on themselves to shield all hydrocarbon chains from water forming vesicular structures
- they are self-healing because a hole is energetically unfavourable

Spherical liposomes which are comprised of a phospholipid bilayer surrounding an aqueous core can be created by a number of methods which result in different sizes from tens of nanometers to micrometers [95]. Crucial for the formation of liposomes is the lipid concentration in the aqueous solution. Only when this concentration is above the critical micelle concentration (CMC) vesicular structures can form. The exact concentration depends on the properties of the lipid. The simplest method for liposome formation is the mechanical dispersion of dry lipid in water. The resulting structures are usually multilamellar vesicles (MLVs) which consist of concentric bilayers separated by narrow aqueous channels. MLVs have been employed extensively to determine details of bilayer structures. Their regular arrays of bilayers are ideally suited for X-ray studies, whereas their relatively large size (2400 nm diameter) favours structural and

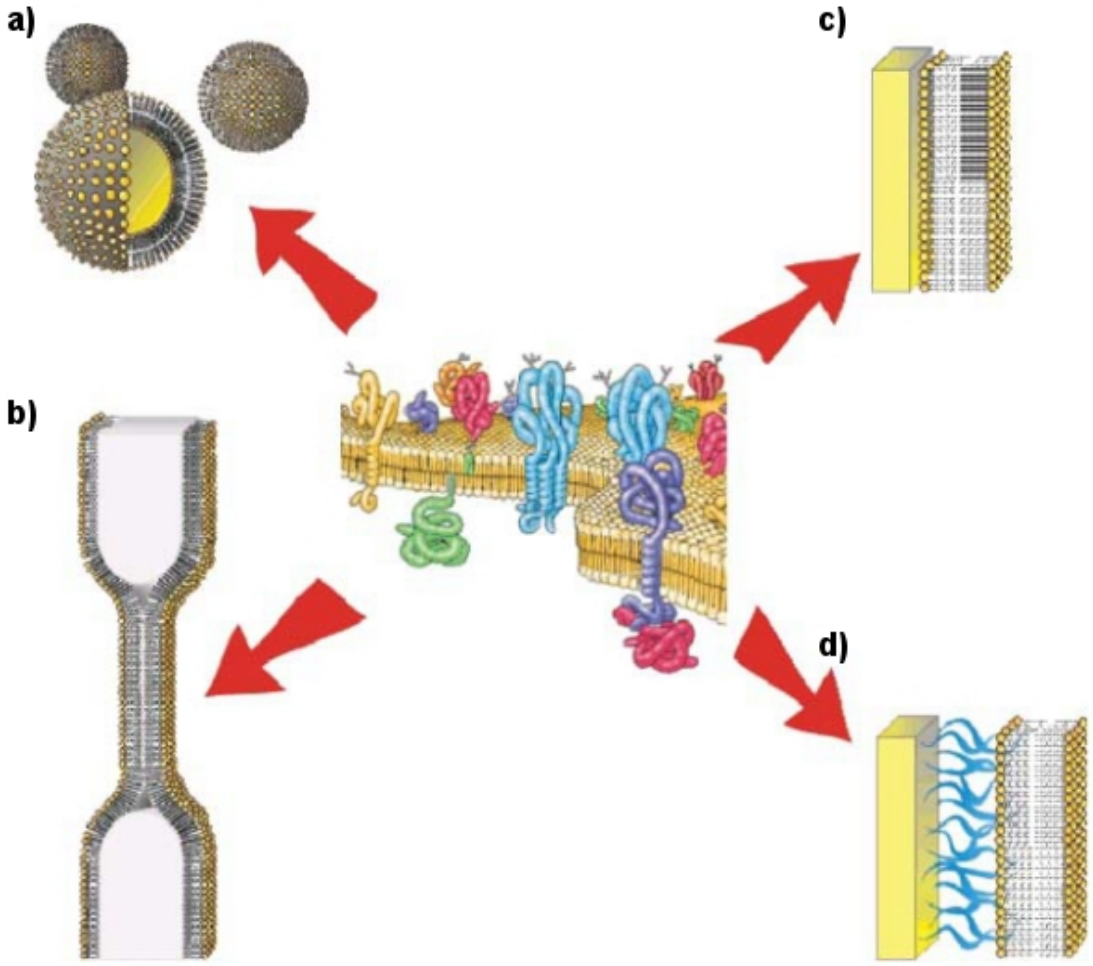

Figure 7: Schematic of bio-mimetic lipid model membranes (original from [175]). Four model systems have emerged to be most suitable for mimicking a biological membrane. a) Vesicles are mostly used to study membrane fusion processes and for drug delivery applications b) Black lipid membranes (BLMs) are useful to study electrical properties of lipid bilayer membranes but suffer from instability. c) Solid supported bilayer lipid membranes (sBLMs) provide increased stability but interactions of the solid support with incorporated proteins may alter their functionality. d) Tethered bilayer lipid membranes (tBLMs) are stabilised due to spacers which covalently anchor the inner leaflet to the support and offer a reservoir between the bilayer and the support. Therefore interactions between support and incorporated proteins are reduced. The reservoir also allows electrochemical characterisation of the membranes and channel proteins.

motional analysis using NMR compared to smaller systems [96]. On the other hand their size heterogeneity and the presence of different compartments hamper the investigation of permeability and fusion processes. To obtain unilamellar vesicles (ULVs) different methods [96] have been devised like disruption of preformed MLVs by sonication [97] or extrusion [98]. Also methods for the direct production of ULVs have emerged like some solvent evaporation procedures [99], [100], detergent dialysis techniques [101] or extrusion in combination with several freeze-thaw-cycles [98]. The extrusion of the formed vesicles results in a homogene size distribution of the vesicles in solution. The ULVs can be sub-divided according to their size into three groups: small unilamellar vesicles (SUV, Ø$\leq$100nm), large unilamellar vesicles (LUV Ø100nm-1μm) and giant unilamellar vesicles(GUV Ø$\geq$1μm).

Liposomes are rather fluid entities with dynamic properties. Different lipid compositions and the relatively easy manipulation of properties lead to a wide range of morphologies. This diversity, the possibility to enclose and protect many types of therapeutic biomolecules, the lack of immunogenic response, low cost and fast production, and their differential release characteristics give rise to their use in analysis, cosmetics, food technologies as well as encapsulation and delivery of drugs and DNA [102]. Liposomes are also suitable formats for the reconstitution of membrane proteins yielding higher protein densities compared to native membranes for subsequent characterisation. LUVs and GUVs can be used in fluorescence microscopy allowing the study of transport processes across the membrane or mediated by channel or pore-forming proteins using fluorophores [103]. Whereas the measurement of ion currents caused by ion channels is only possible with patch-clamp measurements in giant vesicles [105]. Also the mobility of lipids and proteins within the bilayer can be analysed by fluorescence correlation spectroscopy [104].

For array applications liposomes can be immobilised on different surfaces (Au, SiO, sBLMs) with various anchoring techniques (oligonucleotides, biotin-streptavidin binding) [106].

Liposomes are easy to prepare and suitable model systems for flux measurements, functional reconstitution of membrane proteins and the study of some membrane properties like phase separation and lipid mobility. However, they also have some shortcomings. Their inner compartment is small and inaccessible to chemical manipulation and electrical measurements. To overcome these problem several planar lipid bilayer systems have been devised.

Free standing bilayer lipid membranes

The first free standing bilayer lipid membrane was reported in 1962 by Paul Müller and Donald O. Rudin [107]. Their method of preparation is still one of the simplest techniques. A 1% lipid solution, mostly phospholipids or oxidised cholesterol in an organic solvent [107], [108],

is painted onto an aperture (hole with typical diameters of about 100µm in a teflon or polyethylene cup or thin teflon or silicon foil) separating two aqueous compartments. Today several preparation techniques [109] are available including Langmuir-Blodgett [106] and a solvent free method [110]. The formation of the lipid bilayer in the aperture can be observed with a microscope. The colour of the lipid layer changes as its thickness changes. Therefore in the beginning the relatively thick lipid film appears gray, then shows intensive rainbow colors as thinning occurs ending in a black colour as the bilayer is formed [109]. The black colour is caused by negative interference of the reflected light at the two lipid/water interfaces. Thus these free standing bilayer lipid membranes are often referred to as black lipid membranes (BLMs). Today these BLMs are an established model system in membrane biophysics allowing studies of ion channels and their ion current across the bilayer. The BLMs offer controlled compositional and environmental parameters, such as protein concentration, ion strength, pH and electrical field combined with the electrical and physical properties of a native membrane. The experimental setup easily allows the acces of both sides of the membrane making it favourable for electrical measurements as well as structural characterisation by x-ray analysis [111]. One major shortcoming of the BLMs is their limited lifetime due to their high susceptibility to mechanical vibrations. Recently a promising approach to overcome this inherent stability has been published. Malmstadt and coworkers devised a hydrogel encapsulated BLM [112](HEM). These HEMs showed higher stability compared to the traditional BLMs while still supporting the measurement of incorporated pore proteins at single-channel resolution [112]. Several researchers also proofed this concept for their applications making it a promising platform for portable molecular sensing elements. Another approach towards more stability is the use of different nanoporous supports, such as anodised alumina or silicon devices with customised properties [124], [125], [126].

Solid supported bilayer lipid membranes

Another approach to more stable planar bilayer lipid membranes is the strategy to deposit or attach them to a solid support. These solid supported bilayer lipid membranes (sBLM) allow the use of a wide range of surface sensitive techniques such as total interference fluorescence, NMR, FT-IR spectroscopy, surface plasmon resonance, quartz crystal microbalance, and neutron reflectivity [113] to study membrane characteristics or protein-membrane interactions.

SBLMs can be generated by vesicle fusion [114] or Langmuir-Blodgett-transfer [115], [116] on hydrophilic surfaces such as silicon, silica, quartz or mica. These planar membranes permit lateral fluidity and good electrical sealing properties. Substrates with electrical conductivity such as metals or metal oxides (Au, Indium Tin Oxide (ITO))may be used as electrodes allowing electrochemical measurements but reducing the lateral mobility of the lipids or even preventing direct vesicle fusion (aluminum oxide, titanium oxide) [93]. But all those architectures also bear another problem. Due to the direct physisorption of the bilayer on the substrate there is only a very thin water film between the bilayer and the supporting substrate. This close proximity hampers the functional incorporation of integral membrane proteins into sBLMs. The proteins may show altered function or degradation and loose their lateral mobility [117] due to the interaction of substrate-exposed domains with the hydrophilic substrate.

To circumvent this problem different constructions of sBLMs spaced out from the surface have been developed. These tethered bilayer lipid membranes (tBLMs) are attached to spacer molecules or layers which intercalate between the substrate and the bilayer. The additional space gained results in a non-denaturing environment as well as an ion reservoir beneath the membrane and, in consequence, improved conditions for the study of membrane proteins. In the literature several structural concepts for tBLM-formation can be found [93], [106], [121]:

- cushioned bilayer lipid membranes (cBLMs): polymers, hydrogels or peptides are adsorbed to the substrate prior to bilayer deposition [93], [118]
- tethered bilayers using functionalised lipids: lipid head groups are chemically coupled to spacer molecules which exhibit an end group which can bind to the substrate. These functionalised lipids form a self-assembled monolayer (SAM) on the substrate [93] as scaffold for bilayer formation.
- SAMs of spacer molecules as scaffold for subsequent bilayer formation [120], [123]
- protein tethered bilayers: Membrane proteins are anchored to the substrate via his-tag or biotin-streptavidin coupling. Subsequent addition of lipid/detergent solution leads to the formation of a lipid bilayer around the proteins [93], [122]

- deposition of vesicles containing directly the anchor molecule onto activated substrates [93], [119]

The molecular diversity resulting from the various preparation methods for supported lipid bilayers allows to envisage the reconstruction of various protein environments. The choice of substrate and spacer molecule or layer is determined by the surface techniques which will be used for characterisation and by the substrate properties that are required for the selected analysis method. The chosen substrate and tether assign the assembling strategy. Noble metals (gold, silver) are commonly encountered for surface plasmon resonance (SPR) monitoring and electrochemical methods while transparent surfaces (silica, quartz, glass) are necessary for optical techniques. Atomically flat surfaces (mica, silicon, flat gold) being candidates for atomic force microscopy (AFM) imaging [121]. Certain techniques such as quartz crystal micro-balance with dissipation (QCM-D) permit a wider panel of substrate nature to be used [93].

2.5.3 Block-Copolymer based bio-mimetic membrane platforms

As shown in the last paragraph a lot of progress was made in the use of lipid based membrane systems as models of biological membranes. However there are still some bottlenecks in the use of these systems. Their relative membrane instability, difficulties in reproducibility especially for the incorporation of membrane proteins and the challenging chemical modification of lipids encouraged the search for alternative materials. One promising class of molecules are amphiphilic block copolymers (Fig.8).

These synthetic polymers consist of at least two blocks with different solubility [127]: one hydrophilic and one hydrophobic block. Due to this amphiphilic structure they, like lipids, self assemble in aqueous solutions into various superstructures like micelles and at higher concentrations into different lyotropic liquid-crystalline phases (Fig.9).

The assembling process is driven by hydrophobic interactions [131] leading to a hydrophobic core surrounded by a hydrophilic corona [128]. The resulting shape and structure of the aggregates is not only determined by thermodynamic and kinetic aspects, but also influenced by numerous parameters like the initial concentration of block copolymer, molecular properties and geometrical constraints of the polymers themselves (e.g. chain length, polydispersity) as well as the preparation method (temperature, solvent, additives like ions or surfactants) and the assembling mechanism [129]. For amphiphilic block copolymers similar trends for tuning the shape of aggregates as for small amphiphiles and lipids could be observed: decreasing of the hydrophilic block size at constant hydrophobic chain length changes the shape of the aggregates from micelles to tubular micelles and finally to vesicles [147]. For small amphiphiles the

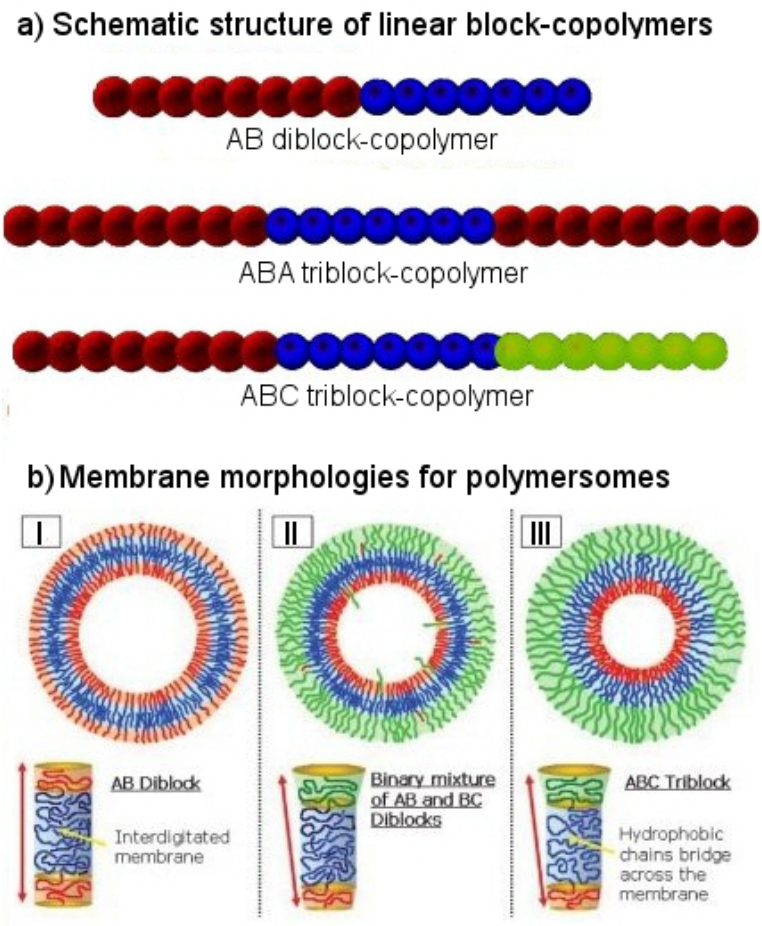

Figure 8: Schematic of the structure of amphiphilic block-copolymers used for bio-mimetic membrane structures. a) Types of linear block-copolymers. AB or BC diblock-copolymers as well as symmetric ABA or asymmetric ABC triblock-copolymers can be used for the formation of bio-mimetic membranes. Hydrophobic blocks are symbolised by blue spheres. Red and green spheres are used for hydrophilic blocks. b) Morphologies for block-copolymer membranes [161]: I) Diblock copolymers form bilayer-membranes. Depending on the hydrophobic block length the degree of interdigitation and entanglement within the hydrophobic core varies. II) Polymersomes prepared from a mixture of AB and BC diblock-copolymers show separation of the different block-copolymers according to their hydrophilic block length. III) Triblock-copolymers form monolayer membranes. The hydrophobic middle block builds the hydrophobic core of the bio-mimetic membrane. Asymmetric triblock-copolymers form asymmetric membranes due to the different block length of the hydrophilic blocks.

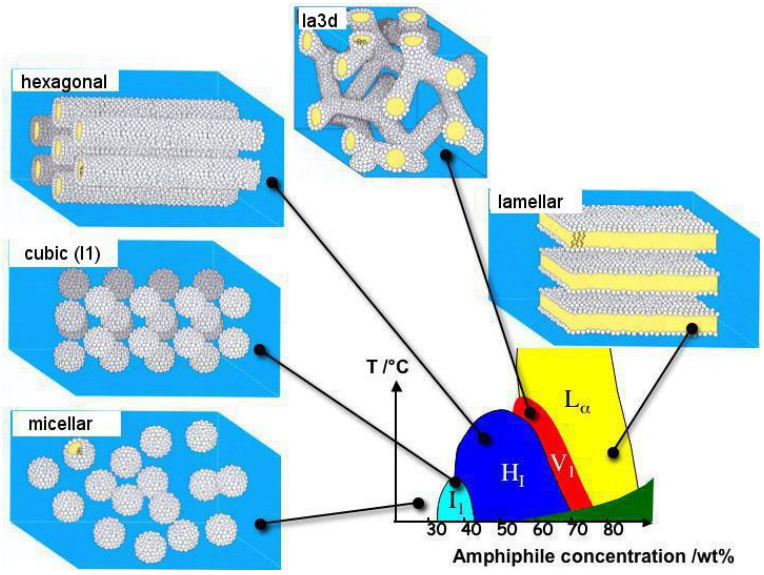

Figure 9: Schematic of the aggregation of amphiphiles into micelles and then into lyotropic liquid crystalline phases (cubic, hexagonal arranged tubular structures, bicontinuous cubic phase and lamellar) as a function of amphiphile concentration and temperature (original from http://en.wikipedia.org/wiki/File:Lyotropic1.jpg#filelinks).

shape can be determined by the size of the hydrophobic group which is described by the packing parameter [129]. For the high molecular weight block copolymers the use of the volume or weight fraction f of the hydrophilic block is more convenient. This parameter determines the curvature of the resulting hydrophilic-hydrophobic interface and therefore the resulting shape of the aggregates Fig.10, [130, 161]. So far, experienced data for block copolymers showed, that block copolymers with $f > 45\%$ tend to form micelles or with $f \approx 35\%$ polymersomes whereas those with $f < 25\%$ are expected to form inverted structures [129].

However, the obtained morphology does not only depend on the geometrical aspects represented by the weight fraction f but also on the minimisation of the free energy. The free energy relies on the interfacial energy of the hydrophilic-hydrophobic interface as well as the loss of entropy of the polymer chains during aggregation [130]. Which of these effects mainly determines the morphology of the aggregates differs according to the wide variety of chemical structures for block copolymers. Therefore there is no valid theory for the prediction of the morphology of polymeric aggregates but the predicted morphology still has to be verified after the formation procedure. Furthermore not only the shape of the aggregates differ according to the molecular properties of the block copolymers, but also the structure of the formed bilayers. Low-molecular weight diblock copolymers tend to form bilayer structures like lipids, whereas the longer hydrophobic chains of high-molecular weight diblock copolymers are likely interdig-

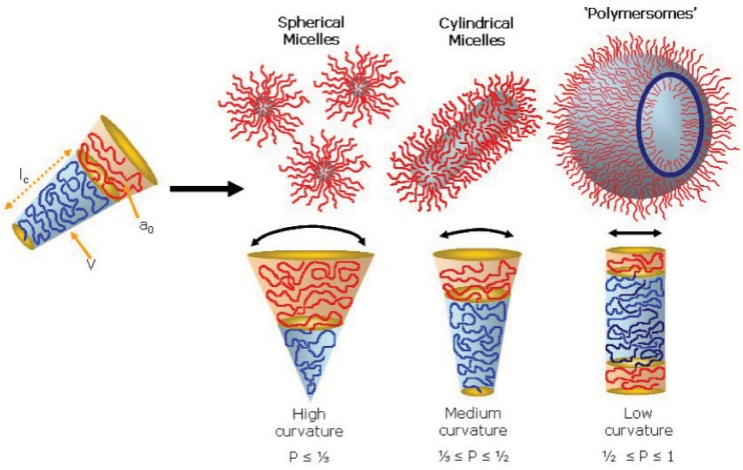

Figure 10: Schematic of the aggregation of block copolymers into various structures due to the inherent curvature of the molecule. Here the curvature is determined by the packing parameter $P = \frac{v}{a_0 l_c}$ (v: volume of hydrophobic chains; a_0: optimal area of hydrophilic head group and l_c: length of the hydrophobic tail) which is used for smaller amphiphiles. (original from [161]).

itated and entangled [135]. This entanglement increases the bending rigidity of the membranes but on the other hand also decreases the lateral membrane fluidity [129, 135]. The limited mobility of the polymer chains obstructs the dissolution of the membrane by detergents [129], and this increased viscosity has two main effects on pore formation within polymer membranes. It considerably increases the energy barrier for pore formation within the membrane by incorporation of pore forming peptides or membrane proteins. But on the other hand pores once formed in the polymer membranes exhibit a longer lifetime than in lipid membranes [137]. Triblock copolymers normally form monolayers [134].

Due to the higher molecular weight of their building blocks, compared to lipids, block copolymer membranes exhibit a greater mechanical stability towards areal strain and bending [127, 130,133] and an increased membrane thickness (≈5-30nm depending on the hydrophobic block length) [130, 135]. This stability can be further enhanced by a certain extent of cross-linking of the block copolymers [130, 137]. The increased membrane thickness also influences the permeability of the membrane. Discher et al. showed, that polymer membranes have a lower permeability to water and low-molecular-weight solutes than common lipid analogues [130, 132]. The permeability can be adjusted by changing the molecular weight and chemical structure of the hydrophobic block [135], by the use of block copolymers containing heteroatoms like oxygen, silicon or sulfur in their hydrophobic blocks [129] or by the incorporation of stimuli-responsive block copolymers to trigger permeability with stimuli like light, temperature, pH or oxidation/reduction [152]. Also the incorporation of pore or channel forming peptides, den-

dritic esters and membrane proteins can be used to specifically alter the permeability of the membrane [130]. The increased membrane thickness leads to a size mismatch with membrane proteins, as the architecture of their hydrophobic parts is optimised for the hydrophobic thickness of natural lipid membranes. Despite the mismatch of membrane thickness and protein sizes the successful reconstitution of active membrane proteins into polymer membranes was demonstrated [141]. Most of these membrane proteins were pore forming or channel proteins. But also more complex membrane proteins like bacteriorhodopsin [173], the F_0F_1-ATP synthase [155] or the NADH-ubiquinone complex [142] have been successfully reconstituted. Most reconstitution experiments so far have been done in triblock copolymer membranes with PDMS as the hydrophobic block [130, 141]. The extremely flexible hydrophobic blocks of the polymers seem to allow the block copolymer membrane to adopt the specific geometrical and dynamical requirements of the membrane proteins to remain their functionality [130]. This adoption is achieved by two mechanisms [142]:

- the compression of the hydrophobic block in the vicinity of the incorporated membrane proteins Fig.11 [143]and
- the local segregation of block copolymers with shorter chains around the protein [143, 144]

The compression is a special feature of the polymer membranes. Lipid membranes are due to their low number of possible configurations of their hydrophobic parts within the bilayer structure nearly incompressible and therefore can not adopt to the size of membrane proteins [130]. The hydrophobic chains of polymers on the other hand are in an unfavourable, stretched conformation in polymer membranes. Therefore, the compression in the vicinity of the membrane proteins decreases the stretching energy which facilitates the protein incorporation [146]. This compression was demonstrated in simulation studies upon pore incorporation into block copolymer membranes [145]. These simulations also pointed out, that the hydrophilic corona may obstruct the incorporated channel proteins and shield them from the bulk solution Fig.12. The degree of obstruction depends on the hydrophilic block length and flexibility and may reduce the activity of the incorporated membrane proteins [129, 145].

Using NADH-ubiquinone complex reconstituted into ABA-triblock-polymersomes Meier and coworkers recently demonstrated, that the activity of a reconstituted membrane protein can also be modulated by the respective sizes of the hydrophobic and hydrophilic blocks [142]. The use of asymmetric ABC triblock copolymer membranes revealed a favoured orientation of reconstituted membrane proteins, whereas symmetric ABA triblock copolymer membranes showed statistical orientation of reconstituted membrane proteins [140]. Experimental studies also showed, that the quantitative reconstitution of membrane proteins in polymer membranes

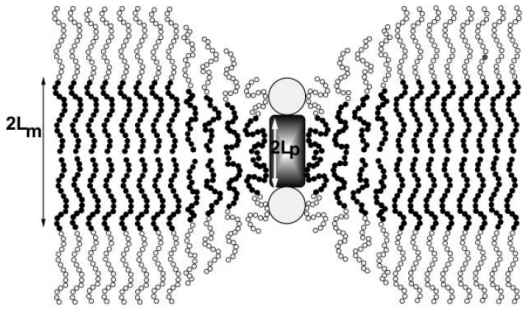

Figure 11: Schematic of the incorporation of membrane proteins into block copolymer membranes. In the vicinity of the membrane protein the hydrophobic blocks of the polymer are compressed. In the unperturbed flat bilayer the polymer chains are highly stretched. This compression allows for the membrane protein to incorporate into the polymer membrane in spite of a thickness mismatch [143]

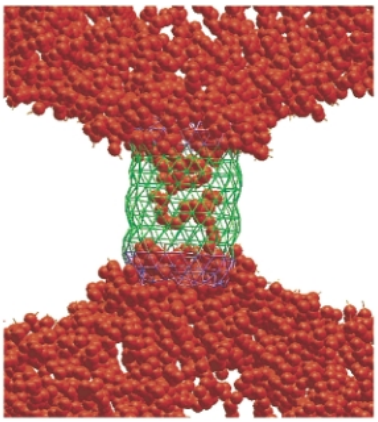

Figure 12: Simulation snapshot of a channel protein, incorporated into a block copolymer membrane. The hydrophobic blocks have been removed. A hydrophilic corona enters the channel and thus affects water diffusion. [145]

depends on the nature of the protein as well as on the nature of the polymer [141]. But still the underlying mechanism of protein reconstitution into polymer membranes is far from being solved. Therefore the optimum ratio of protein to polymer concentration for efficient reconstitution has to be determined experimentally for every membrane protein and polymer membrane.

Another advantage of block copolymers as building blocks for bio-mimetic membranes is obvious: their synthetic nature offers a great versatility in terms of chemical nature, flexibility and interaction allowing easily the tuning of membrane morphologies and properties [130] being in accordance with the recommendations of the membrane protein of interest. Owing to their favourable properties and their lipid-like behaviour in aqueous solutions block copolymers have emerged as a promising alternative to mimic biological cell membranes.

Polymersomes

Like lipids, di- and triblock copolymers form vesicular structures in diluted aqueous solutions. However, they have a lower critical micelle concentration (CMC) which in a better resistance against dissolution. The CMC can be controlled by the chemical structure of the block copolymer and pushed to extremely low limits due to the high diversity in block copolymer chemistry. Those spherical polymer membranes enclosing an aqueous compartment are commonly named polymersomes in analogy to their lipid based relatives, the liposomes. Owing to their preparation from block copolymers they also exhibit all the properties common to polymeric membranes addressed in the last paragraph. Depending on their macromolecular parameters (like structure, composition and molecular weight of the polymers) and the preparation method (solvent switch, rehydration, electroformation, bulk rehydration [130, 146, 147]) those polymersomes can be formed with diameters ranging from 50nm up to approximately 100µm [127]. Like the liposomes they are also divided into small (Ø$\leq$100nm), large (Ø100nm-1μm) and giant (Ø$\geq$1μm) polymersomes. Especially the molar mass of the polymers and the polydispersity of the hydrophilic block play an indispensable role on the size and size distribution of polymersomes. It has been demonstrated [136], that polydispers diblock copolymers segregate upon polymersome formation according to their hydrophilic chain length with the shorter ones on the inner leaflet and the longer ones on the outer leaflet of the bilayer. This segregation results in a lower curvature energy of the polymersomes and the formation of an asymmetric bilayer membrane. This phenomenon leads to the formation of smaller polymersomes with increasing polymolecularity of the hydrophilic chains [130]. The exact mechanism of vesicle formation is still under discussion. Two hypothetic mechanisms are proposed. One suggests the formation of flat bilayers from micelles or clusters prior to a change in curvature which leads to the closing of the bilayer membrane to form polymersomes [148]. This mechanism would lead to an efficient encapsulation of hydrophilic molecules from the bulk solution. The second more

complex mechanism suggests that polymersomes evolve from micelles that grow and change morphology [149]. This mechanism would result in a lower loading efficiency of hydrophilic compounds since there is no closing step for encapsulation. Anyway, encapsulation of both hydrophilic and hydrophobic compounds either in the aqueous lumen of the polymersomes or the hydrophobic core of the membrane have already been reported [139]. Brown et al. recently suggested a new preparation method for polymersomes to enhance the encapsulation efficiency. They used a microfluidic device to induce self-assembly upon deprotonation of diblock copolymers by changing the pH of the flows within the microchannels [170].

Also post-functionalisation of the outer polymersome corona with biological conjugates, chemical compounds, target molecules like ligands or antibodies for cell targeting or even enzymes is possible [129, 139, 141]. This functionalisation of polymersomes Fig.13 in addition with controlled permeability and release of entrapped compounds make them potential candidates for biomedical applications and the use as nanoreactors.

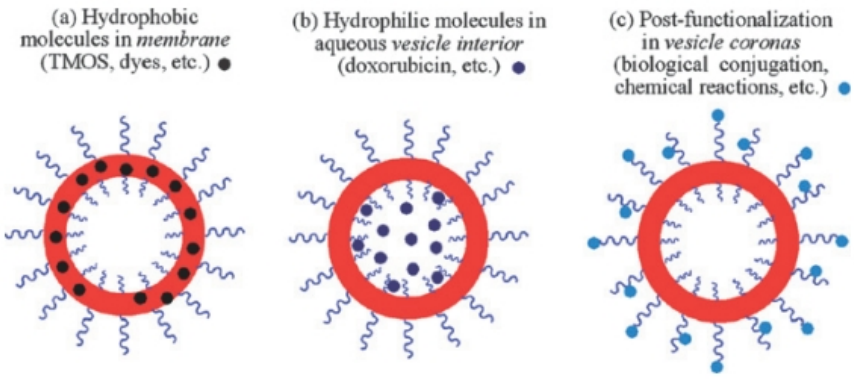

Figure 13: Possible functionalisation strategies for polymersomes. a) entrapped hydrophobic molecules in the hydrophobic core of the membrane b) encapsulated hydrophilic molecules in the aqueous lumen of the polymersomes c) functionalisation of the outer shell of the polymersome with biological conjugates, chemical entities, target molecules like ligands and antibodies or enzymes. Original from [139]

For biomedical applications like drug and gene delivery or *in vivo* imaging [129, 147] the block copolymers for the formation of polymersomes must consist of at least a biocompatible hydrophilic block. More favourable would even be the use of biodegradable polymersomes. So far different synthetic or biohybrid (partly based on natural building blocks like peptides or sugars) polymers have been used [147]. The use of non-fouling polymers like poly(ethylene glycol) (PEG), dextran and poly(acrylic acid) (PAA) lead to the formation of polymersomes with strongly reduced *in vivo* and *in vitro* nonspecific protein adsorption, resulting in stealth behaviour and therefore prolonged circulation times since they are not recognised by the immune

system [150, 151]. Their enhanced stability, the possibility to control release of encapsulated molecules, by incorporation of specific pores and channels [130, 138, 139], the use of stimuli responsive polymers [152] or the formation of inherently leaky polymersomes e.g. based on PS-b-PIAT block copolymers [153] and their prolonged circulation times make them promising candidates for drug and gene delivery [129, 139, 154, 157].

Encapsulated enzymes within the aqueous lumen of the polymersomes in combination with the incorporation of channels or pores into the polymersome membrane produced nanoreactors or synthosomes [158]. Owing to the encapsulation enzymes would be protected against proteolysis and can be easily removed by size exclusion chromatography after the reaction. Educts and products of the bioreactor can diffuse through appropriate pores or channels into the polymersomes and bulk phase. Therefore synthosomes can also be used to entrap products from reactions in the bulk phase due to selective permeability of the polymersome membrane allowing selective product recovery Fig.14.

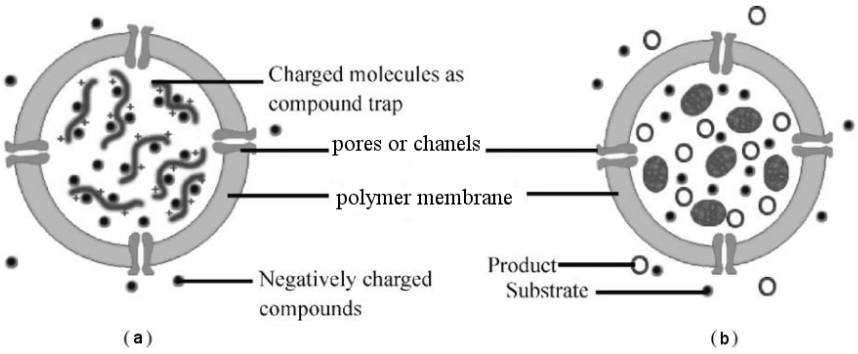

Figure 14: Synthosomes designed a) for selective product recovery. Encapsulated charged macromolecules trap charged products from the bulk phase b) as bioreactors. Encapsulated enzymes are used for selective substrate conversion in a protected environment. Original from [158]

Also their use as artificial cell organelles is in the focus of current research. Choi and Montemagno already demonstrated ATP-synthesis in polymersomes by a coupled reaction between reconstituted bacteriorhodopsin and F_0F_1-ATP synthase motor protein [155]. Meier and coworkers even demonstrated the target-specific intracellular uptake of polymersome based organelles, their biochemical functionality within target cells and their cellular trafficking [156]. Recently even more complex nanoreactors have been realised with a cascade of three enzymes. The first enzyme was entrapped in the aqueous lumen of the polymersome, the second enzyme was attached to the inner hydrophilic corona of the polymersome and the last enzyme was anchored to the outer membrane [147]. Also the further development of synthosomes not only to organelles, but to minimal cells [135, 159] or viruses [135] is under investigation.

For application of polymersomes in biosensors their immobilisation on appropriate surfaces is an essential prerequisite. One approach is the attachment of protein functionalised polymersomes to a modified surface via an anchoring effect due to biomolecules. The most well-known example is the use of the strong interaction of biotin-functionalised polymersomes with streptavidin for immobilisation [162]. Another approaches for the immobilisation of functionalised polymersomes is the use of metal-His-tag protein coupling [141].

Planar polymer membranes

As for lipid based membrane systems planar polymer films either free standing or at interfaces are of particular interest because they allow for surface studies and also allow excess of both sides of the membrane e.g. for electrochemical studies and transport studies across the membrane. Furthermore solid supported membranes exhibit an enhanced stability and permit detailed structural investigations of the membranes and their components.

Although it seems to be obvious that the amphiphilic block copolymers could be used to prepare, in analogy to BLMs, planar free-standing polymer membranes, in 2000, Meier and coworkers were the first to report the successful preparation of such **"'black polymer membranes"'** [168]. Using a PMOXA-PDMS-PMOXA triblock copolymer they yield stable giant membranes with a mean hydrophobic thickness of 10nm. Polymerisation lead, as also demonstrated for polymersomes, to a considerable mechanical stabilisation. Recently a bio-mimetic triblock copolymer membrane array has been reported. Mouritsen and coworkers could demonstrate the formation of a stable ABA triblock copolymer membrane with a long life-time within apertures (300µm diameter) and the functional incorporation of the channel protein gramicidin A [169].

Solid supported polymer membranes are attractive for sensor applications but also for the study of membrane transport and diffusion. Most membranes on solid supports are obtained as grafted films [129]. But also the spreading of tri- and diblock polymersomes onto solid supports [164, 167] and the formation of a bilayer by consecutive Langmuir-Blodgett transfer [165] have already been reported. Gonz*á*les-P*é*rez and coworkers demonstrated the formation of a polymer membrane from deposited ABA-polymer on mica with excellent properties of uniformity and low roughness suitable for membrane protein reconstitution [166]. Meier and coworkers also demonstrated that diblock copolymer membranes formed by vesicle spreading on a gold support exhibit highly sealing properties with resistances resembling those of lipid bilayers. They also demonstrated the feasibility of solid supported polymer bilayers for the incorporation of peptides. A reduced membrane resistance could be observed in EIS measurements due to transient membrane defects caused by the detergent like interactions of the circular peptide Polymyxin B with the polymer membrane [166]. These results hint at the feasibility of solid supported polymer bilayers to also accommodate reconstituted membrane proteins. In the

case of solid supported polymer membranes, the compression of polymeric membranes upon protein insertion may be favourable to avoid direct contact between the membrane protein and the substrate by creating an effective reservoir of solvent between the protein and the substrate.

Polymer membranes deposited on a surface can also be used to create so called "'activated"' surfaces when biomolecules are chemically bound, electrostatically attached or inserted into the polymer membrane [141]. If the biomolecules are enzymes a catalytically active surface can be generated. Those catalytic surfaces permit rapid responses with a very high specificity to various stimuli of interest. So far such systems based on conductive polymers (cp) are of great interest as sensors for diagnostic or technical applications, as the signal produced by the enzyme is recognised by the cp and directly transferred to an electric device [141, 163]. This direct signal transduction is a great advantage to earlier biosensors, where the reaction products had to diffused to the electronic device in order to create a signal. Another advantage of these enzyme-polymer hybrid materials is the longer lifetime of the enzymes, compared to free enzymes in solutions. The interactions with the polymers stabilise the active conformation of the enzymes and additionally protect the enzyme from proteases [141]. Also the reversible loading of the polymer membranes with enzymes has been reported. This reversible adsorption allows to reuse the support after inactivation of the adsorbed enzymes. But it also bears the risk of unintended release of the adsorbed enzyme decreasing the activity of the surface [141]. Also other biomolecules like antibodies or DNA have already been successfully immobilised on polymer membranes [141] to obtain highly active surfaces.

3 Aim of this work

Nowadays about 40-60% of all descriptive drugs on the market or in development target GPCRs [23]. Therefore, screening systems to identify both endogenous ligands as well as new potential drugs are of great interest for the pharmaceutical industry. These screening systems should be cheap, easy to handle, stable and reusable and allow fast identification and characterisation of a great variety of potential substances. Therefore it is crucial to find feasible methods to immobilise GPCRs in a functional conformation onto appropriate hydrophobic surfaces. These functionalised surfaces should be stable against air and strain as well as capable for parallel and high throughput screening.

The aim of this work was the generation of a GPCR-functionalised bio-mimetic membrane system, which should be feasible for ligand binding studies and functional characterisation of the incorporated GPCR. This GPCR functionalised platform should be generated by combining *in vitro* synthesis of membrane proteins and polymeric membrane systems. The synthesis of the membrane proteins with cell-free expression systems should skip the time-consuming bottleneck of cellular overexpression, purification and reconstitution. The use of polymeric bio-mimetic membrane systems should provide increased stability against air and strain. Due to this combination, the novel platforms can easily be adapted to customer needs for screening of any membrane protein of interest. Owing to the increased resilience of the novel platform it should also be applicable for biosensors, structural analysis as well as high throughput screening applications. The pharmaceutical relevant dopamine receptors 1 and 2 were used as model GPCRs for the development of the GPCR-functionalised platform.

In the first step the successful *in vitro* expression with cell-free expression systems into polymeric membranes had to be established. Therefore a suitable bio-mimetic membrane system based on block-copolymers had to be chosen. Also a suitable cell-free expression system for the *in vitro* synthesis of the mammalian model receptors had to be determined. The successful expression as well as the incorporation of the dopamine receptors into the polymeric membrane had to be demonstrated by appropriate methods.

In the second step a surface feasible for screening applications had to be established. This surface should be reproducible, applicable for the *in vitro* synthesis of the membrane proteins and allow for easy detection and characterisation of ligand binding.

In the last step the functionality of the *in vitro* expressed and incorporated dopamine receptors had to be demonstrated.

4 Materials and Methods

4.1 Block-copolymers and polymersome preparation

4.1.1 Preparation of ABA Triblock-polymersomes (PMOXA-PDMS-PMOXA)

The vesicle solutions were prepared and characterised by Zhikang Fu according to the following film rehydration procedure. ABA polymer (5 mg, Polymer Source; structure Fig.15) was dissolved in chloroform(200 µl) and dried slowly under a stream of nitrogen in a conical bottom glass tube to form a thin polymer film. The film was further dried for at least 4 h in a vacuum dessicator. Subsequently the thin polymer film was rehydrated with 1ml ultrapure water (R=18,2MΩ ; 4ppm; Millipore) for at least 18 h. This rehydration allows the spontaneous formation of polymersomes. The resulting suspension was extruded through 0.45 µm PVDF syringe filters (Millipore). Free single ABA molecules were removed by dialysis (MWCO 50 kDa, Spectra/Por® 7, Spectrum Laboratories) against ultrapure water for at least 24 h. The resulting ABA polymersomes were characterised by TEM (Fig.32).

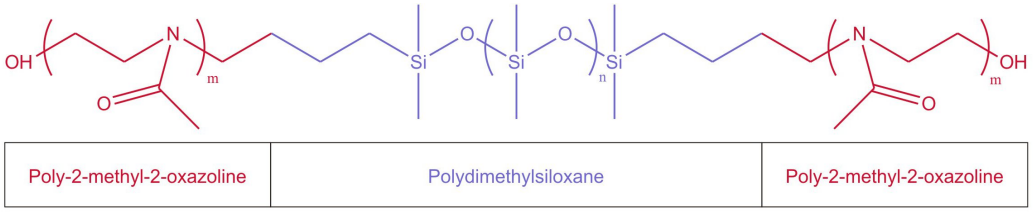

Figure 15: Structure of ABA triblock-copolymer: block length: 12A-55B-12A; ABA stands for PMOXA-PDMS-PMOXA; A=PMOXA = poly(2-methyloxazoline); B=PDMS = poly(dimethylsiloxane)

4.1.2 Preparation of AB Diblock-polymersomes (BD21; PBd-PEO)

The vesicle solutions were prepared and characterised by Zhikang Fu according to the following direct dissolution procedure. BD21 polymer (20 mg; Polymer Source, structure Fig.16) was dissolved in THF (100 µl) and added dropwise to ultrapure water (900 µl). The mixture was stirred at 1000 RPM for at least 18 h to allow self assembly of polymersomes. THF was removed by dialysis (MWCO 50 kDa, Spectra/Por® 7, Spectrum Laboratories) against ultrapure water for at least 24 h. The resulting suspension was extruded through 0.45 µm PVDF syringe filter (Millipore). Free single BD21 molecules were removed by dialysis (MWCO 50

kDa, Spectra/Por® 7, Spectrum Laboratories) against ultrapure water for at least 24 h. The resulting polymersomes were characterised by TEM (Fig.33).

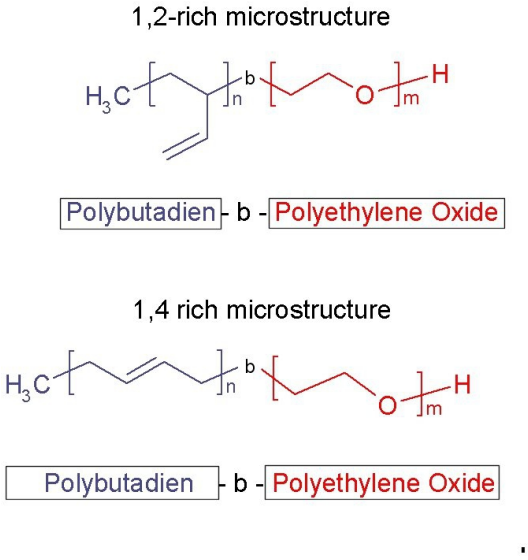

Figure 16: Structure of BD21 diblock-copolymer: the polymer consists of 89% of the 1,2 rich structure; block length: BD21 = [PBd]22-b-[PEO]13 (M_n - 1200-b-600); PBd/PEO stands for Polybutadiene/Polyethylene Oxide(Polymer Source)

4.2 Cloning of recombinant DRD1 and DRD2 receptor for cell-free expression

4.2.1 Cloning of fluorescent pCMVTNT-DRD2-EYFP

The cDNA (Source Bioscience Lifescience: OmicsLink ORF Expression Clone: A0740; Human BAC (RPCI-11) -1; transcript variant 1 (long); LOCUS NM_000795) for the DRD2 receptor was obtained from Sandra Ritz [7] cloned into a pEYFP-N1 vector (Clontech) (Appendix:A2; Fig.51). In the first cloning step the DRD2-EYFP gene was cloned into a pCMVTNT-vector (Promega; Cat.:L562A) (Appendix:A2; Fig.52) appropriate for mammalian and cell-free expression. Therefore the original construct and the new vector were digested with EcoRI (NEB;Cat.:R01015) and NotI (NEB; Cat.:R01896) in NEBuffer3 (NEB; Cat.:B70035). Subsequently the restriction reactions of the pCMVTNT-vector were dephosporylated using the FastAP^{TM}Thermosensitive Alkaline Phospatase (Fermentas; EF0651). All restriction fragments were purified with a 1% Agarose gel (1x TAE-buffer, SYBR Safe DNA gel stain) and subsequent gel extraction (QIAquick gel Extraction Kit; Qiagen; 28704). The ligation reaction

was carried out using T4 DNA ligase (Fermentas; EL0016) and a ratio of plasmid to insert of 1:1 or 1:3. The amount of insert cDNA for the ligation reaction with xng pCMVTNT-vector was calculated according to the following equation:

ng insert = (ng $_{vector}$ x kb$_{insert}$/ kb$_{vector}$) x molar ratio insert/vector

The constructs from the ligation reaction were transformed into Top10 competent cells (invitrogen; 44-0301) and selected on agar-plates (imMedia AmpAgar; Invitrogen; Cat.:45-0034) containing ampicillin. The positive colonies were amplified in LB-medium (Tab.:1) containing ampicillin (0,01 mg/ml). The pCMVTNT-DRD1-EYFP construct was obtained by the same cloning procedure. The successful cloning of both, DRD1 and DRD2 constructs, was verified by DNA-sequencing (Genterprise, Mainz) of the purified plasmids (Plasmid Maxi Kit; Qiagen).

amount	component	supplier
10g	Bacterial Peptone (enzymatic hydrolysate)	SIGMA Cat.:P0556-250g
10g	NaCl (puriss)	Riedel-de-Haën; Cat.:31434)
5g	Hefeextract pulv.f.d. Bakteriologie	Roth; Cat.:2363.3
top up to 1l	ultrapure water	

Table 1: Recipe LB-medium: before use the medium was autoclaved and subsequently supplemented with 10 µg/mL ampicillin.

4.2.2 Cloning of fluorescent pCMVTNT-DRD2-GFP2

Afterwards a fluorescent GFP2-tag was added to the recombinant DRD2 receptor. Therefore the pCMVTNT-DRD2-EYFP construct and the pTagGFP2-N (evrogen; Cat.:FP192) (Appendix:A2; Fig.52) were cut with NotI and AgeI. The fragments from the pCMVTNT-DRD2-EYFP digestion were again dephosphorylated with FastAP^{TM} Thermosensitive Alkaline Phosphatase (Fermentas; Cat.:EF0651). All fragments were purified with a 1% Agarose-gel and subsequent gel-extraction (QIAquick gel Extraction Kit; Qiagen; 28704). The ligation reaction was carried out using the T4 DNA ligase (Fermentas; Cat.:EL0016) and a ratio of plasmid to insert of 1:1 or 1:3. The positive colonies from the agar-plates with ampicillin(imMedia AmpAgar; Invitrogen;Cat.:45-0034) were amplified in LB-Medium (Tab.1) with ampicillin (0,01 mg/ml). The pCMVTNT-DRD1-GPF2 plasmid was cloned with the same procedure. The

purified pCMVTNT-DRD2-GFP2 and pCMVTNT-DRD1-GFP2 plasmids (Plasmid Maxi Kit; Qiagen) were analysed by DNA sequencing (Genterprise, Mainz).

4.2.3 Cloning of pCMVTNT-DRD1 and pCMVTNT-DRD2

The genes for DRD1 and DRD2 were amplified with PCR from the pCMVTNT-DRD1-GFP2 and pCMVTNT-DRD2-GFP2 plasmids (Appendix:A2; Fig.53), respectively, using the primers in Tab.2 and the summarised PCR program in Tab.3. In this step an EcoRI restriction site and a Kozak sequence (ref [8]) were introduced before the dopamine receptor genes.

Primer	Sequence
DRD2 forward	5'-CCGGAATTCTTTTTTTTTTAAACCACCATGGATCCACTGAATCTGTCC-3'
DRD2 reverse	5'-GCCGCGGCCGCTTAGCAGTGGAGGATCTTCAGG-3'
DRD1 forward	5'-CCGGAATTCTTTTTTTTTTAAACCACCATGAGGACTCTGAACAACTCTG-3'
DRD1 reverse	5'-GCCGCGGCCGCTTAGGTTGGGTGCTGACCGTTTTG-3'

Table 2: Primers for amplification of DRD1 and DRD2 genes with insertion of EcoRI restriction site and Kozak Sequence .

step	T °C	t	cycles
initial denaturation	95	2min	1
denaturation	95	15sec	30
annealing	55	30sec	
extension	72	1min	
final extension	72	10min	1
hold	16	for ever	

Table 3: PCR programm for the amplification of DRD1 and DRD2 cDNA from pCMVTNT-DRD1-GFP2 and pCMVTNT-DRD2-GFP2, respectively, with insertion of EcoRI restriction site and Kozak sequence.

Afterwards the PCR fragments were purified by gel extraction from a 1% agarose-gel using the QiaQuick Gel Extraction Kit (Cat:28706). Then the purified PCR fragments and the original pCMVTNT vector were digested (table4) with EcoRI and NotI followed by a ligation reaction using the Rapid DNA Ligation Kit (Roche,Cat.:11635379001). The ligation was carried out with a molar ratio of plasmid:insert of 1:3.

Subsequently the plasmids were transformed into competent DH5α cells by heat-shock (from IMCB Singapore) and plated on agar-plates with ampicillin (0,025mg/ml; IMCB Singapore).

The positive colonies containing the new plasmid with the ampicillin resistance were picked and amplified in LB-Medium(IMCB, Singapore) containing 0.1% ampicillin(1g/ml) over night. The plasmids for analysis of the cloning were purified using the QIAprep Spin Miniprep Kit(Qiagen, Cat.No:27104). The ligation was controlled by double digestion with EcoRI and NotI and subsequently agarose-gel(1%; 1x TAE buffer; ethidiumbromide staining) analysis. For complete analysis of the construct the plasmid (Appendix:A2; Fig.54) was sequenced by the sequencing lab of IMCB Singapore. Large overnight bacterial cultures for amplification of the plasmid were purified using the Nucleo Bond Xtra Midi Kit (Macherey-Nagel). DNA concentrations were determined using the NanoPhotometer (IMPLEN).

component	amount
plasmid cDNA	1µ g
10x fast digest buffer(Fermentas)	2µ l
ultrapure water	top up to 20µ l
NotI(Fermentas Cat:FD0594)	1µ l
EcoRI(Fermentas FD0274)	1µ l

Table 4: Double digestion reactions: the reactions were started with NotI and incubated for 25 min at 37°C then the EcoRI was added and the reactions were incubated for 5 more min at 37°C.

All primers for the above cloning steps of the different pCMVTNT-DRD-constructs were designed using the Vector NTI 11 program (invitrogen). Sequencing results were analysed using the alignment tool from the Vector NTI program (invitrogen) to compare the sequencing results with the theoretical constructs designed with Vector NTI 11. For all constructs glycerol-stocks (33% glycerol) of overnight bacterial cultures were stored at -80°C for later supply of new plasmids.

4.3 Specifications of Dopamine-receptors and fluorescent ligand

Protein sizes

- DRD1-GFP2: 76,69 kDa
- DRD1: 49,29 kDa
- DRD2-GFP2: 79,06 kDa
- DRD2: 50,61 kDa

kds of Dopamine receptor 2 [6]

DRD2 high affinity: 2.8 -474 nM (=4.7μM)

DRD2 low affinity: 1705-2490 nM (=2.5μM)

Therefore the working solution of dansyldopamine should be around 25 μM. The stock solution was prepared as a 10 mM stock in DMF.

Structure dansyldopamine

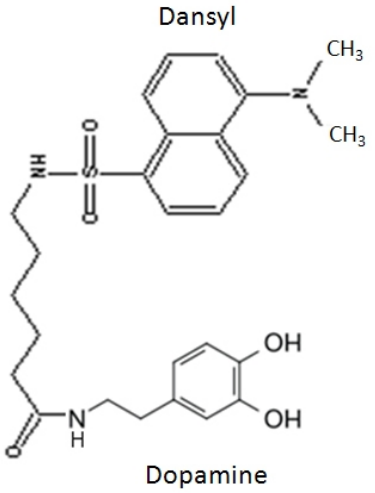

Figure 17: Structure of dansyldopamine(dopamine labeled with dansyl attached through a 5-Carbon linker (DnsylD-1, FIVEphotonBiochemicals).

Specifications dansyldopamine

- MW 499.62g/mol
- solubility : DMF
- Spectral characteristics: 333/515nm
- use a 10xkd of unlabeled dopamine for respective dopamine receptor isoform
- purity 98%

4.4 Expression of GFP2 labelled dopamine receptors in SH-SY5Y cells

To control the new recombinant pCMVTNT-DRD2-GFP2 SHSY-5Y cells were transfected with the plasmid. The expression was controlled with a microscope (Leica TCS SP5). The SHSY-5Y cells were cultivated in DMEM:HAM's F12 medium (BioWhittacker; Cat.:BE12-719F)

with 15% FCS (CCpro; cat.:S-10-L). For the transfection the cells were trypsinised (0.05% Trypsin-EDTA; GIBCO; Cat.:25300) and 2x10^5 SHSY-5Y cells were seeded in each well of a 6-well plate. For later fixation a glass cover slip was put into each well before seeding of the cells. 100µl of transfection reactions (Tab.5) were added to each well. The transfected cells were incubated for 2 days at 37°C and 5% CO_2 in DMEM:HAM's F12 medium (BioWhittacker; Cat.:BE12-719F). The expressed DRD2 receptors were activated with 10mM Dopamine-hydrochloride (SIGMA; Cat.:H8502-5G) in Leibovitz medium (SIGMA; Cat.:L5520). After 15min the cells were fixated with 4% PFA. The receptor internalization was detected with the Leica microscope(Leica TCS SP5).

component	company	Art.No	amount
serum-free DMEM:HAm's F12	BioWhittacker	BE12-719F	up to 100µl
pCMVTNT-DRD2-GFP2			2µg
Fugene HD transfection Reagent	Roche	04709691001	6µl

Table 5: Transfection reactions for the transfection of SHSY-5Y cells with DRD2

4.5 *In vitro* expression

The *in vitro* expression was carried out with the *in vitro* kits from Promega. For expression of DRD2 with the fluorescence protein tag the TnT® T7 Quick Coupled Transcription/Translation System (Promega; Cat.:L1170) was used. DRD2 without tag was expressed using the TnT® T7 Coupled Wheat Germ Extract System (Promega; cat.:L4140). For Western Blot analysis both expression systems were used for all recombinant dopamine receptor variants. The reactions were carried out according to the protocols provided by the supplier. For all *in vitro* reactions for Western Blot analysis ultrapure water was replaced with polymersome solution. Each reaction was run with 1600 ng of cDNA. For expression of DRD2 and DRD1 with the wheat germ expression kit for Biacore, FC and binding and replacement experiments ultrapure water was replaced by polymersome solution in each reaction.

4.6 Western Blot

The first proof for the successful synthesis of the recombinant DRD2 gave the Western Blot analysis. Therefore 5μl of the *in vitro* reactions or 10μl of the different purified fractions were used. The samples were mixed with 5,4 μl autoclaved ultrapure water (0,4μl for the purified samples), 4 μl LDS sample buffer (NuPage invitrogen; Cat.:NP0007) and 1,6 μl sample reducing agent (NuPage invitrogen; Cat.:NP0009) and subsequently denatured for 10min at 70°C in

an Eppendorf thermomixer. The SDS-Page was carried out with 10% Bis-Tris Gels (Nupage invitrogen; Cat.:NP00302BOX) and MES SDS running buffer (20x diluted with ultrapure water to 1x; NuPage invitrogen; Cat.:NP0002). To determine the size of the protein bands in the blot two protein markers were loaded: the invisible MagicMark XP Western Standard (3,5μl, invitrogen; Cat.:LC5602) for later detection in the Western Blot and the visible SeebluePlus 2 Prestained Standard (8μl,invitrogen; Cat.:LC5925) for the immediate control of the SDS-Page.

The gels were blotted with the iBlot® Dry Blotting System (invitrogen; P3, 7min) onto PVDF membranes(iBlot gel Transfer stacks PVDF mini; invitrogen; Cat:IB4010-02). The immunodetection of the proteins was carried out with the Western Breeze Chemiluminescent Detection System mouse primary antibody (invitrogen; Cat.:WB7104). As primary antibody the DRD2 monoclonal antibody purified mouse IgG (abnova; Cat.:H00001813-MO1) was used with a dilution of 1:333 or 1:1000.

4.7 Detection of *in vitro* synthesised DRD2-GFP2 by GFP2 emission

50µl of *in vitro* expression reaction(Promega;Quick coupled Rabbit Reticulocyte Lysate System) were prepared according to the vendors protocol. Instead of water ABA polymersomes were added to the reaction mixtures. After the expression the samples were purified with Durapore PVDF 0.1µm Ultrafree centrifugal filters (Millipore CatNo.:UFC30VV00) for 10min at 3000rpm. Then they were washed(resolved and centrifuged 10min,3000rpm)3 times with ultrapure water. Thereafter the samples were resolved in 100µl of ultrapure water and the emission spectra(400-520nm; excitation 475nm; emission GFP2 506nm) was recorded. As control a dilution series in ultrapure water of free GFP(Recombinant Protein expressed in E.Coli; Millipore; Cat No: 14-392; c=1µg/µl in PBS containing 20% glycerol) was measured.

4.8 Biacore system

This system allows label-free interaction analysis between proteins and other molecules, such as antibodies (www.biacore.com). The detection is based on the SPR (surface plasmon resonance) technology. The Biacore system has 4 flow-cells which are formed by pressing the microfluidic cartride against a sensor chip (Fig.18) with an appropriate surface modification for the experiment. The BIACORE 3000, which was used for the experiments, has a serial flow-cell system (Fig.19). In this configuration the injected sample flows consecutively through the flow cells. The different flow-cells can be opened and closed by a system of valves. For the experiments two serial flow cells were used. Hence one of the flow-cells could be used as on-line reference cell. This arrangement allows the direct monitoring of the blank-subtracted data.

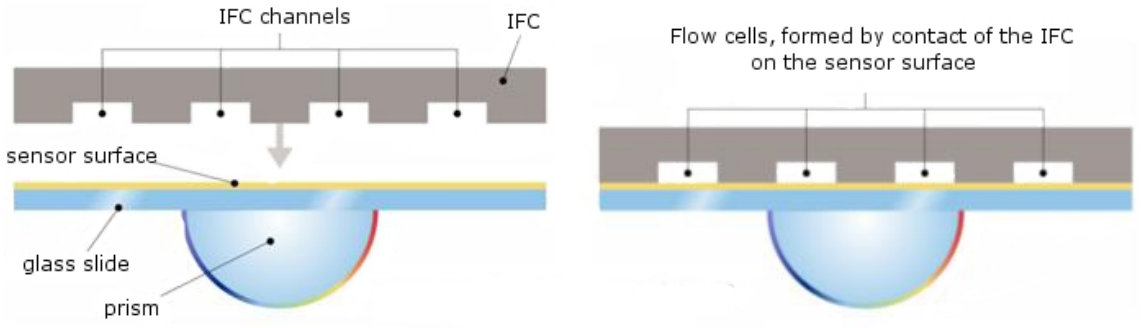

Figure 18: Flow cell formation in the BIACORE machine: the flow-cells are formed when the microfluidic cartridge is pressed against the sensor surface (www.biacore.com)

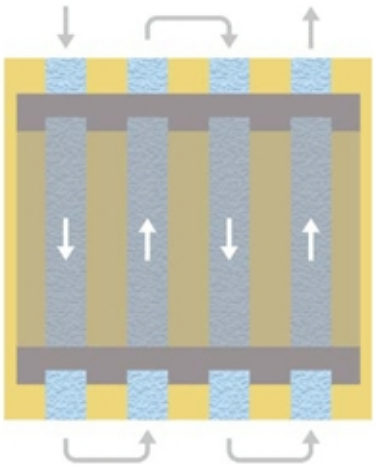

Figure 19: Serial arrangement of flow-cells in the BIACORE machine: for the experiments only two serial flow-cells were used (www.biacore.com)

4.8.1 Protocol

75μl of *in vitro* synthesis reaction were prepared according to the vendors protocol. Instead of water vesicle solution was added to the reactions. Afterwards the polymersomes were purified using Durapore PVDF 0.1μm Ultrafree centrifugal filters (Millipore CatNo.: UFC30VV00). To capture the purified polymersomes on the Biacore CM5 chip (Dextran Matrix; GE Healthcare), Protein A (GE Healthcare) was first immobilised onto the surface using an amine coupling procedure. For this purpose, the carboxylic groups on the surface matrix were transformed into an active ester with a mixture of 0.2 M 1-ethyl-3-(3- dimethylaminopropyl) carbodiimide and 0.05 M N-hydroxysuccinimide (0.2 M EDC- 0.05M NHS, GE Healthcare) (10 μl/min, 10 min). The reactive succinimide esters formed react spontaneously with the amino groups of protein A (level of immobilization 2500 RU) and form amid bonds. Remaining reactive ester groups were inactivated with ethanol-amine (1 molar, pH 8.5; GE Healthcare) (10 μl/min, 10 min)(Lit**??**). For all measurement steps HBS-EP buffer (Tab.6) was used. All centrifugations were performed in an eppendorf MiniSpin® centrifuge at 3000rpm.

component	company	Art.No	amount
HEPES $\geq$ 99,5 %	Sigma	H4034-500g	10mM
NaCl	Merck	1-06404-5000	150mM
EDTA 2Na*H_2O	USB	15701	3.4mM
P20	Biacore		0.005 %
HCl/NaOH	adjust	pH7.4	

Table 6: recipe HBS-EP buffer

Measurement procedure

- flow path 3,4
- First the BIACORE chip was twice rinsed with 10mM HCL(in HBS-EP buffer) solution for 30sec, flow rate = 30µl/min
- passivation of chip surface with BSA(Sigma A3059; stock 100mg/ml): BSA(10mg/ml in HSB-EP) 160µl flow rate: 5µl/min
- flow path 4
- injection of antibody: 2µl Anti-DRD2 (1-110)Mab (Abnova Cat: H00001813-MO1; c=0.37mg/ml) + 98µl HSB-EP buffer; flow rate: 2µl/min

- flow path 3,4
- rinse with HBS-EP buffer; flow rate: 2µl/min
- wait for 30 min for equilibrium of antibody binding
- purification of DRD2-functionalised polymersomes:
  - calibrate the centrifugal filters with 50µl HBS-EP buffer: centrifuge 3min, 3000rpm
  - centrifuge the *in vitro* reaction mixture in the centrifugal filters 3min 3000rpm
  - wash the filters with 50µl HBS-EP buffer: centrifuge 3min, 3000rpm
  - resolve the retentate with the remaining buffer on the filter and adjust volume to 100µl HBS-EP buffer
- injection of vesicle solution: 50µl of purified vesicle solution flow rate: 2µl/min
- wait for 10min for equilibration of bound polymersomes to surface
- rinse the surface twice with 10mM HCl flow rate 30µl/min
- rinse the surface with NaOH
- start new measurement

4.8.2 Surface Plasmon Spectroscopy

Surface-plasmon spectroscopy is by now an established method for the characterization of interfaces and thin films. It can also be used for monitoring of kinetic processes and interfacial binding processes without labelling of the reagents used in the reactions. This advantage guarantees that the reactions are not disturbed or changed by labelling molecules. The surface plasmon spectroscopy is based on the optical contrast within the evanescent field of the surface plasmon propagating along the metal/dielectric interface caused by a molecule bound to the interface. The limit of detection is a layer thickness of about 0.1 - 0.2nm. If binding processes add up in very thin layers or rather marginal effects on the evanescent field the angular shift is too low to be detected. In such cases the signal of the interfacial binding processes may be enhanced by the use of fluorescence labelled reagents.

4.8.3 Theoretical background

The surface-plasmon spectroscopy is based on the phenomenon of the total internal reflection (TIR) which occurs at interface between glass and a dielectric. This phenomenon can be monitored by the reflectivity R, the reflected light intensity Ir scaled to the incoming light intensity Io, as a function of the angle of incidence θ. If a plane wave (i.g.p-polarised laser beam) impinges on such an interface at a certain critical angle (θ_c) the reflectivity reaches a maximum intensity because of the total internal reflection. This critical angle is given by the refractive indices of the solid and the liquid by Snells law. Below this critical angle the reflectivity is low, because most of the light is transmitted and it increases steeply when approaching the critical angle.

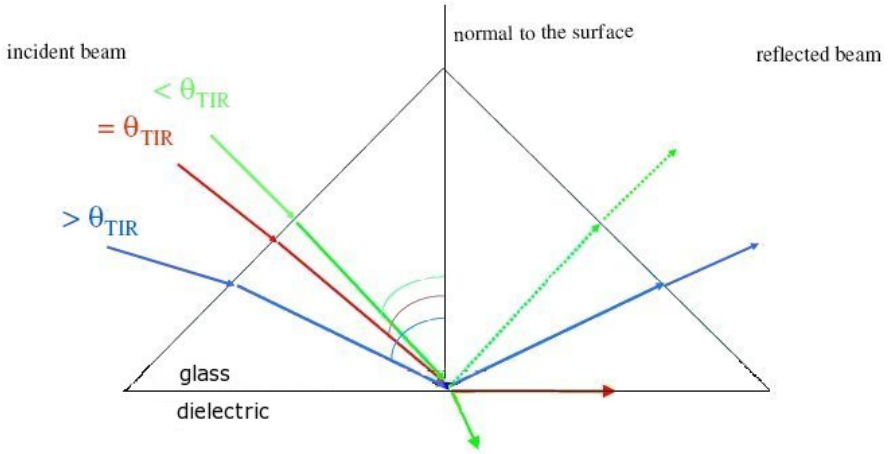

Figure 20: Reflection of light at a glass/dielectric interface:Both the angle of incidence and the angle of reflection are defined as the angle between the corresponding light beam and the normal to the surface

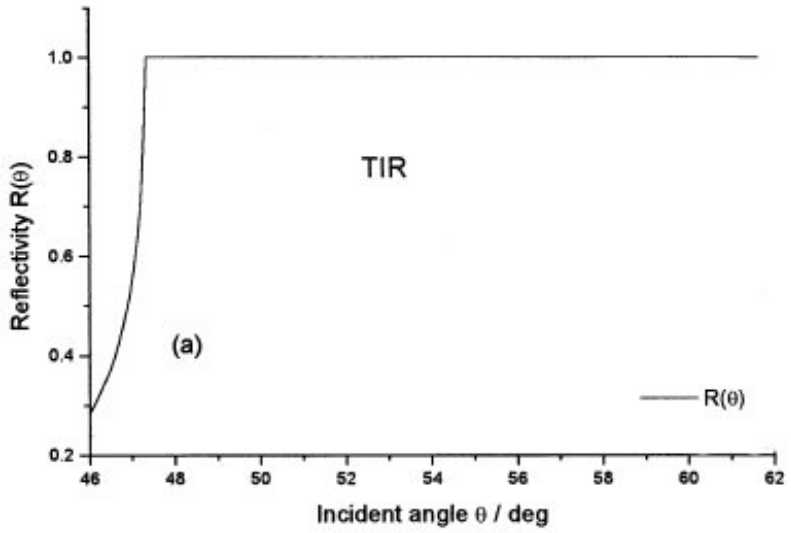

Figure 21: Reflectivity R scaled to the incoming intensity as a function of the angle of incidence (θ) for a mere total internal reflection geometry i.e. a glass/water interface [1]

The intensity of the evanescent light at the interface is enhanced of a factor of 4 at θ_c due to the constructive interference of the two amplitudes of the incoming and reflected electromagnetic field. This enhanced surface light is used in surface selective fluorescence spectroscopy. If the prism is covered with a thin gold layer, the nearly free electron gas of the metal can act as an optical resonator. In this case below the critical angle the reflectivity is already rather high, because the gold layer acts as a mirror. It reflects most of the otherwise transmitted light. The critical angle still shows the highest reflectivity and occurs still at the same value of θ because it is only dependent from the refractive index of the glass and the dielectric, respectively. Above θ_c the free electron gas of the thin gold layer absorbs energy from the photons and oscillate. This absorption of energy leads to the excitation of a surface-bound electromagnetic wave, which propagates along the interface, the so-called surface plasmon. The evanescent field associated with the surface plasmon is perpendicular to the interface. It extends into the metal and the dielectric layer with the highest intensity located at the surface. The evanescent field decays exponentially.

This excitation of a surface plasmon causes a narrow dip in the reflectivity curve with a minimum intensity which depends on the thickness of the gold layer and can reach nearly 0. The half width of the dip depends on the damping of the excitation mode which is dominated by the losses in the metal described by the imaginary part of its dielectric function.

The surface light intensity shows a maximum near the minimum of the reflectivity. The intensity

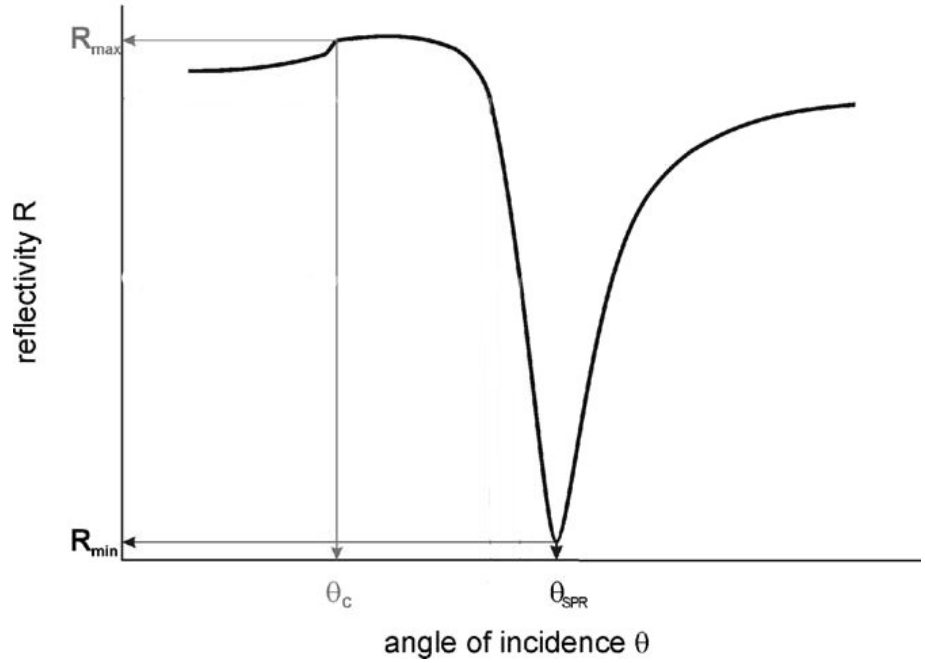

Figure 22: Reflectivity R as a function of the angle of incidence (θ) for a plasmon surface polariton excitation at a Au/water interface

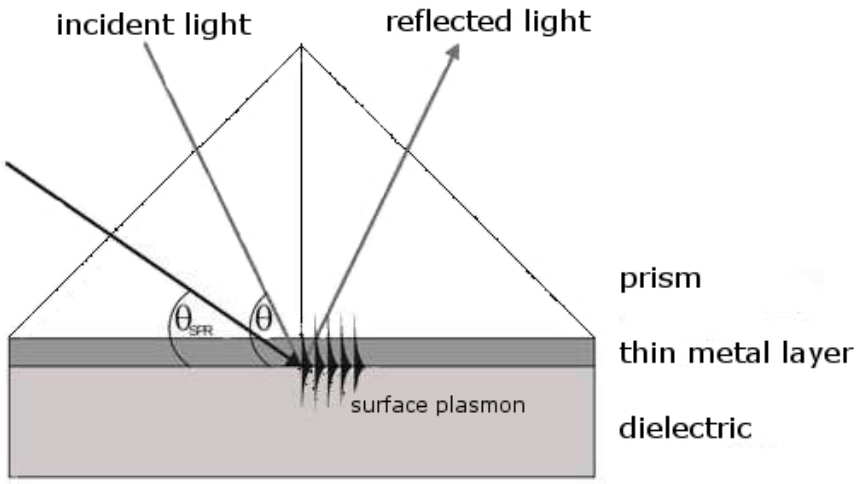

Figure 23: Excitation of an evanescent field at a gold/dielectric interface by p-polarised light [3]

scaled to the incoming intensity shows an enhancement factor of about 16 for gold layers, depending on the real and imaginary part of the dielectric function of the gold. Therefore it can vary from sample to sample. But in general, the lower the imaginary part, the higher the enhancement factor. The highest surface light intensity is found at a slightly lower angle than the minimum of the reflectivity. Because the minimum of the reflectivity is the destructive interference of the directly reflected wave and the evanescent field re-radiated via the prism. And this minimum is reached just above the angle of maximum intensity of the evanescent field (surface light). The exact position again depends from the imaginary part of the dielectric function of the gold, because this part causes the phase change of the two waves. The position of the maximum field intensity can be calculated by the Fresnel theory [2].

In the Biacore system the prism is coupled in the Kretschmann-Räther configuration [4], [5]. In this configuration the photons travel through a high index prism and couple through a gold film(chip surface) that is in contact with the dielectric medium.

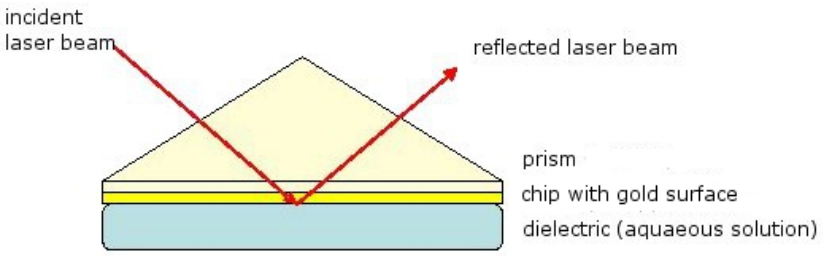

Figure 24: Prism coupling in the Kretschmann configuration. The incident laser beam passes through the prism before it is reflected at the gold/dielectric interface

4.9 Flow cytometry

Flow cytometry is a common method to analyse small particles (cells, vesicles, polymersomes) according to the light scattering pattern they cause by passing through a single wavelength light beam. Therefore the sample of particles must be ordered into a single stream of particles. This ordering is achieved by the so called hydrodynamic focusing (fig.25). In this process the sample is injected into a central core enclosed by a sheath. The faster flowing sheath fluid generates a massive drag effect on the central core chamber. This outer force leads to a higher velocity in the center of the core chamber and no velocity at the walls(ref. [11]. The outcome of this effect is a stream of single particles.

Subsequently this stream of single particles passes through the beam of light with a single wavelength. By passing this beam, the light is scattered by the particle. The scattered light

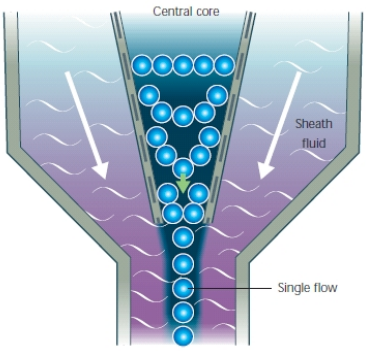

Figure 25: Generation of a single particle stream by hydrodynamic focusing in a FCM machine(picture from ref. [11]

is collected and detected at two different positions(fig.26): the front scatter(forward scatter channel FSC) is detected up to 20% offset to the laser beam axis and the side scatter (side scatter channel SSC) is detected 90° to the laser beam‘s axis.

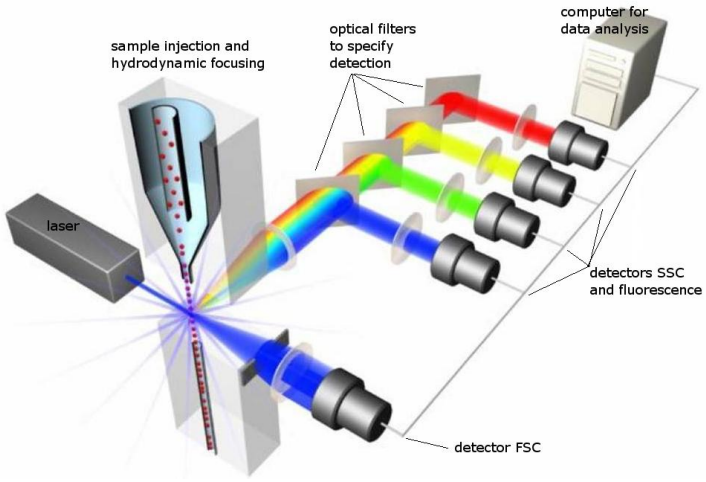

Figure 26: Schematic representation of a common flow cytometer (picture from invitrogen)

The FSC correlates to the size of the particles. The SSC provides information about the granular content of the particle(ref. [11]). The combination of both signals can be used to identify different populations of particles within a sample. The flow cytometry can also be combined with fluorescence labels. This allows for example to mark distinct proteins with fluorescently labelled antibodies in particles. If fluorophores with the same excitation, but different emission wavelengths are used, the flow cytometry offers a comfortable way for simultaneous multiparametric analysis. To ensure the specificity of the analysis the side scattered light is selected by optical filters before reaching the distinct detectors. Commonly three types of filters are used:

long-pass filters(light above a certain wavelength can pass) short-pass filters (light below a certain wavelength can pass) and band-pass filters (light in a narrow bandwidth around a certain wavelength can pass). For multiparametric analysis the error of the filters is crucial. The measured signals can -after transformation into electronic signals in the detector - be plotted in different types of diagrams. In a histogram one parameter (FSC, SSC or fluorescence) is plotted on the x-axis against the number of events (particles with properties of interest)on the y-axis. In a dot plot two parameters of interest are plotted. The density of events with the properties of interest is represented in the number of dots in the plot. To clearly represent the measured data, regions of interest(gates) and a threshold can be defined. Thus only particles with the characteristics of interest appear in the plots.

4.9.1 Protocol for the detection of DRD2 in polymersomes with fluorescent labelled anti-DRD2

50µl *in vitro* expression reactions were prepared according to the vendors protocol. Instead of water BD21 vesicle-solution was added to the reactions. Subsequently the polymersomes were purified with Durapore PVDF 0.1µm Ultrafree centrifugal filters (Millipore CatNo.:UFC30VV00). The purified protein-functionalised polymersomes were then analysed by antibody binding. Therefore the vesicle solutions were incubated with different concentrations of Anti-DRD2 (1-110)Mab (Abnova Cat:H00001813-MO1; c=0.2mg/ml). Subsequently unbound antibody was removed by centrifugal purification. For detection with the flow cytometer a secondary Alexa Fluor® 488 (F(ab')2 fragment of goat anti-rabbit IgG (H+L);invitrogen; Cat: A11070; 2mg/ml) labelled antibody was bound to the primary antibody. The unbound antibody was not removed because it will not be detected by the flow cytometer. For the measurements the vesicle solutions were diluted 1:4 with PBS. A BD LSRII (5 lasers special ordered system; software BD FACS DIVA Software at SIgN Singapore) was used for the measurements. The Alexa-488 measurements were performed with an excitation wavelength at 488 nm and an emission wavelength at 505-550 nm. The data was presented as a two dimensional dotplot using forward and side angle scatter (FSC/SSC) gating to exclude particles and background noise from the system. About 1000 gated events were recorded for each measurement.

4.10 Ultrafiltration binding assay

The *in vitro* reactions were prepared according to the vendors protocol. As negative controls *in vitro* reactions containing Cld2-cDNA or no cDNA were used. Afterwards the polymersomes were purified using ultracentrifugation cartridges (vivaspin 500 sartorius stedim biotech

MWCO 100kDa). Therefore the reaction mixtures were diluted with TMN buffer and centrifuged (1h, 3000rpm). Then the retentate was washed twice with TMN buffer (1h, 3000rpm). For the ligand binding the purified polymersomes were resolved in TMN buffer and transferred into a microcentrifuge tube. The vesicle concentration was controlled by absorption measurement and the volumes were adjusted with TMN buffer + 0.1% Digitonin. Subsequently the vesicle surface was passivated with 4% BSA in PBSA for 30min at room temperature. For the ligand binding dansyldopamine(10mM stock in DMF) was added to a final concentration of 25µM and incubated for 30min was added at 37°C and 600rpm in an Eppendorf thermomixer. Subsequently unbound dansyldopamine was removed in an additional centrifugation(1h 3000rpm) and washing step(1h;3000rpm). The binding of the dansyldopamine to the protein-functionalised polymersomes was determined by measuring the fluorescence intensity with the TECAN plate reader(TECAN i-contol infinite 200; 384 well plate)

4.11 BCA assay

To determine the protein concentration in the purified vesicle solutions after *in vitro* expression the BCA(Bicinchoninic Acid) assay was used. The detection of proteins is based on the reduction of Cu^{2+} to Cu^{1+} by proteins in an alkaline environment(biuret reaction) (ref. [9]). The amino acids cysteine, cystine, tryptophan, tyrosine, and the peptide bonds are capable for the reduction reaction (ref. [10]). The produced Cu^{1+}-ions form coloured complexes with the BCA. The absorbance of these complexes is measured at 562nm. Due to the relative linearity of the complex formation with protein concentration the assay can be used to determine a wide range of protein concentrations (ref. [9]). For the BCA assay the Pierce® BCA Protein Assay Kit (Thermo Scientific; Cat:23227) was used. The calibration curve and the assay was carried out according to the vendors protocols. The samples were incubated for 30min at 37°C in an Eppendorf thermomixer and subsequently transferred to a 96-well plate for the absorbance reading with a TECAN plate reader(TECAN i-contol infinite 200).

4.12 Replacement assay for ligand binding to DRD2

For the replacement assay ABA-polymersomes were covalently attached to an ultrasticky slide (precleaned gold seal Rite-on microslide; Gold-seal Products 20 Post road Portsmouth NH 03801 made in USA of swiss class, Cat:3099; 75x25mm; 1mm thick glass) [177].

The slides were cut into 10 small chips and rinsed with isopropanol and ultrapure water and then dried with N_2-stream.

For the coupling of the polymersomes to the amino-surface (Fig.45) of the chips equal volumes of ethanolic solutions of Tetrazol(4-(2-phenyl-2H-tetrazol-5-yl)benzoic acid) (3.5mM; from co-operation partner: Hans-Peter de Hoog; NTU Singapore), (N-Hydroxysuccinimide)(0.1M;Tokyo chemical industries(TCI) Cat:B0249) and (N-(3-Dimethylaminopropyl-)N'-ethyl-carbodiimide-hydrochlorid) (0.4M;TCI Cat:D1601) were mixed. Each chip was covered completely with the solution and incubated for 1h in a saturated environment at room temperature. Thereafter the chips were rinsed with EtOH and dried with N_2-stream.

The PDMS stamps were plasma treated for 60sec at 80W. Directly afterwards a vesicle(ABA with 10% methacrylate in ultrapure) solution was applied to the stamps and incubated for 1h at room temperature. Thereafter the vesicle solution was removed and the stamps were dried with N_2.

The dried stamps were carefully put on the chips and gently pressed onto the chips. Then the photoinducible 1,3-Dipolar Cycloaddition between the tetrazol and the methacrylate was induced by 15min incubation under UV light(260nm) and the stamps were carefully removed from the chips.

The *in vitro* reactions were prepared according to the vendors protocol and evenly distributed onto the chips. Subsequently the chips were incubated on an Eppendorf thermomixer at 33°C for 90min. Thereafter the chips were rinsed with ultrapure water. Then the chip surface was passivated with 3% BSA solution in TMN buffer for 30min at room temperature. To remove excess BSA the chips were rinsed with ultrapure water. Afterwards the chips were incubated with a 25µM dansyldopamine-solution (in TMN bufffer) for 30min in the dark at room temperature. Subsequently the chips were rinsed again with ultrapure water.

Then the chips were placed on a glass slide and pictures were taken with an Olympus microscope (IX51; 10x magnification, ISO200, 200msec). To get a reliable value for the fluorescence intensity pictures of three different spots were taken. For the determination of the fluorescence intensities the free programm ImageJ was used.

After taking the pictures, the chips were incubated for 30min at room temperature in the dark with different concentrations(0(=TMN buffer), 1µM, 10µM, 100µM and 1mM) of unlabeled dopamine. After rinsing with ultrapure water pictures were again taken with the Olympus IX51 microscope(10x magnification, ISO200, 200msec).

5 Results and discussion

The aim of this work was the generation of a GPCR-functionalised membrane system by combining both promising alternatives: *in vitro* synthesis and polymeric membrane systems. This novel platform should be feasible for the characterisation of incorporated GPCRs. Due to their pharmacological relevance dopamine 1 and 2 receptors were chosen as model GPCRs.

Two different constructs of both receptors were cloned: one with a fluorescent GFP2 (enhanced green fluorescence protein) and one without any tag. The pCMVTNT-vector was chosen because it contains promotors for both, cell-free expression and expression in cell lines. The constructs with the fluorescence tag were used for the direct detection of expression in human SH-SY5Y cells. The fluorescence tag allowed to observe the successful expression, the localisation and functionality of the recombinant dopamine receptors by fluorescence microscopy. Therefore the expression in cells allowed for the easy and fast verification that the cloned plasmids are suitable for functional expression of the recombinant dopamine receptors (Chapter:5.2).

The next step was the *in vitro* expression of the recombinant dopamine receptors with and without the fluorescence tag. Immunodetection in Western blot analysis (Chapter:5.3) and in Flow cytometry analysis (Chapter:5.4.2) of Dopamine receptor 1 and 2 expressed in diblock- and triblock-polymersomes demonstrated the successful *in vitro* expression of GPCRs in polymeric membranes. Antibody binding studies with the Biacore system suggested a favoured orientation of dopamine receptors in triblock-polymersomes. In this experiment the binding of DRD1 or DRD2 functionalised ABA-polymersomes to the specific antibodies was observed. Only for the DRD2-N-terminal specific antibody a specific binding of the DRD2 functionalised polymersomes could be observed. For the DRD1-C-terminal specific antibody only unspecific binding could be observed (Chapter:5.4.1).

The binding of the endogenous ligand dopamine to the dopamine receptor functionalised polymersomes should demonstrate the functional incorporation into the polymersomes. But the specific ligand binding in solution was hindered by residual proteins from the cell-free expression kit (Chapter:5.5.1).

Finally the incorporation and functionality of the *in vitro* synthesised receptors was confirmed by a dopamine-replacement assay on DRD2-functionalised immobilised triblock-polymersomes. As the binding pocket for the endogenous ligand dopamine is formed by several amino acid residues of the three transmembrane regions 3,5 and 6 specific binding and replacement can only occur, if the receptor is incorporated in the right conformation into the polymersome membrane. The altered binding curve suggests an effect of the altered hydrophobic environment presented by the polymer membrane on protein activity (Chapter:5.5.2).

5.1 DRD1 and DRD2 plasmids used for this work

The original cDNAs for DRD1 and DRD2 obtained from Sandra Ritz were cloned into a pEYFP-N1 vector [7]. For this work the pCMVTNT-vector was used because this vector contains promotors suitable for expression in cell lines (CMV promotor) as well as in cell-free expression systems (SP6 and T7 promotor). The fluorescent GFP2 tag (Fig.27) was added to gain a simple detection method for the successful expression of the recombinant proteins in human neuroblastoma cells (SH-SY5Y cells) or the *in vitro* reaction mixture. The detection of the fluorescence tag only worked for expression in cells. Therefore for all following experiments with the cell-free expression systems the tag free dopamine receptors (Fig.28) were used as the determination of successful expression was done by immunostaining with antibodies and determination of functionality with binding of fluorescent labelled dopamine (dansyl-dopamine) as ligand for the receptors.

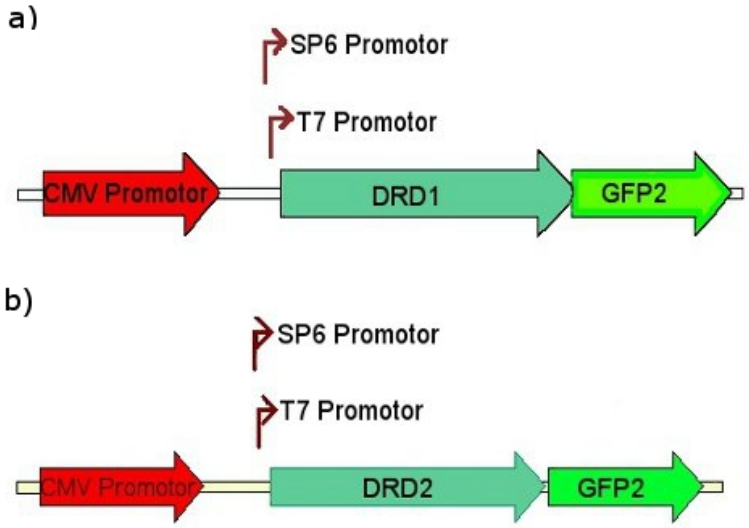

Figure 27: DNA constructs with fluorescence protein tag for DRD2 and DRD1 used for *in vitro* expression and expression in SH-SY5Y cells. a)pCMVTNT-DRD1-GFP2 b) pCMVTNT-DRD2-GFP2; CMV promotor for expression in eukaryotic cells; T7,SP6 promotor for expression in cell free expression systems.

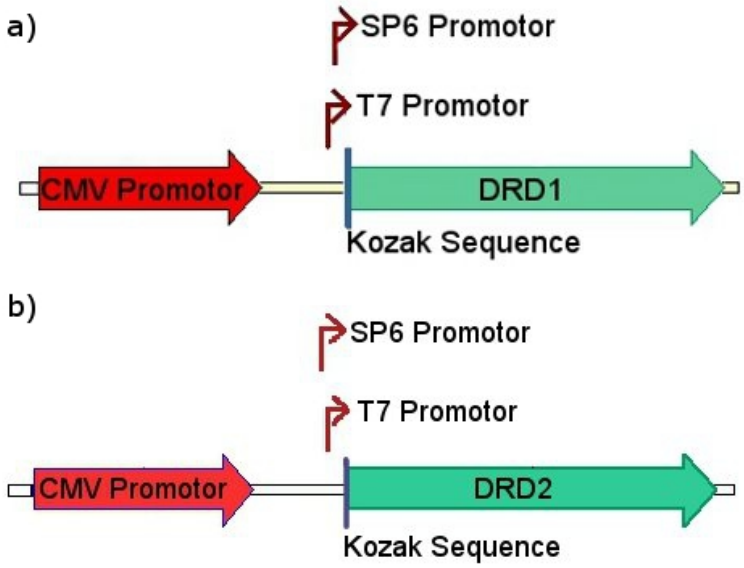

Figure 28: DNA constructs used for *in vitro* expression reactions: a) pCMVTNT-DRD2 b) pCMVTNT-DRD1; CMV promotor for expression in eukaryotic cells; T7,SP6 promotor for expression in cell free expression systems; Kozak sequence added to enhanced expression.

5.2 Expression and proof of functionality of DRD1 and DRD2 recombinant plasmids in human SH-SY5Y cells

To verify the functional expression of the cloned recombinant plasmid DNAs with the fluorescence protein tag GFP2 (enhanced green fluorescence protein Fig.27a) DRD1, b) DRD2), SH-SY5Y cells were transiently transfected with pCMVTNT-DRD1-GFP2 and pCMVTNT-DRD2-GFP2. This human neuroblastoma cell line was chosen, due to their natural expression of dopamine receptors. Therefore the expression of the recombinant dopamine receptors should not cause any cytotoxicity and the natural localisation of the receptors in the outer cell membrane should be supported by the protein expression system of the cells. The pCMVTNT-vector was chosen because it contains promotors for expression in mammalian cells as well as promotors commonly used in cell-free expression systems. Due to the fluorescence protein tag, the localisation in the outer cell membrane as well as the functionality of the receptors could be observed under the microscope. For proof of functionality the transfected cells were incubated with dopamine-hydrochloride to provoke an internalisation of GFP2-tagged dopamine receptors as response upon dopamine binding. This internalisation would confirm the functional expression of the recombinant receptors in the cells and therefore the suitability of the cloned plasmids for dopamine receptor expression.

The successful expression of the dopamine receptors could be observed 48h after transfection

by lipofection with a fluorescence microscope. The brighter rim of the transfected cells results from the correct localisation of the fluorescence protein tagged dopamine receptors in the outer cell membrane.

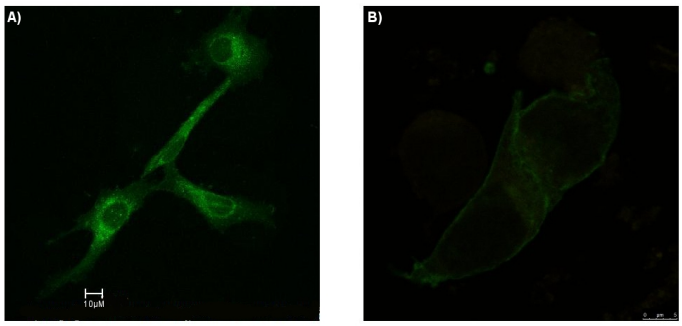

Figure 29: SH-SY5Y cells transiently transfected with pCMVTNT-DRD1-GFP2. A) Activated with 10 µM dopamine-hydrochloride for 20min. In response to dopamine binding to DRD1-GFP2, the cells start desensitisation by internalisation of the receptors, which can be seen as fluorescent vesicles within the cytosol. B) Cross section of transfected cells. The brighter rim of the cells show that the DRD1 receptors were localised within the outer cell membrane.

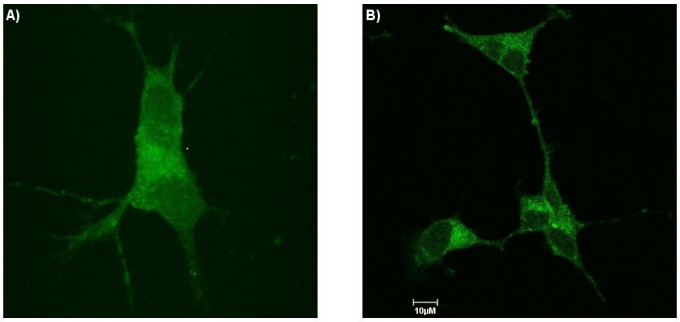

Figure 30: SH-SY5Y cells transiently transfected with pCMVTNT-DRD2-GFP2. Activated with dopamine-hydrochloride for 30min. In response to dopamine binding to DRD2-GFP2, the cells start desensitisation by internalisation of the receptors, which can be seen as fluorescent vesicles within the cytosol. The slightly brighter rim of the cells show that the DRD2-GFP2 receptors were localised within the outer cell membrane. Due to the long incubation time of 30 min most of the receptors are already internalised and therefore significantly amounts of cytosolic fluorescence was detected.

To proof functional expression of the recombinant dopamine receptors the transfected cells were incubated with 10 µM dopamine-hydrochloride for 20-30 min. Already after 10min of incubation with dopamine-hydrochloride the cell starts, in response to the binding of dopamine

to its receptors in the outer cell membrane, desensitisation of the receptors by internalisation of the dopamine receptors, which can be seen as fluorescent vesicles within the cytosol.

Fig.29 and Fig.30 show clearly brighter rims which confirm the localisation of the GFP2-tagged dopamine receptors 1 and 2 in the outer cell membrane. The fluorescent vesicles detected in the cytosol after incubation with dopamine-hydrochloride proofed the functionality of the expressed dopamine receptors. These results confirmed the successful functional expression of the recombinant dopamine receptors in SH-SY5Y cells. Therefore the cloned recombinant plasmids are suitable for functional expression of the dopamine receptors. As the vectors also contain promotors usually used in cell-free expression systems, the same plasmids could be used for the *in vitro* expression of the receptors.

5.3 *In vitro* expression of recombinant DRD1 and DRD2 receptors

After the successful expression of the recombinant dopamine receptors in cells the next step towards the functionalised bio-mimetic surface was the *in vitro* expression with cell-free expression systems. For the first experiments a rabbit reticulocyte based cell-free expression system was used. This system was chosen due to the mammalian origin of the recombinant dopamine receptors. Therefore no complications in expression due to different codon usage or differences in post-translation modification should be expected. The successful *in vitro* expression of pCMVTNT-DRD1-GFP2 and pCMVTNT-DRD2-GFP2 was verified by Western Blot analysis.

Fig.31 shows the Western blot for the expression of DRD1-GFP2 and DRD2-GFP2 with the rabbit reticulocyte based cell-free expression kit. The specific bands for DRD1-GFP2 and DRD2-GFP2 were detected around 60 kDa. Although the recombinant GFP2-tagged dopamine receptors have a formula molecular weight of 77 kDa (DRD1-GFP2) and 79 kDa (DRD2-GFP2). This mismatch in protein size and migration in the Western blot is common for helical membrane proteins and is called gel-shifting. The helical hydrophobic membrane regions and incomplete denaturation cause an anomalous SDS binding to membrane proteins. Therefore membrane protein migration on SDS-gels does not correlate with their actual molecular weight [171]. The immuno-staining of the Western blot with DRD1 and DRD2 specific antibodies revealed, that the detected bands around 60 kDa correlated with the respective expressed recombinant receptor. This deduction is also supported by the fact that these bands were not detected in the negative control without plasmid DNA. Therefore unspecific binding of DRD1 mAb and DRD2 mAb to proteins of the cell extract causing a false positive result is unlikely. These results proofed the successful expression of the recombinant dopamine receptors with the mammalian cell-free expression system. Therefore the cloned constructs are also suitable for cell-free expression systems.

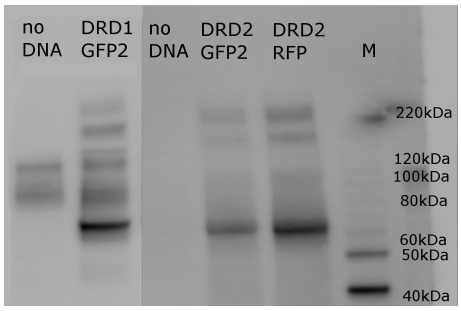

Figure 31: Western Blot of pCMVTNT-DRD1-GFP2 and pCMVTNT-DRD2-GFP2 expressed with the rabbit reticulocyte cell-free expression kit. Detected with chemiluminescence detection kit and anti-DRD1 (two lanes from the left) and anti-DRD2 (3 lanes from the right), respectively. The strong bands around 60 kDa result from the GFP2-tagged dopamine receptors. The fainter bands at higher molecular weights may result from aggregates of the receptors. no DNA: negative control: *in vitro* expression reaction without plasmid DNA added; DRD2-GFP2: *in vitro* reaction with 1.6 µg pCMVTNT-DRD2-GFP2 added; DRD1-GFP2: *in vitro* reaction with 1.6 µg pCMVTNT-DRD1-GFP2 added; M: magic mark protein standard

5.3.1 *In vitro* expression of DRD1-GFP2 and DRD2-GFP2 into polymersomes

The next step towards the receptor functionalised platform was the incorporation of the *in vitro* expressed receptors into the bio-mimetic membranes. For lipid based bio-mimetic membranes the direct incorporation of membrane proteins by *in vitro* synthesis has already been demonstrated [94]. Therefore in this work the *in vitro* expression of the dopamine receptors was performed in the presence of polymersomes to also achieve their direct incorporation into the polymer membrane. Polymer membrane based functionalised platforms would be interesting for screening applications due to their higher mechanical and chemical stability. Also for medical applications polymer based bio-mimetic membranes would be interesting due to varying possibilities to modify their surface properties as well as their chemical properties like permeability. For the following experiments two different kinds of polymersomes, ABA triblock-polymersomes Fig.32 and AB diblock-polymersomes Fig.33, were tested. The ABA triblock polymersomes were used due to their already proofed applicability for reconstitution of membrane proteins (Chapter:2.5.3). AB diblock polymersomes were used due to their bilayer membrane structure which resembles more the morphology of natural lipid membranes. This leaflet structure may lead to better lateral fluidity, compared to the monolayer triblock-copolymer membrane (Chapter:2.5.3 Fig.8). This increased lateral fluidity may favour incorporation and functionality of membrane proteins. Also two different cell-free expression systems were used. The mammalian rabbit reticulocyte based one as before and a wheat germ based one. The wheat

germ based cell-free expression kit was chosen owing to the possibility of supplementation with larger volumes of polymersome solution and an easier purification due to the properties of the cell extract. For both expression systems 1.6 µg plasmid DNA were used in each *in vitro* reaction. The rabbit reticulocyte based expression system was supplemented with 5 µl and the wheat germ based expression system with 16 µl of polymersome solutions prepared from 5 mg ABA and 20 mg AB block-copolymer in 1 ml and 900 µl ultrapure water, respectively. The successful expression was detected by Western blot analysis. The association of the *in vitro* synthesised dopamine receptors was demonstrated by centrifugal purification of the polymersomes after the *in vitro* expression reaction. All purification steps were also analysed by Western blot analysis.

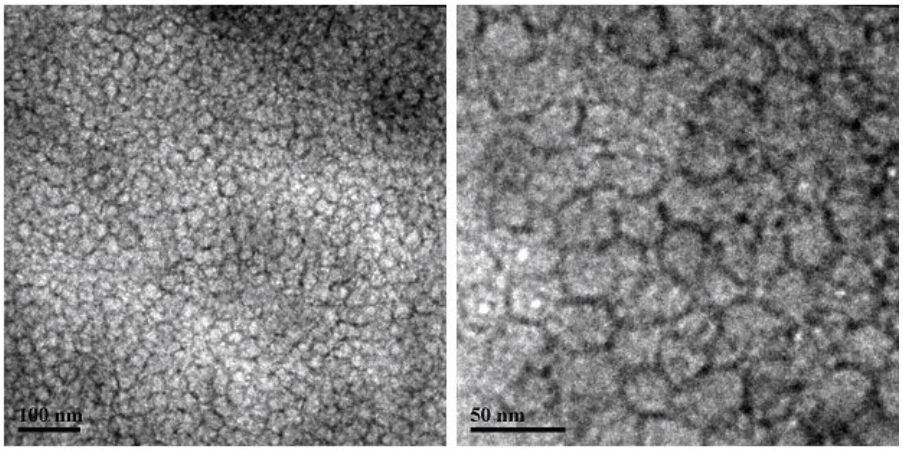

Figure 32: TEM picture of ABA triblock-polymersomes prepared from 5 mg ABA-triblock copolymer by film rehydration in 1 ml ultrapure water. The pictures show clear vesicular structures of about 50 µm in diameter. Preparation and TEM picture done by Zhikang Fu.

Fig.34 shows the Western blot of the expression of DRD2-GFP2 with the rabbit reticulocyte based cell-free expression kit supplemented with the two different polymersomes. Lane GFP is the pure *in vitro* reaction without any polymersomes as a reference. The specific bands for DRD2-GFP2 were for each reaction containing pCMVTNT-DRD2-GFP2, as already shown above, detected around 60 kDa due to the gel-shifting. Therefore the successful expression of DRD2-GFP2 in the presence of two different kinds of polymersomes could be demonstrated (Fig.34 lanes GFP BD21 and GFP ABA). For the *in vitro* reaction supplemented with ABA triblock polymersomes (ABA: PMOXA-PDMS-PMOXA) no clear band could be detected. The signal is blurred within the lane. This might be caused by incomplete denaturation of the polymersomes and aggregation of the expressed DRD2-GFP2 with polymersomes or fragments of that kind. These aggregations may cause unspecific migration in the SDS gel due to various

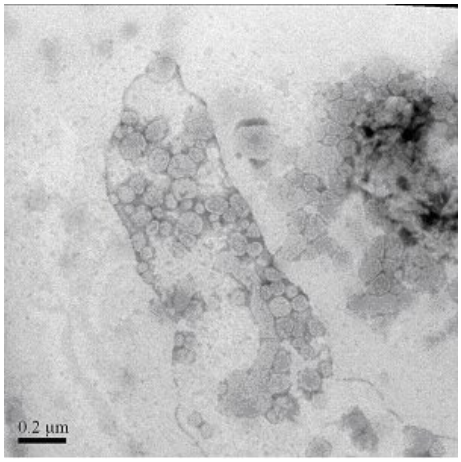

Figure 33: TEM picture of AB diblock-polymersomes prepared from 20 mg BD21 diblock copolymer by direct dissolution in 900 µl ultrapure water. In the center of the picture clear vesicular structures could be detected. Preparation and TEM picture done by Zhikang Fu.

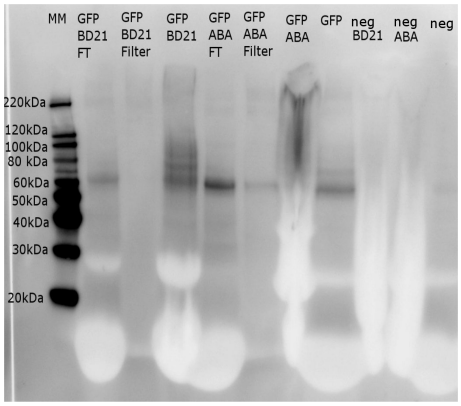

Figure 34: Western Blot of pCMVTNT-DRD2-GFP2 expressed with the rabbit reticulocyte expression kit supplemented with AB (BD21) or ABA polymersomes. Detected with chemiluminescence detection kit and anti-DRD2. neg: negative control, *in vitro* reaction without DNA template; BD21:*in vitro* reaction with BD21 polymersomes added; ABA:*in vitro* reaction with ABA polymersomes added; GFP: *in vitro* reaction with pCMVTNT-DRD2-GFP2; FT: 1st flow through from centrifugal purification; filter: resolved retentate from centrifugal purification; MM: magic mark protein standard

sizes, resulting in the observed signal. For the AB diblock polymersomes (BD21) the DRD2-GFP2 band could be detected. But there were also some faint bands with higher molecular weight which may result from altered molecular sizes due to incomplete dissolution of protein-polymer-interactions or aggregates. The centrifugal purification of the polymersomes from the *in vitro* reactions revealed that only a small part of the expressed protein was stably associated with the polymersomes. The resolved retentates only produced a very faint band for ABA polymersomes and no band for AB polymersomes (Fig.34 lanes GFP ABA filter and GFP BD21 filter). For the missing DRD2-GFP2-band in the filter fraction for AB polymersomes two explanations are possible: either a very low amount of protein below the detection limit was associated with the polymersomes, or even no protein was associated with the polymersomes. The bands in the 1st flow through fractions of the purification procedure (Fig.34 lanes GFP ABA FT and GFP BD21 FT) point out, that most of the expressed protein was not associated with the polymersomes but remained in the bulk solution. Anyway these results demonstrated that at least for the ABA triblock polymersomes a detectable amount of DRD2-GFP2 was stably associated with the polymersomes.

5.3.2 Control experiment for feasibility of GFP2-fluorescence as indicator for DRD2-GFP2 expression

After the proof of association of *in vitro* synthesised DRD2-GFP2 with ABA-polymersomes a control experiment was done to test if the GFP2-tag could also be detected in an emission spectra. This would be a useful detection method for the development of screening applications. The detection of GFP2 by emission spectra would offer an easy and fast way to at least control the efficient expression of DRD2 into the polymersomes. It would also offer an opportunity to detect activation of the receptors in a FRET (fluorescence resonance energy transfer).

For recording an emission spectra *in vitro* reactions with pCMVTNT-DRD2-GFP2 or without cDNA and all supplemented with ABA-polymersomes were performed as before with subsequent centrifugal purification. The retentates were resolved with ultrapure water and an emission spectra was recorded. As control an emission spectra of free GFP in ultrapure water was measured. In a first set of experiments the excitation wavelength was at 480nm and no GFP emission peak (506 nm) could be detected. Only an unspecific emission peak at 480 nm was detected for all samples. Therefore the measurements were repeated with an excitation wavelength of 475 nm. In this set of experiments low broadened GFP emission peaks could be detected (Fig.35). The emission spectras demonstrated, that detection of the fluorescence from the GFP2-tag was not unambiguous for DRD2-GFP2 functionalised ABA polymersomes (Fig.35b)) cause the GFP2 emission peak (506 nm) was partly masked by a broadened emission peak around 475 nm. The detection of the emission peak at 475 nm in the control measurement

with free GFP demonstrated, that the emission peak at 475 nm was not caused by residues of the rabbit reticulocyte expression kit. A concentration series of free GFP also revealed, that only a relatively high GFP concentration (1 µg/100 µl) was detectable at all (Fig.35a). As the emission peak at 480nm was measured for all three samples, free GFP, DRD2-GFP2 and the negative control (Fig.35) it must be caused by the measurement system itself.

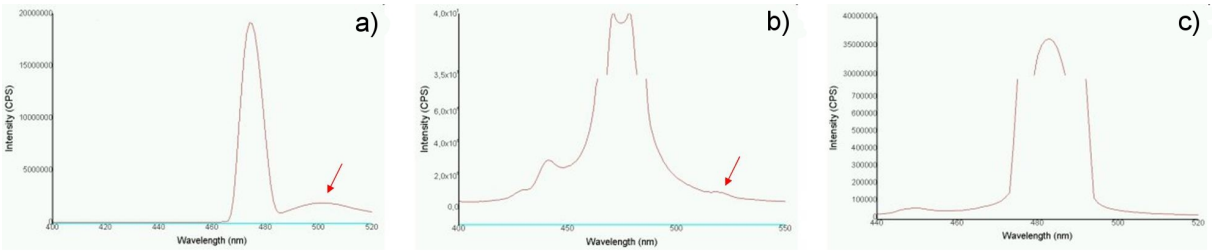

Figure 35: Emission spectra of a) GFP in ultrapure water (c=1µg/100µl); A broad GFP emission peak is detected around 506 nm and an intensive peak around 475 nm resulting from the system itself. b) DRD2-GFP2 functionalised ABA polymersomes purified by centrifugation; Only a tiny hump is left of the GFP2 emission peak because it is masked by the broadened peak at 475 nm. c) Negative control: *in vitro* reaction with ABA polymersomes purified by centrifugation; Only the broadened excitation peak around 475nm is detected. The excitation wavelength was reduced to 475nm (instead of 488nm) to reduce the masking of the GFP emission peak at 506 nm.

These results led to the decision to remove the fluorescence protein tag. Therefore recombinant plasmid DNAs were cloned without the fluorescence protein tags Fig.28. To enhance expression efficiency a Kozak sequence was also introduced into the new constructs.

5.3.3 *In vitro* expression of tag-free DRD1 and DRD1 into polymersomes

The *in vitro* expression of the tag-free DRD1 and DRD2 receptors was also verified by Western blot analysis (Fig.36,37,38) by immuno-staining with monoclonal antibodies specific for DRD1 and DRD2, respectively. Specific bands for DRD1(≈49kDa) and DRD2(≈50kDa) were detected around 40 kDa due to the gel-shifting phenomenon (Chapter:**??**). For all expression experiments an increased expression efficiency compared to the fluorescence protein tagged constructs could be observed.

For DRD2 the expression with the wheat germ based cell free expression kit (Fig.36A),Fig.37A)) produced distinct bands at 40kDa with only two weaker bands around 60 and 80kDa representing dimers or aggregates which are common for dopamine receptors. For the DRD2-BD21

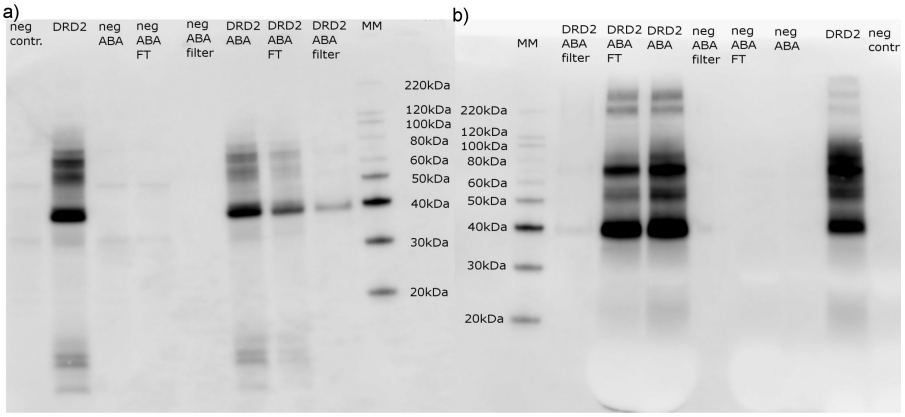

Figure 36: Western blot of pCMVTNT-DRD2 expressed with a) the wheat germ expression kit and ABA polymersomes and b) the rabbit reticulocyte expression kit and ABA polymersomes. Detected with chemiluminescence detection kit and anti-DRD2. neg: negative control, *in vitro* reaction without DNA template; ABA:*in vitro* reaction with ABA polymersomes added; DRD2: *in vitro* reaction with pCMVTNT-DRD2; FT: 1st flow through from centrifugal purification; filter: resolved retentate from centrifugal purification; MM: magic mark protein standard

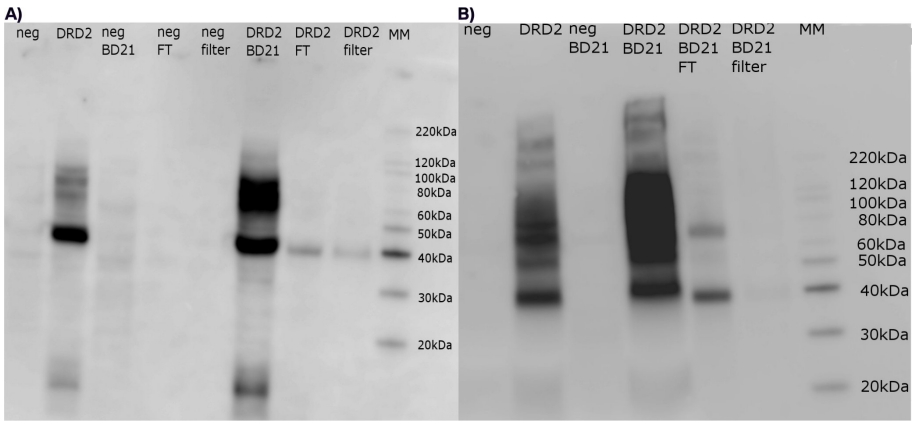

Figure 37: Western Blot of pCMVTNT-DRD2 expressed with A) the wheat germ expression kit and BD21 polymersomes and B) the rabbit reticulocyte expression kit and BD21 polymersomes. Detected with chemiluminescence detection kit and anti-DRD2. neg: negative control, *in vitro* reaction without DNA template; BD21:*in vitro* reaction with BD21 polymersomes added; DRD2: *in vitro* reaction with pCMVTNT-DRD2; FT: 1st flow through from centrifugal purification; filter: resolved retentate from centrifugal purification; MM: magic mark protein standard

samples those aggregation bands are blurred, maybe due to incomplete dissolution from the polymers and therefore altered migration in the SDS gel. For DRD2 a clear band is also detected for the resolved retentates for both kinds of polymersomes, ABA and BD21. But still the majority of expressed DRD2 remains in the bulk solution. Intensity measurement of the DRD2 bands for each purification step revealed, that approximately 25% of expressed DRD2 is stably associated with the polymersomes, either ABA or BD21. Expression of DRD2 with the rabbit reticulocyte based cell free expression kit (Fig.36B),Fig.37B)) seems to produce higher yields of DRD2. But also the amount and variety of dimers and aggregates is increased resulting in two additional bands over 200kDa. Furthermore the centrifugal purification is less effective for the rabbit reticulocyte based system indicated by a very faint DRD2 band for samples with ABA polymersomes and nearly no band for the BD21 polymersomes. Fig.38 shows the same results for expression of DRD1 in the presence of ABA polymersomes with wheat germ(Fig.38A)) and rabbit reticulocyte(Fig.38B)) based cell free expression systems as discussed above for DRD2. The expression of DRD1 in the presence of BD21 polymersomes is not shown, since this expression mode was not used for further experiments. Due to these results from Western Blot

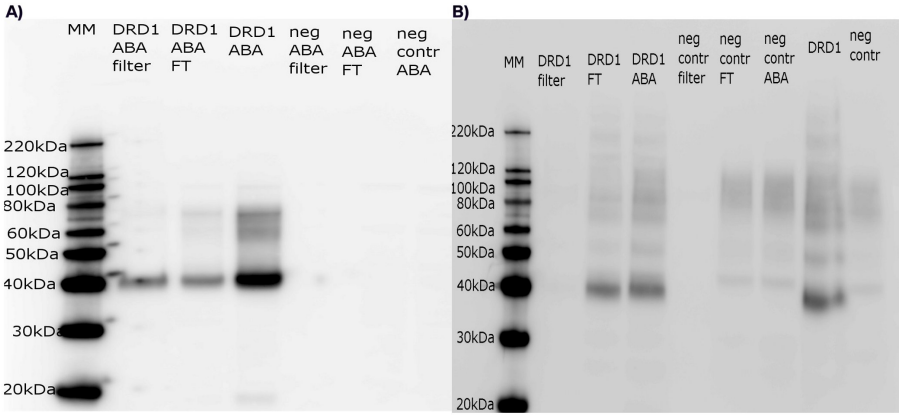

Figure 38: Western Blot of pCMVTNT-DRD1 expressed with A) the wheat germ expression kit and ABA polymersomes and B) the rabbit reticulocyte expression kit and ABA polymersomes. Detected with chemiluminescence detection kit and anti-DRD1. neg: negative control, *in vitro* reaction without DNA template; ABA:*in vitro* reaction with ABA polymersomes addded; DRD1: *in vitro* reaction with pCMVTNT-DRD1; FT: 1st flow through from centrifugal purification; filter: resolved retentate from centrifugal purification; MM: magic mark protein standard

analysis the wheat germ based cell free expression system was used for further experiments. Furthermore ABA polymersomes were mostly used for further experiments due to better purification properties.

In summary we could show the successful *in vitro* expression of dopamine receptor 1 and 2 with two different cell-free expression systems. Western blot analysis of polymersomes purified by centrifugal centrifugation after the *in vitro* reaction revealed a stable association of a sufficient amounts of synthesised dopamine receptors with both ABA-triblock and AB-diblock polymersomes.

5.4 Proof of stable association of *in vitro* expressed dopamine receptors with polymersomes

The Western blot analyses of purified dopamine receptor functionalised polymersomes suggested a stable association of the recombinant proteins with the polymersomes. To verify this association two control experiments were done. In one control experiment the stable association with the polymersomes was investigated by SPR spectroscopy. Therefore binding of dopamine receptor functionalised ABA-triblock polymersomes to immobilised DRD2 mAb was observed by SPR measurements with a Biacore device (Chapter:5.4.1).

In another control experiment the association of the *in vitro* expressed dopamine receptors with the polymersomes was detected by flow cytometry (Chapter:5.4.2). Therefore the dopamine receptors were first labelled with their specific antibodies. In a second step the primary antibodies were labelled with a fluorescently labelled antibody. Due to the gating process in the flow cytometry only labelled dopamine receptors which were associated with polymersomes could be detected.

These experiments should demonstrate the stable association of the *in vitro* expressed dopamine receptors with the polymersomes. In the event, that the dopamine receptors are not only associated but incorporated into the polymersome membrane different binding properties would be expected for DRD1- and DRD2-functionalised polymersomes in both experiments. These differences in binding arise from the different location of the epitopes of the dopamine receptors recognised by the antibodies. The epitopes for anti-DRD1 and anti-DRD2 are located at the N-terminus and the C-terminus of the respective receptor, respectively. For an incorporation in the natural orientation into the polymersome membrane an external N-terminus and internal C-terminus will be expected (Chapter:2.2.1, Fig.1). Therefore, if the receptors are incorporated in the natural orientation into the polymersome membrane, only DRD2-functionalised polymersomes will be able to bind to their specific antibody.

5.4.1 Biacore: Binding of dopamine receptor functionalised ABA polymersomes to immobilised antibodies

For further investigation of the association of the *in vitro* expressed dopamine receptors with ABA polymersomes binding of receptor functionalised polymersomes with immobilised antibodies was tested. Therefore the specific antibody for DRD1 or DRD2 was immobilised on a ProteinA coated Biacore chip. Subsequent incubation with DRD1 or DRD2 functionalised ABA-polymersomes should result in increasing reflectivity due to polymersome binding to the immobilised antibodies and therefore increase of layer thickness.

For experiments with DRD2-functionalised polymersomes a significant increase in reflectivity could be detected with the Biacore 3000. Pure ABA polymersomes only generated a small increase of reflectivity due to unspecific adsorption to the surface (Fig.BiacoreDRD2ABA). This specific binding of the functionalised polymersomes to the immobilised antibody suggests a stable association with ABA polymersomes. For the DRD1-functionalised polymersomes no

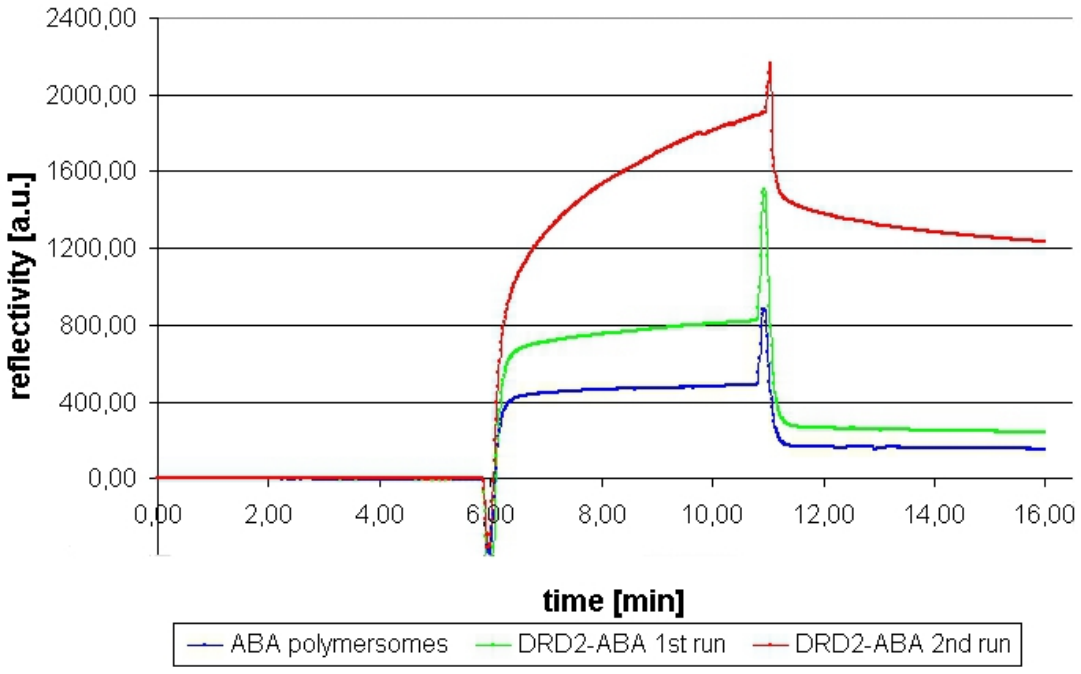

Figure 39: Binding of pure ABA polymersomes and DRD2-functionalised ABA polymersomes to mAb DRD2 immobilised on the surface. The binding of the polymersomes was detected with SPR in a Biacore 3000. The DRD2 functionalised polymersomes (green and red curve) show a significant higher binding to the mAb DRD2 than the pure ABA polymersomes (blue curve).

specific binding to the immobilised anti-DRD1 could be detected with the Biacore. The increase of reflectivity is the same as for the unspecific adsorption of pure ABA polymersomes

(Fig.BiacoreDRD1ABA). Normally this result would suggest, that no DRD1 is associated with

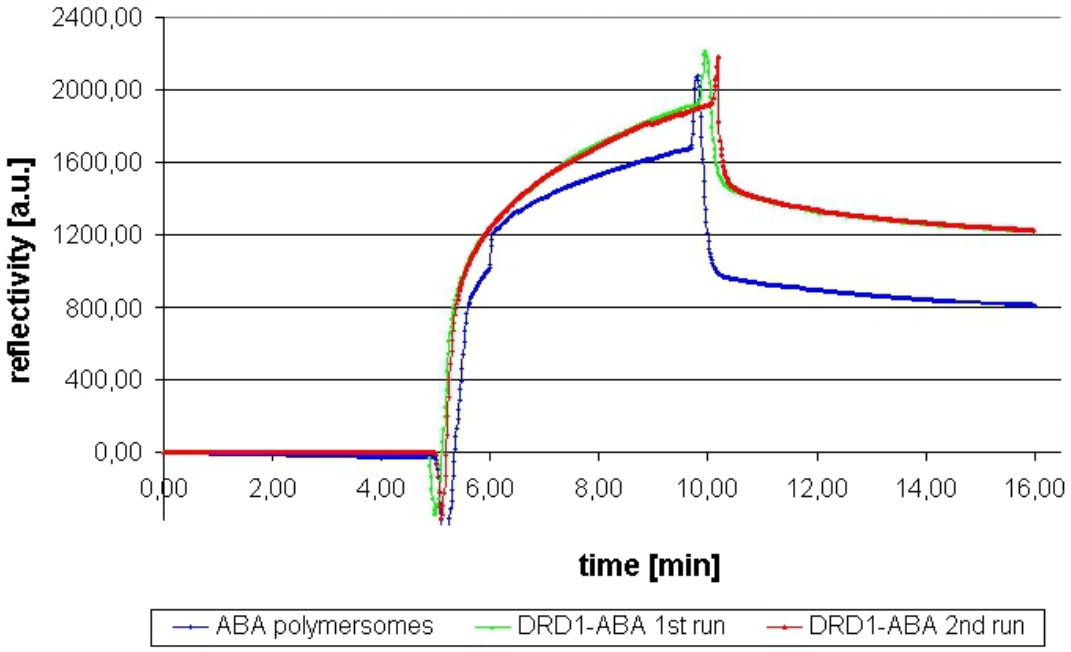

Figure 40: Binding of pure ABA polymersomes and DRD1 functionalised ABA polymersomes to mAb DRD1 immobilised on the surface. The binding of the polymersomes was detected with SPR in a Biacore 3000. The DRD1 functionalised polymersomes (green and red curve) and the pure ABA polymersomes (blue curve) show the same binding efficiency to the immobilised mAb-DRD1, indicating unspecific adsorption.

the ABA polymersomes. But the Western blot and centrifugal purification already demonstrated, that there are DRD1-receptors associated with the polymersomes. Therefore the unspecific adsorption of DRD1-functionalised ABA polymersomes to immobilised anti-DRD1 can only be explained by prevented binding of the antibody. This scenario can only occur, if DRD1 is incorporated into the poylmersomes in the natural orientation with external N-terminus and internal C-terminus (Chapter:2.2.1, Fig.1), since the anti-DRD1 used in this experiment binds to the C-terminus of DRD1. This conclusion is also supported by the successful binding of the DRD2-functionalised ABA-polymersomes to immobilised anti-DRD2 which binds to the N-terminus of DRD2.

For further verification it would be helpful to repeat the experiment with anti-DRD2 and anti-DRD1 which bind to the C-terminus and N-terminus, respectively. If these experiments generate results showing that DRD2-functionalised polymersomes do not bind and DRD1-functionalised ones bind, a correct incorporation of the dopamine receptors into the polymer membrane would

be most probably. Conclusive proof for the exact orientation of the *in vitro* expressed dopamine receptors in the polymer membrane would be a proteolytic digestion of radio-labelled *in vitro* expressed dopamine receptors and subsequent Western blot analysis of the digestion fragments. Due to the protection of membrane incorporated protein regions a specific incorporation will generate a specific pattern of digestion fragments.

5.4.2 Flow cytometry measurements

To scrutinise the findings from the Biacore experiments DRD1- and DRD2- functionalised polymersomes were incubated in solution with DRD1 and DRD2 specific antibodies, respectively. Subsequently the bound antibodies were labelled with fluorescently labelled antibodies. Polymersomes containing antibody labelled DRD1 or DRD2 receptors could be detected by flow cytometry.

Again only for DRD2-functionalised ABA polymersomes specific antibody binding could be detected (Fig.41b)). For the negative control with ABA polymersomes only unspecific adsorption of approximately 35% was detected.

For DRD1-functionalised ABA-polymersomes (Fig.41a)) the binding of antibody was less than 30% increased compared to the unspecific binding of pure ABA polymersomes, indicating also only unspecific adsorption of anti-DRD1 to the DRD1-functionalised polymersomes.

These results corroborate the suggested oriented incorporation of the dopamine receptors into the polymersome. Maybe a minor amount is incorporated in the opposite orientation generating slightly increased binding to the DRD1-functionalised polymersomes compared to the negative control.

For DRD2 the successful association with AB (BD21) diblock-polymersomes could also be demonstrated by detection of antibody binding in solution by Flow cytometry (Fig.42b)). The unspecific adsorption of anti-DRD2 to BD21 polymersomes ($\approx$36%) is in the same order as for ABA triblock-polymersomes ($\approx$35%). For this experiment a second membrane protein (claudin2) was *in vitro* expressed with AB polymersomes. Claudin2 plays a major role in tight junction-specific obliteration of the intercellular space, through calcium-independent cell-adhesion activity. This membrane protein was chosen as control cause it was also commonly used for *in vitro* expression in polymersomes in this group [176]. This second negative control also only showed unspecific adsorption ($\approx$36%) in the same order as the pure polymersomes. This strengthens the conclusion that the increased binding to DRD2-functionalised polymersomes results from specific receptor antibody interaction and not from general unspecific protein-antibody interactions.

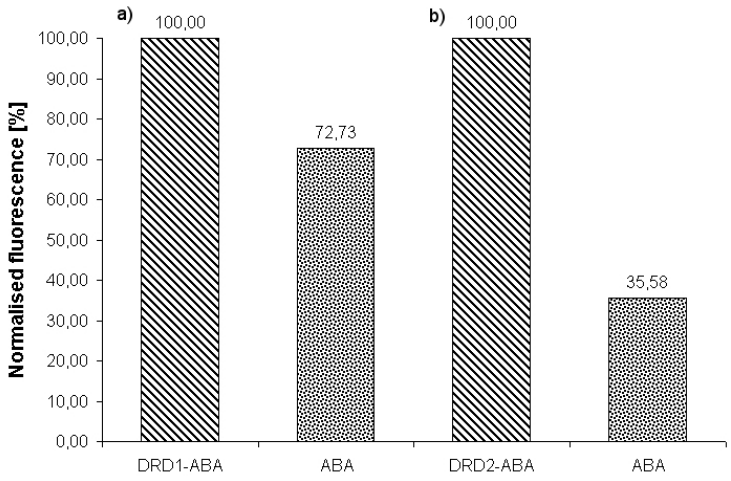

Figure 41: Flow Cytometry measurements of binding of fluorescently labelled mAb to a) pure ABA polymersomes (73%) and DRD1 functionalised polymersomes (100%). There is no specific binding of mAb DRD1 to the receptor functionalised polymersomes detected. b) pure ABA polymersomes (35%) and DRD2 functionalised poylmersomes (100%). For the DRD2 functionalised polymersomes a specific binding of mAb DRD2 could be detected.

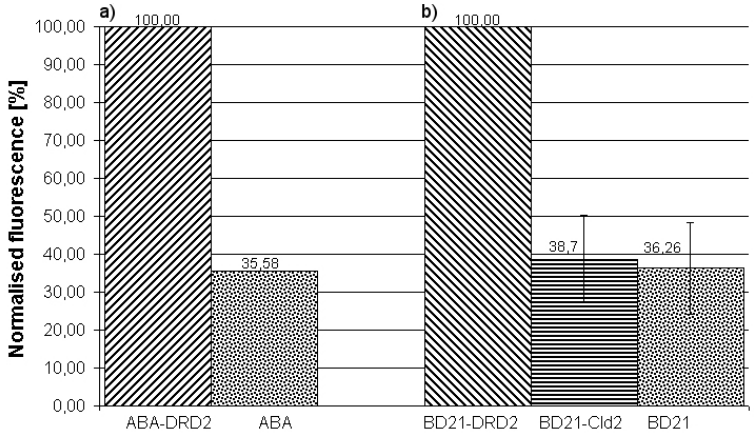

Figure 42: Flow Cytometry measurements of binding of fluorescently labelled mAb to a) pure ABA polymersomes (35%) and DRD2 functionalised ABA polymersomes (100%). There is no specific binding of mAb DRD1 to the receptor functionalised polymersomes detected. b) pure AB (BD21) polymersomes (36% $\pm$ 11%), Cld2 functionalised BD21 polymersomes (39% $\pm$ 11%) and DRD2 functionalised BD21 poylmersomes(100%). For the DRD2 functionalised polymersomes a specific binding of mAb DRD2 could be detected. Both negative controls, the pure BD21 and the Cld2 functionalised BD21 polymersomes, only showed a low unspecific adsorption.

In summary we could demonstrate the stable association of the *in vitro* expressed dopamine receptors with the polymersomes. Unspecific binding of C-terminal antibodies to receptor functionalised polymersomes and specific binding to N-terminal antibodies in both experiments suggested the successful incorporation into the polymersome membrane. According to the results the orientation of the incorporated dopamine receptors is supposed to be the same as the natural orientation in the outer cell membrane: external N-terminus and internal C-terminus. Conclusive proof of these observations needs to be produced by further experiments.

5.5 Ligand binding as proof of functionality of *in vitro* expressed DRD2

The results from the antibody binding experiments suggested that the *in vitro* expressed dopamine receptors are incorporated in their natural orientation. Therefore the next step was to show that they are also incorporated in their functional conformation. The binding pocket for their endogenous ligand dopamine is formed by several amino acid residues of different transmembrane domains of the receptor (Chapter:2.2.1, Fig.1). Therefore dopamine binding is only possible if the *in vitro* expressed dopamine receptors are incorporated in their functional conformation. Hence binding of dopamine labelled with the fluorescent dye dansyl (Chapter:4.3, Fig17) to DRD2-functionalised ABA and AB polymersomes was observed in solution (Chapter:5.5.1) and on the surface (Chapter:5.5.2). As controls, like in the antibody binding experiments, pure polymersomes and polymersomes functionalised with the membrane protein claudin2 were used.

5.5.1 Ultrafiltration binding assay

The results from the antibody binding experiments suggested incorporation of the dopamine receptors in a preferred orientation into ABA and AB polymersomes. To verify this conclusion the binding of the endogenous ligand dopamine was examined. Therefore purified DRD2-functionalised ABA and AB polymersomes were incubated with 25µM dopamine labelled with the fluorescent dye dansyl (Chapter:4.3, Fig.17). Subsequently unbound dansyldopamine was removed by centrifugal purification. Bound dansyldopamine was detected by fluorescence measurement with a plate reader.

Fig.43 shows, that no specific binding of dansyldopamine to DRD2-functionalised polymersomes could be detected. The negative controls without any expressed proteins (pure polymersomes) and the claudin2-functionalised polymersomes showed the same binding affinities as the DRD2-functionalised polymersomes. As the assay is performed in solution unspecific binding may originate from interactions of dansyldopamine with residual proteins from the *in vitro*

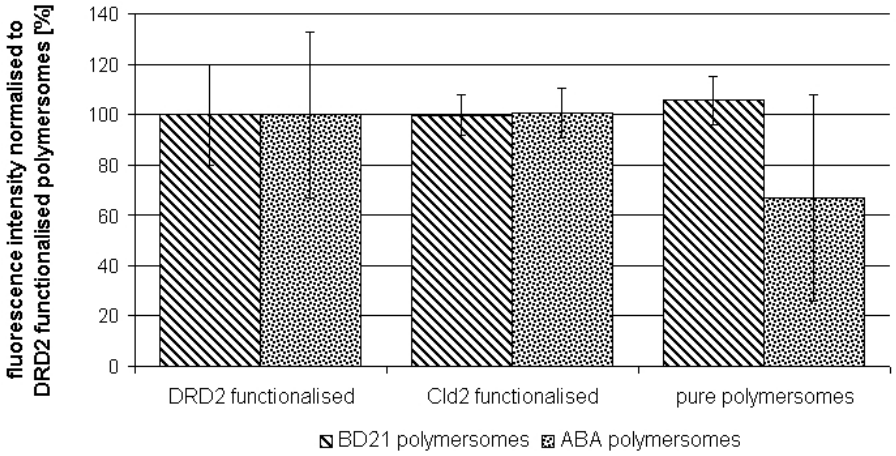

Figure 43: Fluorescence intensities of the ultrafiltration binding assay. The polymersomes were purified after *in vitro* expression with 100kDa MWCO filters. The resolved retentates were incubated with 25µM dansyldopamine. Fluorescence intensities were measured with a plate reader after rinsing. There is only unspecific adsorption of dansyldopamine to any of the polymersome populations detectable.

expression kit or from direct interactions of dansyldopamine with the polymersomes. A BCA assay (Tab.7) and Coomassie gel (Fig.44) revealed that the purification process by filtration is not complete. A lot of residual proteins could be detected in the purified polymersome solutions used for the binding assay. The determined protein concentrations from the BCA assay are far too high for yields from cell free expression systems. Also the high protein concentrations in the pure BD21 sample demonstrate, that the determined protein concentrations originate from the cell extracts and not from the expressed proteins. The protein concentrations detected in the 2nd flow through from the purification process point out, that still a lot of residual protein can be removed and therefore additional washing steps will have to follow for complete purification. But the Coomassie gel also shows that two more washing steps do not completely remove the residual proteins. Therefore this method is not feasible to develop an efficient, fast and easy to handle assay for ligand binding to DRD2 in polymersomes. The complete purification, if at all possible, would be too time-consuming.

5.5.2 Replacement assay on patterned ABA polymersomes

Specific ligand binding was not possible in solution due to incomplete purification of the polymersomes. To ease purification ABA polymersomes containing 10% methacrylate residues were immobilised on an amino-functionalised glass slide (Fig.45). This immobilisation of the

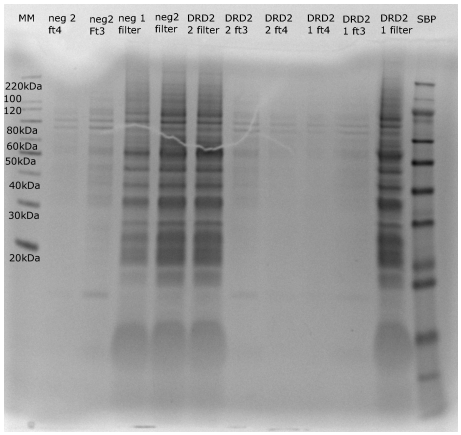

Figure 44: Coomassie gel of purified polymersome samples from the ultrafiltration binding assay.

polymersome population	mean concentration [µg/µl]	SEM [µg/µl]
DRD2	786	190
Cld2	1053	460
BD21 polymersomes	776	225
DRD2 2nd flow through	482	95
CLd2 2nd flow through	882	206
BD21 2nd flow through	715	179

Table 7: Protein concentrations for purified polymersome populations used for the ultrafiltration binding assay determined by BCA assay.

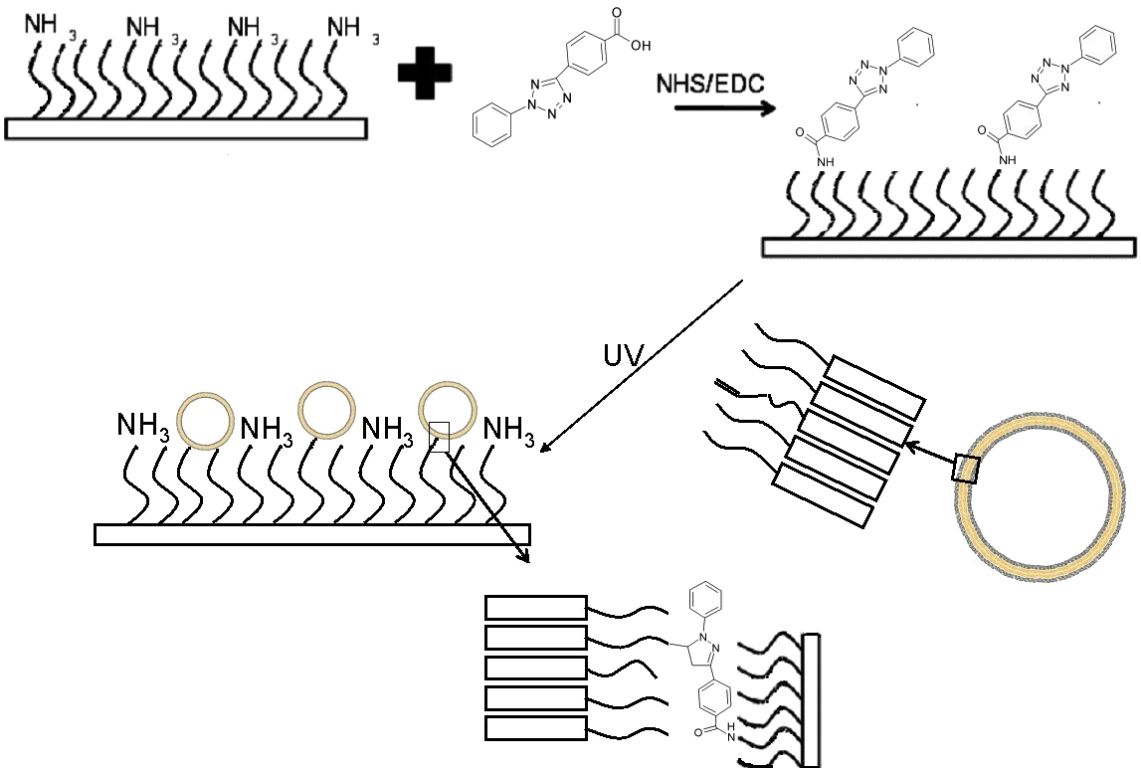

Figure 45: Mechanism of immobilisation of ABA-methacrylate polymersomes on amino-functionalised surfaces. In the first step a 2,5-diaryl-tetrazol is coupled to the amino surface. In the second step a diarylnitirle imine arises from the 2,5-diaryltetrazol by photolysis. This diarylnitirl imine readily reacts with the methacrylate-anchor of the polymersomes in a [3+2] cycloaddition coupling the polymersomes covalently to the surface.

polymersomes is favourable for eased purification by simple rinsing steps and will be advantageous for use in biosensor applications. For better signal recognition the polymersomes were immobilised in line patterns.

For the binding assay *in vitro* expression of DRD2 was performed directly on the immobilised polymersomes. Residual cell extract was removed by thorough rinsing with buffer. Subsequently the DRD2-functionalised polymersomes were incubated with 25µM dansyldopamine. In Fig.46a) specific binding of dansyldopamine to DRD2-functionalised polymersomes could be observed. The line pattern of the immobilised polymersomes is clearly labelled with dansyldopamine bound to the DRD2-functionalised polymersomes. For the negative control with pure ABA polymersomes, the line pattern is nearly not visible indicating very little unspecific adsorption of dansyldopamine to the polymersomes.

These results support the concept that the unspecific adsorption observed in the binding assay in solution is mainly due to residual proteins from the cell-free expression kit due to incomplete purification. And the low unspecific binding also confirms higher purification efficiency for the immobilised polymersomes. The specific binding of dansyldopamine suggests that at least sufficient quantities of DRD2 are incorporated into the polymersomes in an active conformation and physiological orientation, allowing for ligand binding.

To further verify this hypothesis reversibility of ligand binding was tested with a replacement assay. Therefore bound dansyldopamine was replaced with different concentrations of unlabelled dopamine. A decrease in dansyldopamine fluorescence with increased dopamine concentration could be observed (Fig.46b)). This showed, that the dansyldopamine is bound reversible to DRD2 and can be replaced by unlabelled dopamine. Blotting the measured fluorescence intensities against concentration of unlabelled dopamine resulted in a sigmoidal curve (Fig.47), which is characteristic for specific ligand binding.

The estimated EC_{50} value was approximately 30µM. Compared to cellular systems [172] with IC_{50} values around 8nM for replacement of ^{3}H-dopamine the binding curve was shifted to higher concentrations. As according to the vendor dansyldopamine has no altered binding affinity to dopamine receptors, the observed altered affinity for dopamine is probably caused by the different environment provided by the polymer membrane.

Although the mismatch in membrane thickness of polymer membranes and natural lipid membranes successful reconstitution of different membrane proteins into polymersomes have already been demonstrated [141, 142, 155, 173]. Simulation studies for incorporation of channel-forming proteins into polymer membranes suggested a compression of the highly flexible hydrophobic block of the membrane upon incorporation (Chapter:2.5.3,Fig.11; [145]). Hence the polymer membrane can adapt to the specific physical requirements of the membrane protein. It was also demonstrated that the deformation of the polymer membrane may lead to a partial

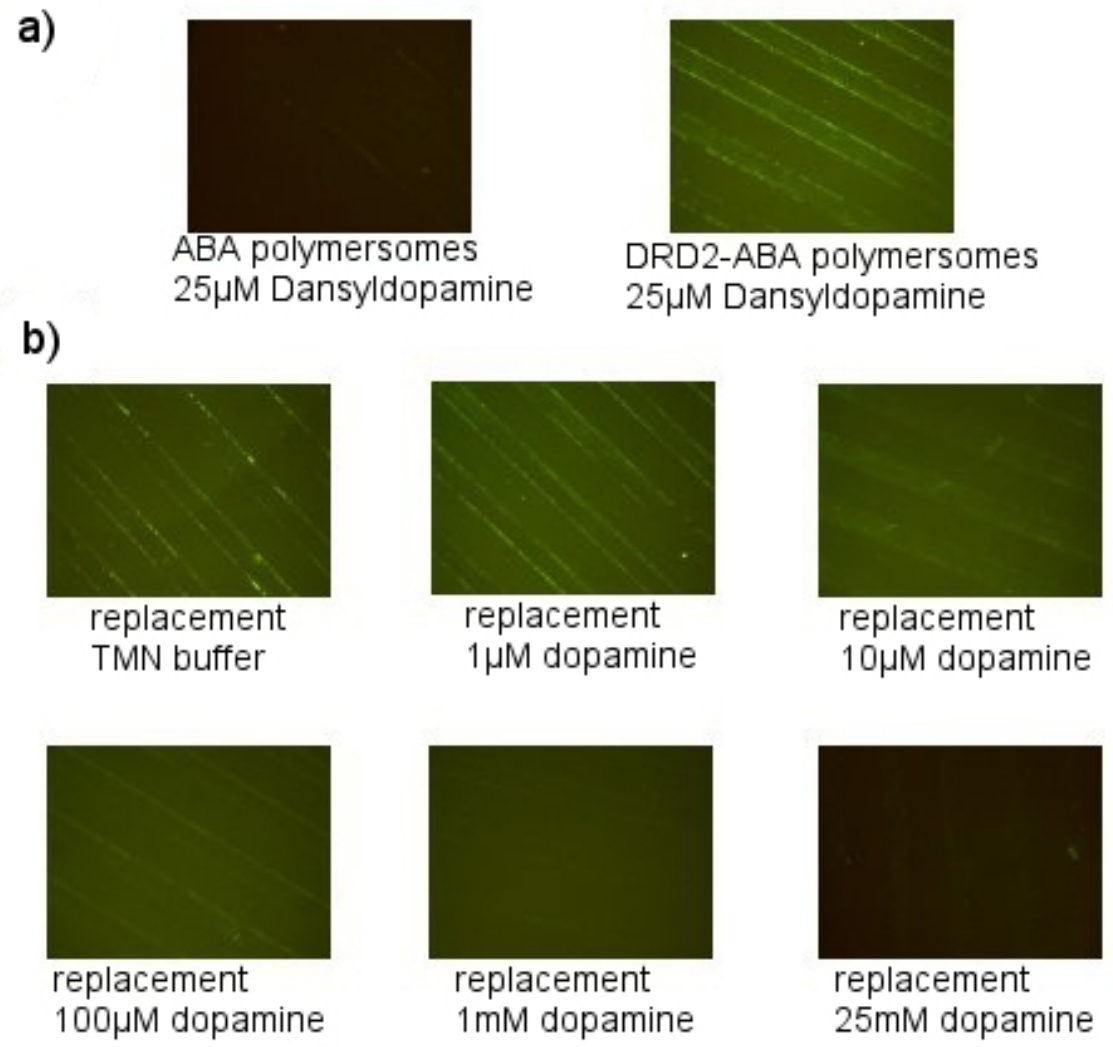

Figure 46: Microscope pictures of stamped ABA-patterns on amino-functionalised glass slides. a) Patterned ABA-polymersomes after *in vitro* expression with(right) and without(left) pCMVTNT-DRD2 and subsequent incubation with 25µM dansyldopamine. The pure ABA polymersomes show very little unspecific adsorption of dansyldopamine. For the patterned DRD2-functionalised polymersomes a clear specific binding of dansyldopamine is detected. b) Patterned ABA-polymersomes with *in vitro* incorporated DRD2 after the incubation with 25µM dansyldopamine and subsequent replacement with different concentrations of unlabelled dopamine.

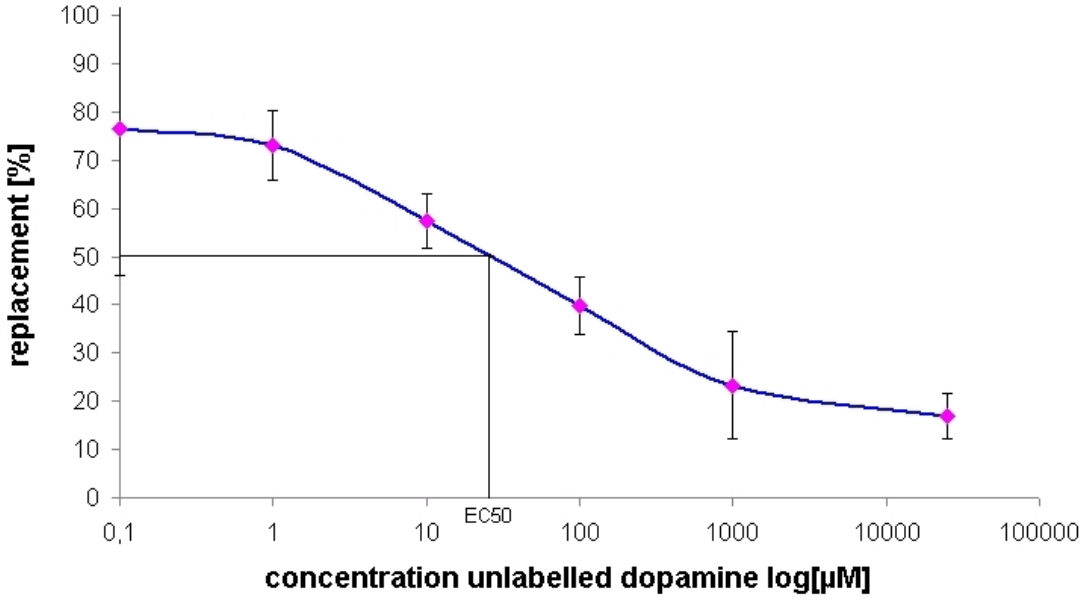

Figure 47: Replacement assay of dansyl-dopamine (25µM) with increasing concentrations of unlabelled dopamine. The replacement shows a sigmoid curve in dependence of unlabelled dopamine concentration. For plotting of the samples with pure TMN buffer an unlabelled dopamine concentration of 0,1 instead of 0 was used due to the logarithmic scale of the x-axis. EC50: estimated approximately 30µM

obstruction of the channel entrance by the hydrophilic corona falling onto the entrance due to the high flexibility (Chapter:2.5.3, Fig.12; [129, 145]).

For the patterned polymersomes there will also be a size mismatch of polymer membrane and the hydrophobic-hydrophilic characteristics of the dopamine receptor resulting in the compression of the highly flexible PDMS core upon incorporation of the receptor. In this case the hydrophilic corona of the thicker polymer membrane might not only fall onto the entrance to the receptor but directly interact with the hydrophilic "'extra-polymersomal"' loops of the DRD2. These interactions may hamper conformational changes of the receptor upon ligand binding or the binding step itself and therefore change the affinity of the receptor for its ligand. Moreover the hydrophilic parts of the ABA-polymer may shield the ligand binding side and therefore hinder the ligand to access the binding pocket.

Also the compressed hydrophobic PDMS core of the polymer membrane may slightly alter protein conformation or influence conformational changes due to different hydrophobic interactions with the transmembrane helices compared to lipid membranes. Altered membrane protein activity in correlation with the length of the hydrophilic and hydrophobic blocks of ABA-polymersomes has been reported recently [142]. Meier and coworkers demonstrated that NADH:ubiquinon reductase activity mostly correlates with the PDMS block length. They measured significantly lower activities for complex1 in polymersomes with similar ABA-structure like the ABA used for the patterned surface. This suggest, that the chosen hydrophobic block length might not offer an optimal hydrophobic environment for the activity of membrane proteins.

Another possible reason for altered receptor activity might be differences in post-translation modifications. Dopamine receptor 2 exhibit several glycosylation and phosphorylation sites on the external N-terminus and at the internal 3rd loop and C-terminus, respectively. Due to the *in vitro* expression of the DRD2 receptors with a non-mammalian cell-free expression system, these post-translational modification might be altered.

These interferences in receptor-ligand interaction recommend higher ligand concentrations to achieve the same effect as in cellular systems, resulting in the observed shift of the binding curve. Which of the above mentioned effects has the major contribution to the alteration of binding affinity and which ABA-type will induce the best affinity needs to be determined experimentally. Therefore the activity of DRD2 incorporated into ABA-polymersomes with different molecular properties will have to be measured.

Also formation of naturally occurring dimers may have an influence on the activity. The reduced fluidity of polymer membranes may also hinder dimer formation. And the formation of dimers in polymer membranes at all still has to be demonstrated.

Nevertheless this result strengthens the conclusion that the interaction of the *in vitro* expressed DRD2 and its endogenous ligand dopamine is specific and therefore DRD2 is expressed and incorporated in a functional conformation into ABA-polymersomes.

In summary it could be demonstrated, that *in vitro* expression of dopamine receptors into ABA polymersomes is possible. The replacement assay with the endogenous ligand dopamine proofed incorporation of DRD2 in an active conformation and physiological orientation into ABA polymersomes.

To determine the reason for altered affinity of the *in vitro* expressed receptors compared to the cellular system several control experiments will have to be evaluated. Ligand binding studies with ABA polymers of different block lengths can be used to determine the contribution of the altered environment provided by the polymer membrane. Binding studies with DRD2-functionalised triblock and diblock polymersomes will demonstrated the contribution of altered lateral membrane fluidity on binding affinity. The *in vitro* expression of DRD2 with a mammalian cell-free expression system may reveal altered binding affinity due to differences in post-translational modifications.

6 Conclusion

The functional expression of the fluorescent fusion protein recombinant plasmids for dopamine receptor 1 and 2 in SH-SY5Y cells could be demonstrated. Microscopic studies showed the correct localisation within the cell membrane. The internalisation of the fluorescence protein tagged dopamine receptors upon dopamine-hydrochloride activation demonstrated the functionality of the expressed receptors.

Furthermore the successful *in vitro* synthesis of dopamine receptor 1 and 2 with and without fluorescence protein tag with both eukaryotic (wheat germ and rabbit reticulocyte based) cell free expression systems could be demonstrated by Western blot analysis. In addition Western blot analysis confirmed the stable association of *in vitro* synthesised receptors with AB and ABA polymersomes added to the *in vitro* reaction mixtures.

Binding studies with monoclonal antibodies with the Biacore system and with flow cytometry revealed specific binding for dopamine receptor 2 to anti-DRD2 mAb. For dopamine receptor 1 no specific binding to anti-DRD1 antibody could be detected. This suggested the oriented incorporation of the dopamine receptors into the polymersomes since the anti-DRD2 mAb and anti-DRD1 mAb bind to the external N-terminus and internal C-terminus of the receptors, respectively.

Further verification of incorporation of the receptors into the polymer membrane was done by ligand binding experiments with fluorescent dansyldopamine. Specific ligand binding could only be observed for immobilised DRD2-functionalised polymersomes. In solution incomplete purification by centrifugal filtration caused a high unspecific adsorption of dansyldopamine to residual proteins from the cell free expression kit.

The replacement assay on the surface showed that the receptor was incorporated in the functional conformation into ABA-polymersomes. The shifted binding curve revealed that the different membrane properties and maybe also differences in post-translation modification alter ligand binding affinity.

These results highlight the general possibility to use *in vitro* expressed membrane proteins in polymersomes as a platform for drug screening or sensing. Although the membrane properties for maximum protein activity may have to be determined experimentally for each membrane protein of interest, this concept can be adjusted for any membrane protein of interest. The use of *in vitro* synthesis for incorporation of membrane proteins into the polymersomes spares the time-consuming traditional way of purification and reconstitution of the membrane protein of interest. Furthermore, the incorporation of different proteins or subtypes, by simply using the specific cDNAs, also offer interesting possibilities for screening applications. The immobilisation of the polymersomes on a surface provides an opportunity for parallel and high throughput screening.

7 Future Perspectives

The proof of principle for the successful *in vitro* expression of dopamine receptors as member of the large protein family of membrane proteins and especially GPCRs has been demonstrated. There are many questions involved that have not yet been adequately researched but need to be answered in order to fully understand the novel platform for functional protein expression and therefore the use in sensor and screening applications.

7.1 Improvement of sensor surface

The "'chip"' used for the replacement assay is still a primitive prototype. The pattern of the polymersomes by manual stamping and rinsing steps is not feasible for high throughput applications. A faster method for the pattern of polymersomes could be a printing method. First trials with printing of methacrylated ABA-polymersomes loaded with Rhodamine B onto the

same activated surface and subsequent covalently binding by photolysis demonstrated the immobilisation of intact polymersomes on the surface Fig.48a). Even after harsh rinsing steps with ultrapure water a reasonable amount of intact polymersomes on the surface could be detected. Fig.48b). Also mounting of the chip into a microfluidic system would be favourable for

Figure 48: Printing of methacrylated ABA-polymersomes onto activated ultrasticky slides(as used for the pattern by stamping) and subsequent covalently binding by photolysis and cycloaddition. a) Polymersomes loaded with Rhodamine B directly after printing and binding. The bright fluorescent spots demonstrate the immobilisation of intact ABA polymersomes on the surface. b) Immobilised ABA polymersomes after harsh rinsing procedure with ultrapure water. Some of the immobilised polymersomes vanished. But still a reasonable amount of immobilised polymersomes could be detected.

screening applications. The microfluidic system would ease rinsing steps and the application of different ligand solutions in a defined environment and controlled amount. Therefore high throughput screening would become possible. The closed environment of a microfluidic system would also prevent the surface from drying and therefore offering a longer lifetime for the incorporated membrane proteins.

Also some preparative parameters will have to be determined like the efficiency of polymersome

immobilisation and the amount of membrane protein incorporated into the polymersomes as well as the concentration of bound ligand. The overall protein concentration on the chips and the absolute amount of bound ligand will allow for calculation of binding constants and IC_{50} values.

Problems may also arise from the prerequisite of fluorescently labelled ligands for the binding assay. This always bears the possibility of altered affinity due to the fluorescent label. Therefore other detection methods for ligand binding will be of interest. One possible approach may be the use of conductive polymers as bio-mimetic surface for the incorporation of membrane proteins. To circumvent these complications a more complex sensor system for GPCRs might be possible. Similar to synthosomes, the immobilised polymersomes could be "'functionalised"' with the respective G-protein, adenylate cyclase and ATP prior to the combined *in vitro* synthesis of the GPCR and an cAMP gated ion channel. In this system the activation of the GPCR would cause an influx of ions into the polymersomes [174]. This inward current might be electronically detected. This would further improve easy handling and skip the labelling step of the ligands of interest.

7.2 Final proof of fully functional incorporation of GPCRs into polymersomes

Although the functionality of the incorporated receptor could be demonstrated, there is still a mismatch in activity compared to cell based systems. Therefore further experiments will have to proof functional incorporation of membrane proteins into polymersomes.

To determine incorporation of the receptors into the polymeric-membrane digestion experiments with radioactive labelled receptors are common. If the receptors are incorporated a characteristic band pattern will be detected in the radio-activity blot, as the transmembrane regions of the receptors and intra-polymersomal loops should be protected against digestion by the polymers. This method may also provide further proof for the orientation of the receptors in the membrane, as different orientations may cause different digestion patterns in the radioactivity blot due to different digestion sites accessible for the digestion-enzyme.

Also the influence of the hydrophobic block length on the ligand affinity of the receptors will have to be determined experimentally. Cause maybe altered hydrophobic core thickness of the polymeric membrane may lead to affinities similar to cellular systems. To further develop the sensor for general screening applications also activities depending on hydrophobic block length of different membrane proteins should be tested. This study should also reveal if there is a general favourable hydrophobic block length for membrane protein activity or if optimum hydrophobic core thickness differs with the protein of interest. A general optimum hydrophobic

block length would be favourable for general screening applications. In this case one general sensor platform could be easily functionalised with the protein of interest.

Further binding studies with different ligands and determination of their receptor affinities in the polymer-system will characterise general properties of the system. These studies may also determine adaptability of the system for general screening applications.

References

[1] LIEBERMANN,T. ; Knoll, W.:Colloids and Surfaces A: Physicochem. Eng. Aspects 171, 115-130 (2000)

[2] KNOLL,W.: Annu. Rev. Phys. Chem. 49, 569-638 (1998)

[3] WILTSCHI,B. et al. :Methods 39, 134-146 (2006)

[4] RAETHER,H.: Springer Tracts in Modern Physics, 111 (1988)

[5] KRETSCHMANN,E.: Zeitschrift für Physik B241, 313-324 (1971)

[6] GINGRICH,J.A. ; M.G. Caron: Annu. Rev. Neurosci. 16, 299-321 (1993)

[7] RITZ,S. Dissertation 2007

[8] KOZAK, M. Nucleic Acids Research 15, 8125-8148 (1987)

[9] SMITH,P.K. et al : ANALYTICAL BIOCHEMISTRY 150,76-85 (1985)

[10] WIECHELMANN,Karen J. et al. : ANALYTICAL BIOCHEMISTRY 175 231-237 (1988)

[11] RAHMAN,Misha: Introduction to flow cytometry; Abd Serotec

[12] LIMBIRD,Lee E.:molecular interventions 4, 6 326-336 (2004)

[13] AHLQUIST, Raymond P. Am.J.Physiol. 155, 586-600 (1948)

[14] ROSS, E.M. et al. J.Biol.Chem. 252, 5761-5775 (1977)

[15] SUTHERLAND, Earl W. Science 177 401-408 (1977)

[16] PALECZEWSKI,K. et al. Science 289, 739-745 (2000)

[17] MARINISSEN, M.J.; Gutkind, J.S. Trends Pharmacol. Sci. 22 368-375 (2001)

[18] NEVES, S.R. et al. Science 296, 1636-1639 (2002)

[19] FERGUSON, S.S.G. Pharmacol. Rev. 53, 1-24 (2001)

[20] HALL,R.A.; Lefkowitz, R.J. Circ. Res. 91 672-680 (2002)

[21] FREDERIKSSON, R. et al. Mol.Pharmacol. 63, 1256-1272 (2003)

[22] JACOBY, Edgar et al. ChemMedChem 1, 760-782 (2006)

[23] YILDIRIM, Muhammed A et al. Nature Biotechnology 25 10 1119-1126 (2007)

[24] KEBABIAN, J.W. and D.B. Calne Natue 277 93-96, (1979)

[25] MISSALE, Christina et al. Physiological Reviews 78, 1, 189-225 (1998)

[26] STRANGE, P.G. Pharmacol. Rev. 53, 1, 119-133 (2001)

[27] LE FOLL, Bernard Biotrend Reviews Review No.6 (5-2000)

[28] VALLONE, D. et al. Neuroscience and Biobehavioral Reviews 24, 125-132 (2000)

[29] BONCI, Antonello and F. Woodward Hopf Neuron 47, 335-338 (2005)

[30] NEVE, Kim A. et al. Journal of Receptors and Signal Transduction 24, No.3, 165-205 (2004)

[31] GIROS, Bruno et al. Nature 342, 923-926 (1989)

[32] USIELLO, A. et al. Nature 408, 199-203 (2000)

[33] BEAULIEU, Jean-Martin et al. Cell 122, 261-273 (2005)

[34] BEAULIEU, Jean Martin et al. The Journal of Neuroscience, 27, 4, 881-885 (2007)

[35] KOSCHATZKY, S. et al. ACS Chem. Neurosci. 2011

[36] ROCHEVILLE, M. et al. Science 288, 154-157 (2000)

[37] HURLEY, M.J. and P.Jenner Pharmacology & Therapeutics, 111, 715-728 (2006)

[38] GARCIA-TORNADU, Isabel et al. Neuroendocrinology, 92 207-214 (2010)

[39] GARCIA-TORNADU, Isabel et al. Neuroendocrinology 151, 1441-1450 (2010)

[40] SCHMAUSS, Claudia The Neuroscientist 6, 2, 127-138 (2000)

[41] ROGERS, Robert D., Neuropsychopharmacology 36, 114-132 (2011)

[42] FRANK, Michael J. and John A. Fossela Neuropsychopharmacology 36, 133-152 (2011)

[43] SARKAR, Chandrani et al. Brain, Behavior, and Immunity 24, 525-528 (2010)

[44] ITOKAWA, Masanari et al. Journal of Pharmacological Science 114, 1-5 (2010)

[45] WANG, Min et al. Molecular Brain 3, 25, (2010)

[46] MAILMAN, Richard B. and Vishakantha Murthy Curr Pharm Des 16, 5, 488-501 (2010)

[47] MANJI, Husseini K. et al. Science Signaling 207, 49-55 (2003)

[48] KÜHHORN, Julia et al. Journal of medical Chemistry 54, 4896-4903 (2011)

[49] BONCI, Antonello and F. Woodward Hopf Neuron 47, 335-338 (2005)

[50] VOLKOW, Nora D. et al. Biol Psychiatry 57, 1410-1415 (2005)

[51] LINGFORD-HUGHES, Anne et al. British Medical bulletin 96, 93-110 (2010)

[52] CAMPBELL, Benjam Charles and Dan Eisenberg Coll. Anthropol. 31, 1, 33-38 (2007)

[53] SASABE, Toschikazu and Shoichi Ishura Int. J. Environ. Res. Public Health 7, 1448-1466 (2010)

[54] STICE, E. et al. Science 322, 449-452 (2008)

[55] STICE, Eric et al. Neuroimage 50, 1618-1625 (2010)

[56] PAVESE, Nicola et al. Brain 126, 1127-1135 (2003)

[57] HASBI, Ahmed et al. PNAS 106, 50, 21377-21382 (2009)

[58] GEORGE, Susan R. and Brian F. O'Dowd The scientific World Journal 7(S2), 58-63 (2007)

[59] MILLAN, Mark J. et al. The Journal of Pharmacology and Experimental Therapeutics 303, 2, 791-804 (2002)

[60] KLEWE, Ib V. Neuropharmacology 54, 1215-1222 (2008)

[61] STIEGE,Wolfgang and Volker A. Erdmann Journal of Biotechnology 41, 81-90 (1995)

[62] KLAMMT, Christian et al. Journal of Structural Biology 158, 482-493 (2007)

[63] LIGUORI, Lavinia et al. Expert Rev. Proteomics 4, 1, 79-90 (2007)

[64] ENDO, Yaeta and Sawasaki, Tatsuya: Current Opinion in Biotechnology 17, 373-380 (2006)

[65] JACKSON, et al. Briefings in Functional Genomics and Proteomics 2, 4, 308-319 (2004)

[66] KALMBACH, Rolf et al. J. Mol. Biol. 371, 639-648 (2007)

[67] KATZEN, F. et al. Journal of Proteome Research 7, 3535-3542 (2008)

[68] CAPPUCCIO, Jenny A. et al. Molecular and Cellular Proteomics 7.11 2246-2253 (2008)

[69] SPIRIN, Alexander S. et al. Science 242, 1162-1164 (1988)

[70] KUBICK, S. Current Topics in Membranes 63, 25-49 (2009)

[71] RIGAUD, J.L. and Levy, D. Methods Enzymol. 372, 65-86 (2003)

[72] SEDDON, Annela M. et al. Biochimica et Biophysica Acta 1666, 105-117 (2004)

[73] SCHWARZ, Daniel et al. Proteomics 8, 3933-3946 (2008)

[74] SOBHANIFAR, S. J. Biomol. NMR 46, 33-43 (2010)

[75] KLAMMT, Christian et al. FEBS Journal 273, 4141-4153 (2006)

[76] KATZEN, Federico et al. Trends in Biotechnology 27, 8, 455-460 (2009)

[77] RAJESH, Sundaresan et al. New Biotechnology (2010)

[78] STAUNTON, David et al. Magnetic Resonance in Chemistry 44, S2-S9 (2006)

[79] CHEN, Y.J. et al. Proc. Natl. Acad. Sci. U.S.A. 104, 18999-19004 (2007)

[80] KOGLIN, Alexander et al. Magnetic Resonance in Chemistry 44, S17-S23 (2006)

[81] KATZEN, Federico et al. Trends in Biotechnology 23, 3, 150-156 (2005)

[82] SCHWARZ, Daniel Methods 41, 355-369 (2007)

[83] KLAMMT, Christian et al. FEBS Journal 272, 6024-6038 (2005)

[84] YANG, Jian-Ping BMC Biotechnology 11, 57 (2011)

[85] SHIMIZU, Yoshihiro et al. nature biotechnology 19, 751-755 (2001)

[86] DOI, N et al. Genome Res. 12, 487-492 (2002)

[87] ADAMS, S.R. et al. J. Am. Chem. Soc. 124, 6063-6067 (2002)

[88] ANGENENDT, Philipp et al. Anal. Chem. 76, 1844-1849 (2004)

[89] KHNOUF, Ruba et al. Anal. Chem. 82, 70221-7026 (2010)

[90] NOIREAUX, Vincent et al. Phys. Biol. 2, P1-P8 (2005)

[91] SINGER, S.J. and Nicolson G.L. Science 175, 720-731 (1972)

[92] STRYER, Lubert Biochemistry Fourth Edition (1999) W.H. Freeman and Company New York

[93] ROSSI, Claire and Joël Chopineau Eur. Biophys. J. 36, 955-965 (2007)

[94] ROBELEK,Rudolf et al. Angew. Chem. Int. Ed. 46, 605 -608 (2007)

[95] LAPINSKI, Monique M. et al. Langmuir 23, 11677-11683 (2007)

[96] HOPE, M.J. et al. Chemistry and Physics of Lipids 40, 89-107 (1986)

[97] HUANG, C.H. Biochemistry 8, 344-352 (1996)

[98] HOPE, M.J. Biochimica et Biophysica Acta 812, 55-65 (1985)

[99] SZOKA, Francis JR. and Demetrios Papahadjopoulos PNAS 75, 4194-4198

[100] DEAMER, D. Biochimica et Biophysica Acta - Biomembranes 443, 3, 629-634 (1976)

[101] ENOCH, Harry G. and Philipp Strittmatter PNAS 76, 1, 145-149 (1979)

[102] BALAZS, Daniel A. and WT. Godby Journal of Drug Delivery (2011)

[103] KORLACH, J. et al. Proceedings of the National Academy of Sciences of the United States of America 96, 8461-8466 (1999)

[104] KAHYA, N. Journal of Biological Chemistry 278, 28109-28115 (2003)

[105] RIQUELME, G. et al. Biochemistry 29, 11215-11222 (1990)

[106] BALLY, Marta et al. small X, XX 1-17 (2010)

[107] MÜLLER, Paul and Donald O. Rudin et al. Nature 194, 979-980 (1962)

[108] TIEN, H.T. et al. Nature 212, 718-719 (1966)

[109] TIEN,H. and A. Ottova-Leitmannova Membrane Biophysics, Elsevier (2000)

[110] MONTAL, M. et al. PNAS 69, 3561-3566 (1972)

[111] BEERLINK, A. et al. Langmuir 24, 4952-4958 (2008)

[112] MALMSTADT, Noah et al. Advanced Materials 20, 84-89 (2008)

[113] TUTUS, Murat Macromolecular Bioscience 8, 1034-1043 (2008)

[114] BRIAN, Adrienne A. and Harden M. McConnell PNAS 81,19, 6159-6163 (1984)

[115] BLODGETT, K. JACS 57, 1007-1022 (1935)

[116] ZASADZINSKI, J.A. et al. Science 263, 1726-1733 (1994)

[117] SALAFSKY, Joshua et al. Biochemistry 35, 14773-14781 (1996)

[118] TANAKA, M. and Sackmann E. Nature 437, 656-663 (2005)

[119] ROSSI, Claire et al. J. Phys. Chem. B 111, 7567-7576 (2007)

[120] KNOLL, W. et al. Electrochimica Acta 53, 6680-6689 (2008)

[121] MULLER, Daniel J. and Andreas Engel Current Opinions in Colloid and Interface Science 13, 338-350 (2008)

[122] GIESS, F. et al. Biophysical Journal 87, 3213-3220 (2004)

[123] STELZLE, M. et al. J. Phys. Chem. 97, 2974-2981 (1993)

[124] HAN, Xiaojun et al. Advanced Materials 19, 4466-4470 (2007)

[125] SIMON, A. et al. Journal of Colloid and Interface Science 308, 337-343 (2007)

[126] KÖPER, Ingo Molecular BioSystems 3, 651-657 (2007)

[127] NARDIN, Corinne and Wolfgang Meier Reviews in Molecular Biotechnology 90, 17-26 (2002)

[128] ALEXANDRIDIS, P. Curr. Opin. Colloid Interface Sci. 1, 490-501 (1996)

[129] MALINOVA, V. et al. Adv. Polym.Sci. 224, 113-165 (2010)

[130] LE MEINS, J.-F., O. Sandre and S. Lecommandoux Eur. Phys. J.E 34, 14 (2011)

[131] TANFORD, C. Science 200, 1012 (1978)

[132] DISCHER, D.E. et al. Science 284, 1143-1146 (1999)

[133] BERMUDEZ, H. et al Macromolecules 35, 8203-8208 (2002)

[134] DELCEA, M. et al. Macromol. Biosci. 10, 465-474 (2010)

[135] MENG, F. and Z. Zhong J. Phys. Chem. Lett. 2, 1533-1539 (2011)

[136] LUO, L. and A. Eisenberg Langmuir 17, 6804 (2001)

[137] NARDIN, C. et al. Langmuir 16, 1035 (2000)

[138] LI, M.H. and P. Keller Soft Matter 5, 927(2009)

[139] DU, J. and R.K. O'Reilly Soft Matter 5, 3544-3561 (2009)

[140] STOENESCU, R., A. Graff and W. Meier Macromol. Biosci. 4, 930-935 (2004)

[141] BAUMANN, Patric et al. Polymers 3, 173-192 (2011)

[142] GRAFF, A. et al. Macromol. Chem. Phys. 211, 229 (2010)

[143] PATA, V. and N. Dan Biophysical Journal 85, 2111-2118 (2003)

[144] DAN, N. and S.A. Safran Macromolecules 27, 5766-5772 (1994)

[145] SIRINIVAS, G. D.E. Discher and M.L. Klein Nano Letters 5, 12, 2343 (2005)

[146] KITA-TOKARCZYK, K. et al. Polymer 46, 3540-3563 (2005)

[147] BRINKHUIS, René P. et al. Polym. Chem. 2, 1449-1462 (2011)

[148] ANTONIETTI,M. and S. Forster Advanced Materials 15, 1323-1333 (2003)

[149] UNEYAMA, T. J. Chem. Phys. 126, 114902 (2007)

[150] BROž, P. et al. Nano Letters 6, 10, 2349-2353 (2006)

[151] PHOTOS, P.J. et al. Journal of Controlled Release 90, 323-334 (2003)

[152] CHEN, Y.M. et al. Macromol. Rapid Communications 27, 741-750 (2006)

[153] VRIEZEMA, D.M. et al. Angewandte Chemie, Int. Edition 42, 772-776 (2003)

[154] ENDRES, T.K. et al Biomaterials 32, 7721-7731 (2011)

[155] CHOI, H.-J. and Carlo D. Montemagno Nano Letters 5, 12, 2538-2542 (2005)

[156] BEN-HAIM, N. et al. Nano Letters 8,5, 1368-1373 (2008)

[157] GRAFF, A. et al. PNAS 99, 5064-5068 (2002)

[158] NALLANI, M. et al. Journal of Biotechnology 123, 50-59 (2003)

[159] RODBEEN, Renee and Jan C.M. van Hest BioEssays 31, 1299-1308 (2009)

[160] BROž, P. et al. Journal of Controlled Release 102, 475-488 (2005)

[161] BLANAZS, A., S.P.Armes and A.J. Ryan Macromolecular Rapid Communications 30, 267-277 (2009)

[162] GRZELAKOWSKI, M. et al. Small 5, 2545-2548 (2009)

[163] AHUJA, T. et al. Biomaterials 28, 791-805 (2007)

[164] DORN, J. et al. Macromolecular Bioscience 11, 514-525 (2011)

[165] BELEGRINOU, S. et al. Soft Matter 6, 179-186 (2010)

[166] GONZáLES-PéREZ, A. et al. Soft Matter 7, 1129-1138 (2011)

[167] RAKHMATULLINA,E. et al. Langmuir 24, 6254 (2008)

[168] NARDIN, C. et al. Langmuir 16, 7708-7712 (2000)

[169] GONZáLES-PéREZ, A. et al. Langmuir 25, 18, 10447-10450 (2009)

[170] BROWN,L. et al. Lab Chip 10, 1922-1928 (2010)

[171] RATH, Arianna et al. PNAS 106, 6, 1760-1765 (2009)

[172] BURT, D.R. et al. PNAS 72, 11, 4655-4659 (1975)

[173] CHOI, H.-J. et al. Nanotechnology 16, 1589 (2005)

[174] PIFFERI, S. et al. FEBS Letters 580, 2853-2859 (2006)

[175] KÖPER, Ingo Molecular BioSystems 3, 651-657 (2007)

[176] NALLANI, Madhavan et al. Biointerphases 6, 4, (2011)

[177] DE HOOG, H.-P.M., Nallani, M., Liedberg, B. Polymer Chemistry 3, 2, 302-306 (2012)

List of Tables

8 Appendix

A1 abbreviations

GPCR	G-Protein coupled receptor
cAMP	cyclic adenosine monophosphate
DNA	Deoxyribonucleic acid
D_{1-5}	Dopamine receptor 1-5
G_s	stimulatory G protein
G_{olf}	olfactory G protein
$G_{i/o}$	inhibitory G proteins
DRD1	Dopamine receptor 1
DRD2	Dopamine receptor 2
MAP kinase	mitogen-activated protein kinase
AkT-GSK3	Protein kinase B/Glycogen Synthase Kinase 3
PP2A	protein phosphatase 2
D_{2L}	long isoform of DRD2
D_{2S}	short isoform of DRD2
ADHD	Attention-Deficit Hyperactivity Disorder
tRNA	transfer Ribonucleic acid
mRNA	messanger Ribonucleic acid
ATP	Adenosine triphosphate
GTP	Guanosine triphosphate
RNA	Ribonucleic acid
PCR	Polymerase chain reaction
PURE	protein synthesis using recombinant elements
E.coli	Escherichia coli
NMR	Nuclear magnetic resonance
NLP	nanolipoprotein particles
BLM	Black lipid membrane
tBLM	tethered bilayer lipid membrane
sBLM	supported bilayer lipid membrane
CMC	critical micell concentration
MLV	multilamellar vesicles
ULV	unilamellar vesicles
SUV	small unilamellar vesicles
LUV	large unilamellar vesicles

GUV	giant unilamellar vesicles
HEM	hydrogel encapsulated BLM
FT-IR spectroscopy	Fourier transform infrared spectroscopy
cBLM	cushioned bilayer lipid membranes
SAM	self-assembled monolayer
his-tag	Histidine tag
AFM	Atomic force microscopy
QCM-D	quartz crystal micro-balance with dissipation
NADH	Nicotinamide adenine dinucleotide, reduced
PDMS	Poly(dimethylsiloxane)
PEG	Poly(ethylene glycol)
PAA	poly(acrylic acid)
PS-b-PIAT	Polystyrene-block-Poly(isocianopeptide)
PMOXA	Poly(2-methyloxazoline)
cp	conductive polymer
PVDF	Polyvinylidenfluoride
MWCO	molecular weight cut off
kDa	kilo Dalton
TEM	Transmission electron microscopy
THF	Tetrahydrofuran
RPM	Revolutions per minute
cDNA	complementary DNA
LB-medium	Lysogeny broth medium
DMF	Dimethylformamide
MW	molecular weight
SHSY-5Y cells	human neuroblastoma cells
FCS	fetal calf serum
DMEM	Dulbecco modified Eagle's minimal essential medium
HAM's F12	nutrient mixture
EDTA	Ethylenediaminetetraacetate
PFA	Paraformaldehyde
FC	Flow cytometry
SDS	Sodium dodecyl sulfate
MES buffer	2-(N-morpholino)ethanesulfonic acid as a buffering agent
GFP2	enhanced green fluorescent protein
PBS	Phosphate buffered saline
SPR	Surface Plasmon Resonance

EDC	1-ethyl-3-(3- dimethylaminopropyl) carbodiimide
NHS	N-hydroxysuccinimide
BSA	Bovine serum albumin
FSC	forward scatter channel
SSC	side scatter channel
Mab	monoclonal antibody
Anti-DRD2	antibody against DRD2
Anti-DRD1	antibody against DRD1
IgG	Immunoglobulin G
H+L	heavy and light chain
Cld2	Claudin 2
PBSA	PBS with sodium azide
BCA	Bicinchoninic Acid
N_2	Nitrogen
EtOH	Ethanol
ABA	triblock co-polymer 12[PMOXA]-55[PDMS]-12[PMOXA]
BD21	diblock co-polymer [PBd]22-b-[PEO]13
EC_{50}	half maximal effective concentration
IC_{50}	half maximal inhibitory concentration

A2 Sequences and plasmidmaps

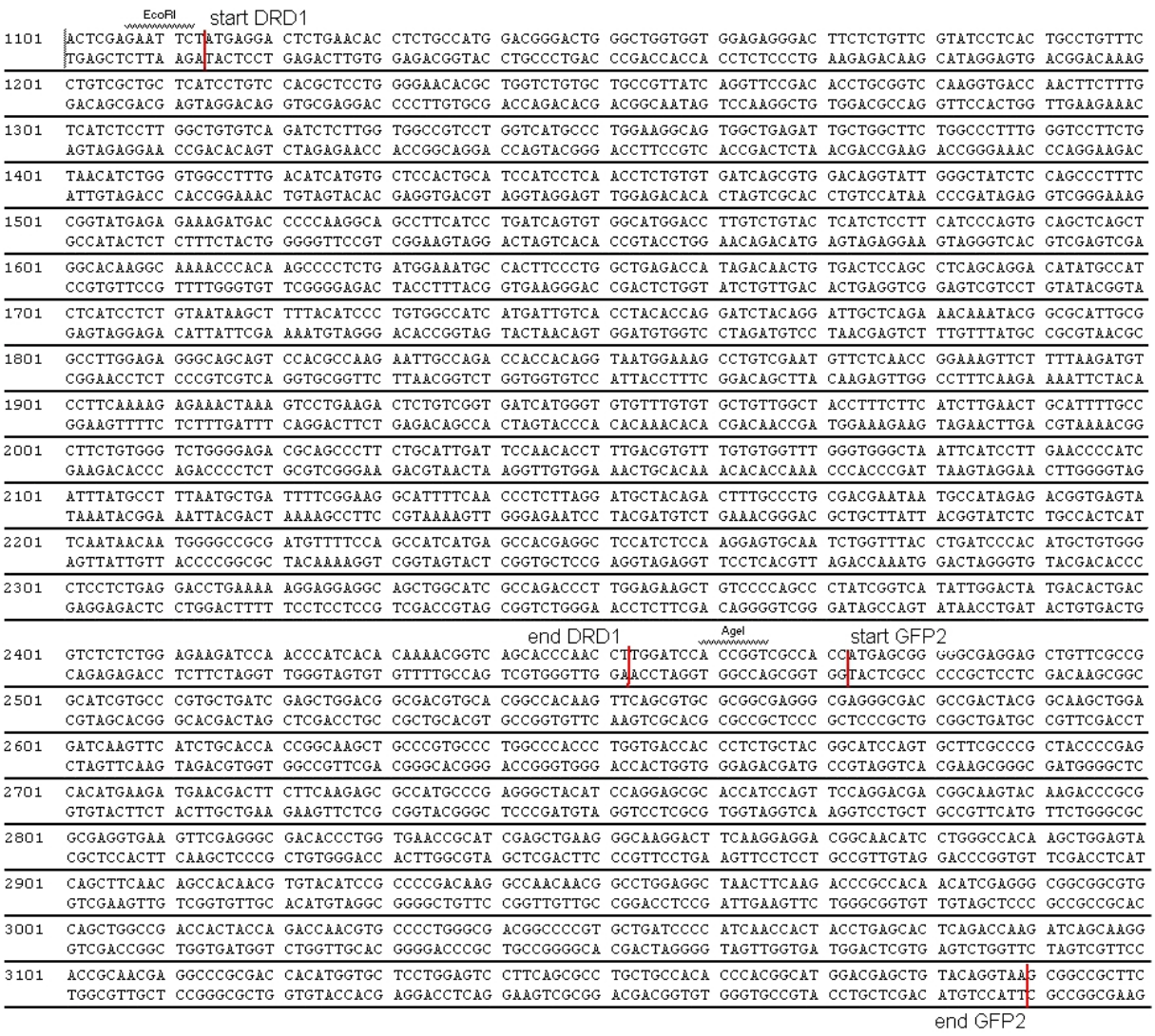

Figure 49: DNA-sequence of recombinant DRD1-GFP2

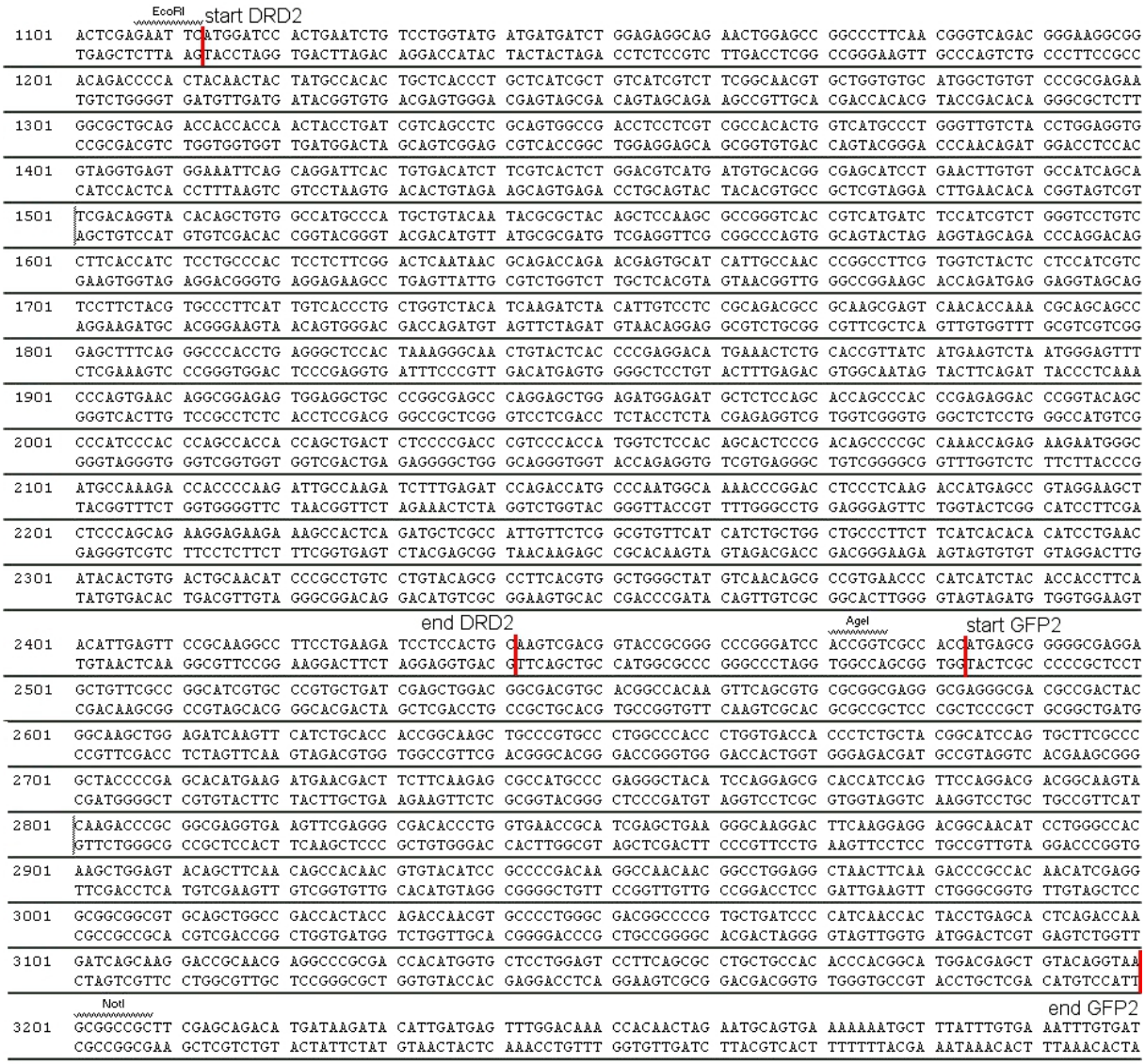

Figure 50: DNA-sequence of recombinant DRD2-GFP2

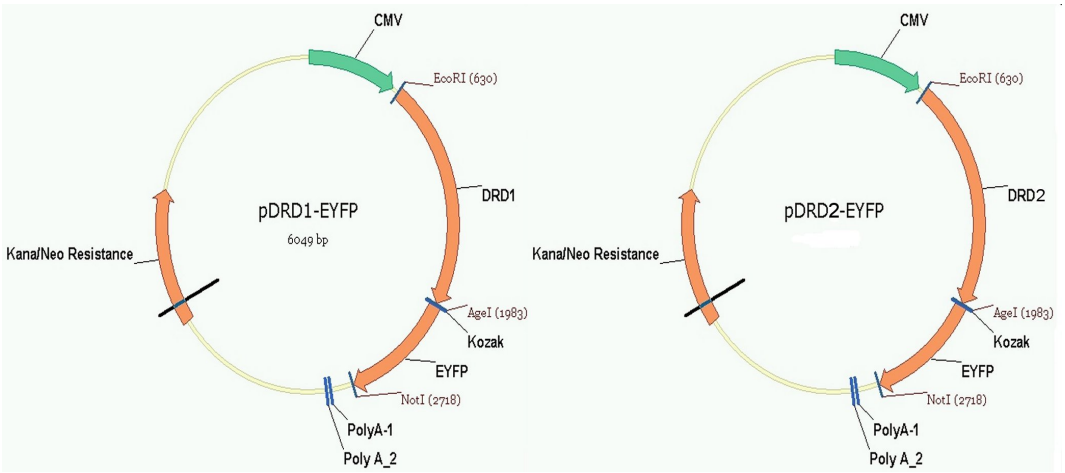

Figure 51: Plasmidmaps: a) pDRD1-EYFP and b) pDRD2-EYFP Both are the original vector from Sandra Ritz.

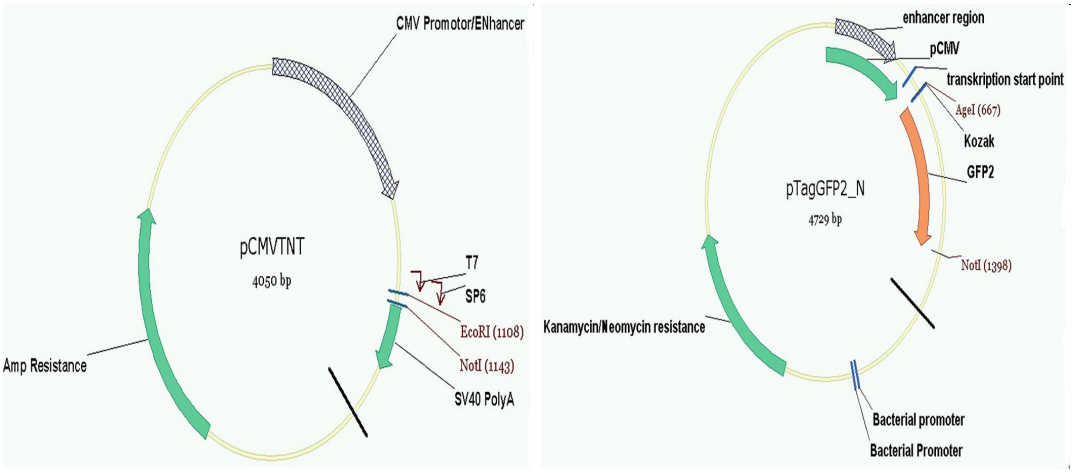

Figure 52: Plasmidmaps: left: pcMVTNT (invitrogen) right:pTag-GFP2-N (invitrogen)

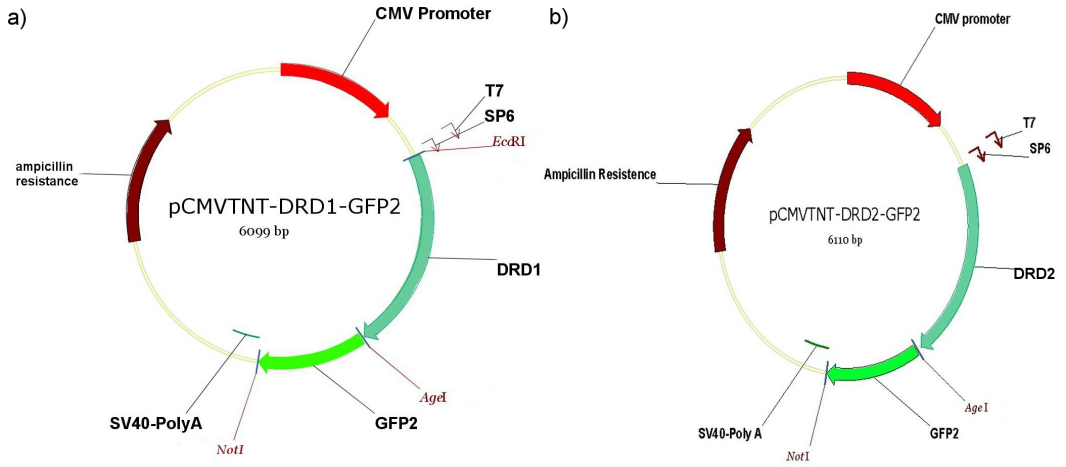

Figure 53: Plasmidmaps: a) pCMVTNT-DRD1-GFP2 and b) pCMVTNT-DRD2-GFP2

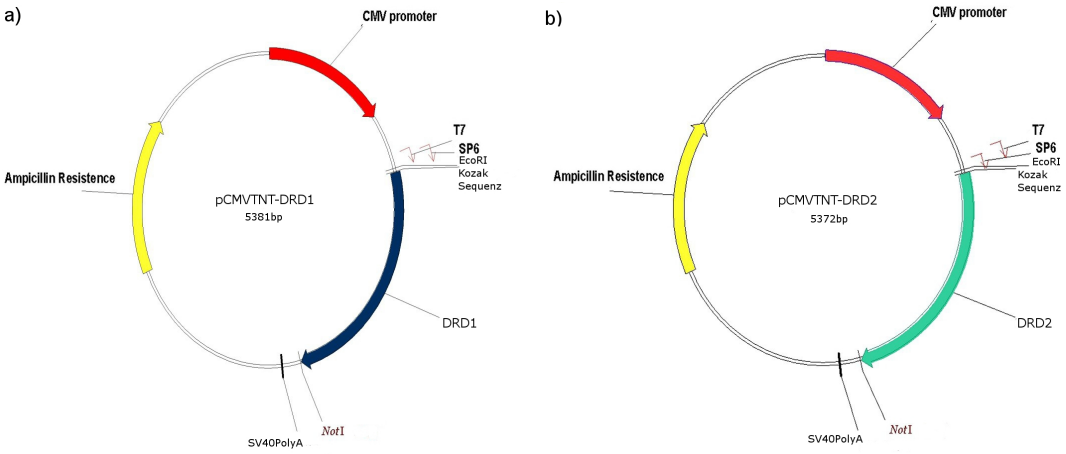

Figure 54: Plasmidmaps: a) pCMVTNT-DRD1 and b) pCMVTNT-DRD2